1951

The use of non-metallic models to study the behavior of submarine structures

Durfee, Elbert Foster

Massachusetts Institute of Technology

THE USE OF NON-METALIC MODELS TO STUDY THE BEHAVIOR OF SUBMARINE STRUCTURES

ELBERT FOSTER DURFEE, JR.
VAN DYKE JOHNSON

March 10
1857

THE USE OF NON-METALLIC MODELS TO STUDY THE BEHAVIOR OF SUBMARINE STRUCTURES

by

ELBERT FOSTER DURFEE, JR., COMMANDER, U.S. NAVY
B.S., Webb Institute of Naval Architecture

and

VAN DYKE JOHNSON, COMMANDER, U.S. NAVY
B.S., Webb Institute of Naval Architecture

SUBMITTED IN PARTIAL FULFILLMENT OF THE REQUIREMENTS FOR THE DEGREE OF

NAVAL ENGINEER

at the

MASSACHUSETTS INSTITUTE OF TECHNOLOGY

1951

Cambridge, Massachusetts

May 18, 1951

Professor Joseph S. Newell
Secretary of the Faculty
Massachusetts Institute of Technology
Cambridge, Massachusetts

Dear Sir:

In accordance with the requirements for the degree of Naval Engineer, we submit herewith a thesis entitled, "The Use of Non-Metallic Models to Study the Behavior of Submarine Structures."

Respectfully,

TITLE: THE USE OF NON-METALLIC MODELS TO STUDY THE BEHAVIOR OF SUBMARINE STRUCTURES

AUTHORS: E.F. Durfee, Jr., Comdr. U.S.N. and V.D. Johnson, Comdr. U.S.N.

Submitted for the degree of NAVAL ENGINEER in the Department of Naval Architecture and Marine Engineering on May 18, 1951.

I. ABSTRACT

The object of this thesis was to investigate the practicability of using plastic models to study the behavior of steel submarine pressure hulls under hydrostatic loading. The conclusion reached in this thesis is that models made of commercially available plastics can be used for such study, but that their range of application is limited.

The need for small scale models in submarine design exists because the formulas for submarine pressure hull strength calculations are limited in application and have not been adequately verified; therefore, design calculations have always been checked by hydrostatic tests of models. Steel models are normally used for these tests although they are costly to construct and must be tested to the same high pressure as will cause collapse of the full-scale submarine. In contrast, plastic submarine pressure hull models offer the advantage of low cost and low test pressures. For example, "Lucite" models cost approximately one-fifth the cost of comparative steel models and collapse at about one-fifth the pressure.

This investigation was conducted in two steps. First, the accuracy of using plastic columns to predict behavior of steel columns was studied; fifteen plastic columns were tested by the authors in this phase of the investigation. Second, the more complex problem of predicting the performance of a steel prototype using a plastic submarine pressure hull model was investigated.

Four plastic submarine models were built, and were tested by the authors in a simple, low-pressure steel tank using tap water.

Three of the four models tested failed sufficiently clear of both the end bulkheads and the longitudinal seam to indicate reliable failure data. The manufacture of

plastic structural models involved new techniques of construction; hence the lack of technical difficulties with the plastic under test was noteworthy.

Analysis of the test results indicates that: (1) plastic submarine models can predict the collapse of a steel prototype, but only when the prototype is not stressed above its proportional limit at collapse; (2) models should have λ similarity rather than geometric similarity to prototypes.

The accuracy of predicting steel prototype performance is affected by the value used for the modulus of elasticity of the plastic, and this value is in turn significantly affected by the rate of loading and temperature during testing. Therefore, plastic models are recommended more for qualitative comparison of the effect of varying one parameter, than for getting the exact quantitative collapse pressure of a specific steel submarine design.

The low cost of plastic models suggests their use in extensive research programs where qualitative predictions are desired. The present limited range in which models made of commercially available plastic can be used might well be extended by development of new plastics with stress-strain curves similar to those of steels used in submarines.

ACKNOWLEDGMENTS

The authors wish to express their appreciation to those individuals at Massachusetts Institute of Technology, David Taylor Model Basin, and Boston Naval Shipyard who materially aided the authors in their work upon this thesis. At each activity named the authors found everyone approached to be most co-operative and helpful.

Special acknowledgment is due the following professors who furnished aid and advice as Thesis Advisors: Professor J.P. Den Hartog, Professor A.G.H. Dietz, and Professor C.H. Norris.

Comdr. R.T. Miller, USN, very generously furnished to the authors for use in this thesis the data he had compiled from column tests using "Plexiglas" conducted at the David Taylor Model Basin in August, 1950.

The authors are particularly indebted to their Thesis Supervisor, J.H. Evans, Assistant Professor of Naval Architecture, for his advice and guidance; to Dr. S. Yurenka of the M.I.T. Plastics Laboratory, for his most helpful aid in regard to plastics and for his cooperation in making column testing apparatus available

to the authors; and to Dr. E. Wenk, Jr., of David Taylor Model Basin who was a continual source of valuable information, encouragement and advice upon all phases of the thesis from its very inception.

SYMBOLS AND ABBREVIATIONS

The following symbols and abbreviations are used throughout this report:

$\sigma_y = \sigma_{y.p.}$ = Yield point stress.

$\sigma_p = \sigma_{p.l.}$ = Stress at proportional limit.

E = Modulus of elasticity - initial slope of stress-strain curve.

E_T = Tangent modulus - slope of stress-strain curve at a particular stress.

E_R = Reduced modulus = $\dfrac{4E\, E_T}{(\sqrt{E} + \sqrt{E_T})^2}$

λ = $\sqrt[4]{\dfrac{(L/2R)^2}{(h/2R)^3}} \cdot \sqrt{\dfrac{\sigma_y}{E}}$ Thinness factor or sturdiness factor.

L = Unsupported distance between frames on submarine pressure hull.

L' = Submarine pressure hull frame spacing.

R = Radius of curvature of submarine pressure hull.

D = Diameter of submarine pressure hull (2R)

h = Thickness of submarine pressure hull.

ψ = $\dfrac{P}{(h/R)(\sigma_y)}$

P = Collapse pressure of model.

$\sigma_{crit.}$ = Buckling stress of a column.

ℓ	= Length of equivalent pin-ended column.
ρ	= Least gyradius of column section.
DTMB	= David Taylor Model Basin, Washington, D.C.
μ	= Poisson's Ratio.

The Use of Non-Metallic Models to Study

The Behavior of Submarine Structures

TABLE OF CONTENTS

TABLE OF CONTENTS (continued)

II.

INTRODUCTION

Objective

The purpose of this thesis is to investigate the practicability of using plastic models to facilitate study of the behavior of, and structural failures of, steel submarine pressure hulls.

Failure of a typical length of cylindrical shell and its attendant transverse frames under non-dynamic conditions of external hydrostatic loading is the specific item of "behavior" or mode of "structural failure" upon which this thesis concentrates.

In assessing the value, if any, which may be indicated for plastic submarine models, the thesis has as its initial objective the determination that such models can, or cannot, predict the performance of steel prototypes in a qualitative sense. Exploration of the quantitative worth of the plastic submarine models (as, for example, the prediction of an exact prototype collapse depth), is an ultimate objective.

Background

The theories concerning the exact cause of the

collapse or failure of a cylindrical thin-walled pressure vessel reinforced by stiffening rings (i.e., a submarine pressure hull) are neither complete, nor uniformly accepted. Similarly, the several formulas for computing or checking submarine pressure hull strength and collapse depth calculations involve simplified boundary conditions and other simplifying assumptions in their derivation and, therefore, owe their authority to such substantiation as test experiments afford, and apply to but one aspect of the collapse depth problem. Thus, the several formulas are used collectively to arrive at an acceptable design.

In addition to the uncertainties of theory and of design formulas as they apply to design parameters, the actual performance of any given submarine pressure hull will be a direct function of the physical characteristics of the material used, the methods of welding and construction, the quality of workmanship, etc.

For a variety of reasons, including the above, it has long been the practice to conduct actual hydrostatic tests to failure of selected submarine pressure hull designs. Some test work has been done upon large scale models of submarines; most of the test work is performed via hydrostatic tests of properly scaled small steel models.

Construction and test of a steel model is a time-consuming and costly procedure. Procurement of steel of the prototype's characteristics, hand machining of H-frames, special small scale welding, etc., are among the problems of model manufacture. Since the model should fail at the same collapse depth as the prototype (for example, over 400 pounds per square inch for 1000 feet collapse depth), the pressures involved are high, the test apparatus is heavy and expensive, and the testing techniques are time-consuming and costly. Time requirements and costs involved in standard steel model tests may be spoken of, conservatively, in "weeks" and "hundreds of dollars," respectively.

In contrast to the use of steel models, the use of a plastic (for example, "Lucite" or "Plexiglas") appeared to offer several promising advantages. First because of the relatively low values of the modulus of elasticity and of the yield stress for these methyl methacrylate plastics, the required test pressures for plastic models geometrically similar to steel models are much lower than the corresponding pressures for steel models. This suggested great simplification in the test equipment required with a lighter test tank, easily removable models, lighter piping, elimination

of pressure pumps and use of tap water as a water and pressure source, ease of securing watertightness, etc. Another saving was foreseen in the use of standard commercially available plastics to quickly and readily build models. The possible speed-up in actual testing offered superimposed savings.

The concept of using plastic submarine pressure hull models was suggested to the authors by some work at David Taylor Model Basin as witnessed by one of the authors during the summer of 1950. DTMB has officially reported the use of a cellulose acetate model in the physical test of a cylindrical gun foundation, Reference (1). Several plastic submarine pressure hull models have been prepared by DTMB, and inspected by the authors, but have not been tested. A sample test of an unfinished plastic model was made in August, 1950, at DTMB with one author assisting; it verified the opportunity for reduction in time, cost and test pressures. This DTMB test suggested another possible advantage of plastic models - the possibility of testing a model to "failure" (as evidenced by collapse lobe formation), but without destruction of the model. It was predicted that plastic models, particularly at the lower pressures, could be unloaded without permanent damage and then re-used. (This last prediction has <u>not</u> been confirmed by the subject work).

Problem

From consideration of the foregoing, the following problem was posed by the authors:

> Can a plastic model of a submarine pressure hull be utilized to predict, in either a qualitative or a quantitative sense, the collapse depth of a steel prototype under hydrostatic loading?

Implicit in the above problem, or in any attempt at its solution, are numerous other questions including the following:

> With commercially available plastics and average workmanship, can a plastic model be expected to behave as an efficient pressure vessel?
>
> Will a plastic model fail in mode similar to a steel model?
>
> Can instability or yield failures be obtained, or will the mechanics of construction provide the sources of failure?

What will be the effects on the steel-plastic correlation of the inherent variations in yield stress-modulus ratios and general shapes of the stress-strain curves?

Because of these variations in material characteristics, what scale factor must be employed between steel and plastic, and how shall it be applied to such difference design parameters as shell thickness, frame stiffness, etc.

Proposed Approach

The method of attack outlined below was established.

(a) Survey the work done in field of steel submarine pressure hull models.

(b) Survey the preliminary work done in the field of plastic submarine pressure hull models at DTMB.

(c) Survey plastics; availability, physical characteristics, stress-strain behavior, etc.

(d) Manufacture and test in compression a series of columns of chosen plastic; including preparation of stress-strain curve.

(e) Compare plastic column data with accepted existing steel column data.

(f) Manufacture and assemble low-pressure steel test tank, gages, piping, etc.

(g) Manufacture a series of plastic submarine pressure hull models, covering a range of frame spacing, and conduct hydrostatic tests of these scale models.

(h) Compare pressure and modes of failure for plastic submarine models with available data from tests of steel submarine models at DTMB.

Details of the actual approach to the problem will be found in the next section, "PROCEDURE." For additional details pertinent to the foreging section, see APPENDIX"A".

III.

PROCEDURE

Outline

In brief, the procedure followed in this thesis may be outlined in the following manner:

(a) Choice of plastic - the study of possible plastics, and the selection of an available, workable plastic with stress-strain and other characteristics not too dissimilar to steel.

(b) Plastic column tests - the selection and test of a series of compression columns of the chosen plastic, including preparation of stress-strain data for selected rate of loading.

(c) Correlation of plastic and steel columns - comparison of behavior of plastic columns with widely documented steel column performance, including correlation on selected non-dimensional basis to exclude variations in E, yield stress, etc.

(d) Design of plastic submarine models - selection of the design parameters, and the variables and range of variables to be studied.

(e) Manufacture of plastic submarine models - including problems of forming shell and frames, maintaining circularity, choice and use of solvents, etc.

(f) Design and manufacture and test of the steel test tank - including provision of gages, control of water pressure and volume, etc.

(g) Plastic submarine model tests - with the attendant problems of watertightness, rate of loading, observation of failure lobes, detection of incipient failure, etc.

(h) Correlation and evaluation of plastic submarine model test data - examination of plastic submarine model test results in view of column test results and all available data; correlation of plastic test data with experimental data from tests of steel submarine models.

(i) Evaluation of thesis and conclusions.

Choice of Plastic

The choice of plastic finally centered upon methyl methacrylate for a number of practical reasons, not the least of which is its availability in readily usable forms and sizes. Other reasons which led to the choice of a methyl methacrylate ("Lucite" and "Plexiglas" are both trade names for materials belonging to this category) included those listed hereafter. The material is readily available in commercial sizes of good uniformity as to size and tolerance, and fair uniformity as to chemical composition and physical characteristics. Much experience and knowledge regarding this material has been amassed by the M.I.T. group under Professor A.G.H. Dietz, and by DTMB. Use of this material would permit direct comparison with column tests by Cdr. Miller in August, 1950, and with projected submarine model tests by DTMB. Use of this material would offer a minimum of new "mechanical" problems in regard to model construction, choice of solvent cement, etc.

A primary disadvantage in the choice of methyl methacrylate lies in its gently rounded stress-strain curve without a distinct yield point. Another serious disadvantage is the fact that, whereas the yield stress

of this material is about 1/10 that of steel, the initial modulus of elasticity is only about 1/100 that of steel.

For a more detailed discussion of the choice of the plastic, refer to Appendix "B".

Plastic Column Tests

In order to achieve a starting point for comparing plastic submarine models with steel submarine models under conditions of hydrostatic (compressive) loading, it was decided to first conduct compression tests upon a series of plastic columns and compare such column test results with Euler's Column Curves and with existing published results of steel columns.

Accordingly, the set of "Lucite" columns specified on Tables IX-XIV were tested in compression. The test set-up was as detailed by Figure I. Columns were tested "fixed-ended", load rates were adjusted for ready comparison with "Plexiglas" column tests by R.T. Miller at DTMB in August, 1950, and short specimens were employed to obtain a compression stress-strain curve for "Lucite" - Figure XII.

For further details regarding "Lucite" columns, refer to Appendix "B".

FIGURE I

DIAGRAMMATIC SKETCH ~ LUCITE COLUMN COMPRESSION TESTS

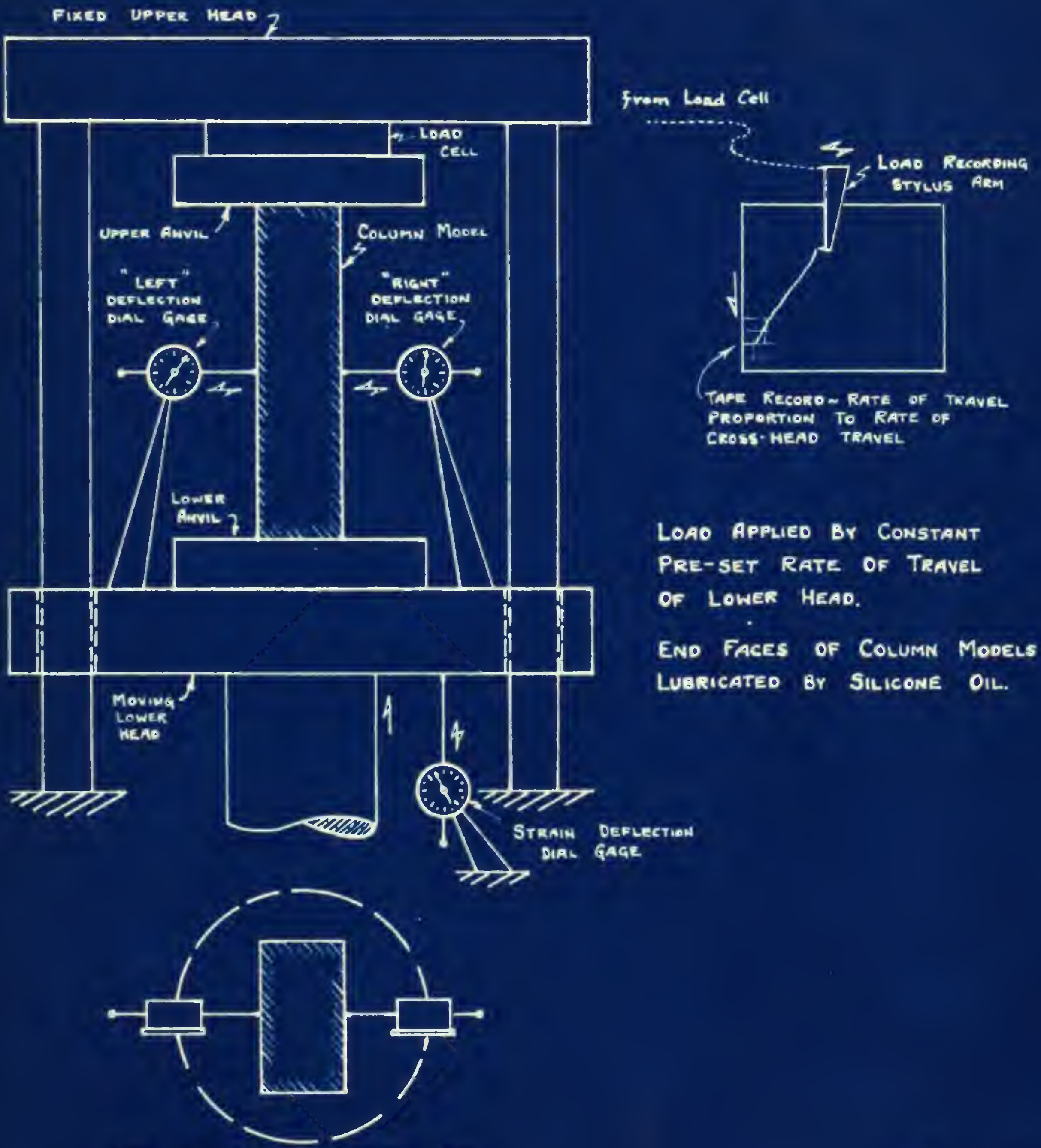

LEFT AND RIGHT DEFLECTION DIAL GAGES MOUNTED IN PLANE OF LEAST SECTION MODULUS AS INDICATED.

D 4/23/61

NOT TO SCALE

Correlation of Plastic and Steel Columns

In correlating the results of the plastic column tests with steel column data, use was made of the vast mass of data regarding steel columns that has been developed, documented in the literature, and accepted as valid. It was not the purpose of this thesis to conduct tests of steel columns, and no such tests were made. For the purposes of this thesis, the steel column data employed was that presented by Shanley in Reference (2).

The basis for correlating comparative steel and plastic column data was to reduce such data to appropriate non-dimensional plots to eliminate the effects of variations in basic characteristics such as yield stress and modulus of elasticity.

For pertinent details of the correlation of plastic and steel column test data, refer to sections on "RESULTS" and "DISCUSSION OF RESULTS."

Design of Plastic Submarine Models

The underlying concept for the design of the plastic submarine models was to cover by experimental tests as large a portion of the significant λ range as could be allowed by limitations of theory, of time, of pressure, and of money.

As a check of the applicability of plastic models to current submarine design, it was further decided to base one plastic model as closely as practicable upon current submarine design practice, using either λ -similarity, or geometric similarity, or both.

From an experimental point of view, the authors felt the desirability of obtaining submarine test spots in sufficient quantity to check against three portions of the λ - ψ curve: the rising "instability" portion of the curve at the higher λ values; the "yield" portion of the curve at low values of λ where ψ approximates unity; and, the transition range between the first and second areas.

The design, number and choice of dimensions for the submarine models actually tested is a compromise. The number of models was limited by cost, and the basis for other decisions is detailed in the APPENDIX. The model specifications were as detailed by Figures II-V; the model scantlings as actually built, where different, are detailed on Figures XVII-XXII. Four (4) models were built and tested; each was a nominal 9" inside diameter by 1/16" shell thickness. All shells were fitted with a longitudinal seam fitted with external butt strap. All frames were 3/16" wide by 5/16" deep,

FIGURE II

SPECIFICATION SHEET ~ MODEL № 50

MATERIAL : METHYL METHACRYLATE
FRAMES : 6 ~ 3/16" × 5/16"
SHELL THICKNESS : 0.060"
KEY DIMENSION: 0.52" BETWEEN FRAMES
0.71" CENTER TO CENTER

SCALE : 1" = 2"

3/17/51

FIGURE III

SPECIFICATION SHEET ~ MODEL № 51

MATERIAL : METHYL METHACRYLATE
FRAMES : 5 ~ 3/16" x 5/16"
SHELL THICKNESS : 0.060 "
KEY DIMENSION : 0.93" BETWEEN FRAMES
1.12" CENTER TO CENTER

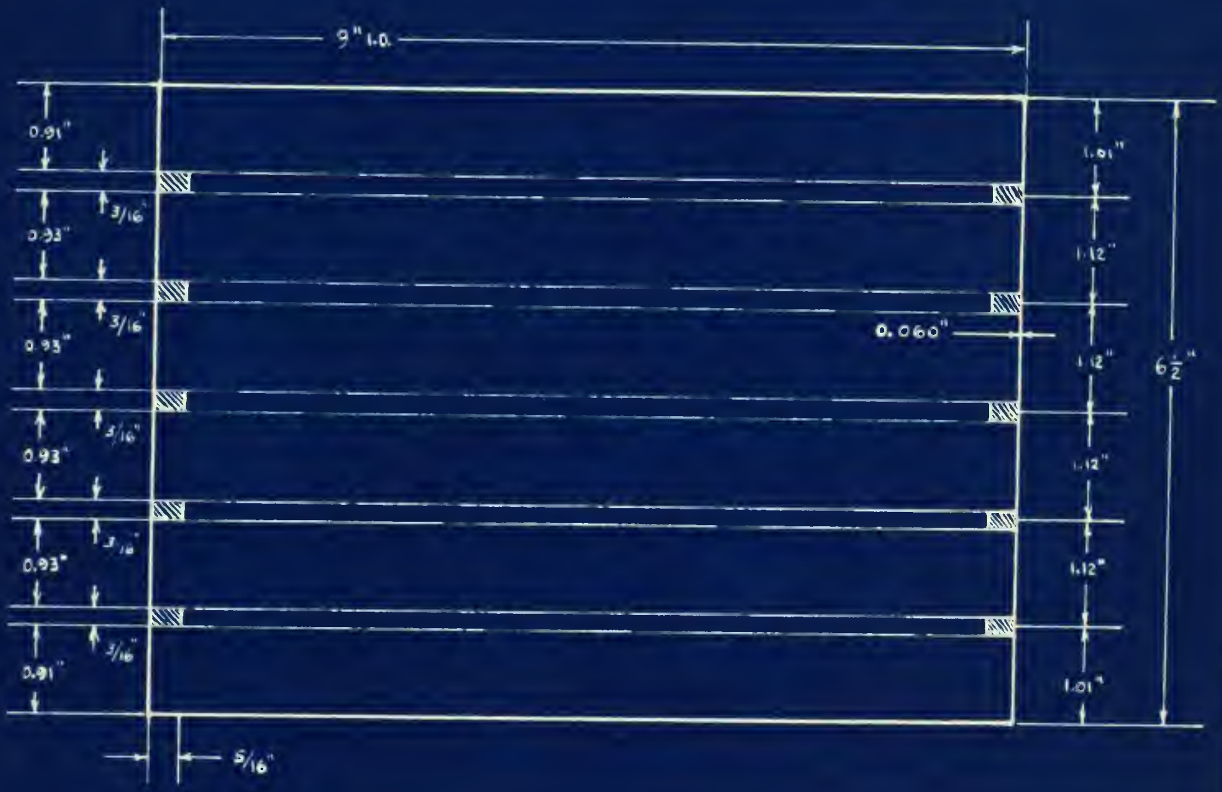

SCALE : 1" = 2"

3/17/51

FIGURE IV

SPECIFICATION SHEET ~ MODEL № 52

MATERIAL : METHYL METHACRYLATE
FRAMES : 5 ~ 3/16" x 5/16"
SHELL THICKNESS : 0.060"
KEY DIMENSION : 1.35" BETWEEN FRAMES
1.54 CENTER TO CENTER

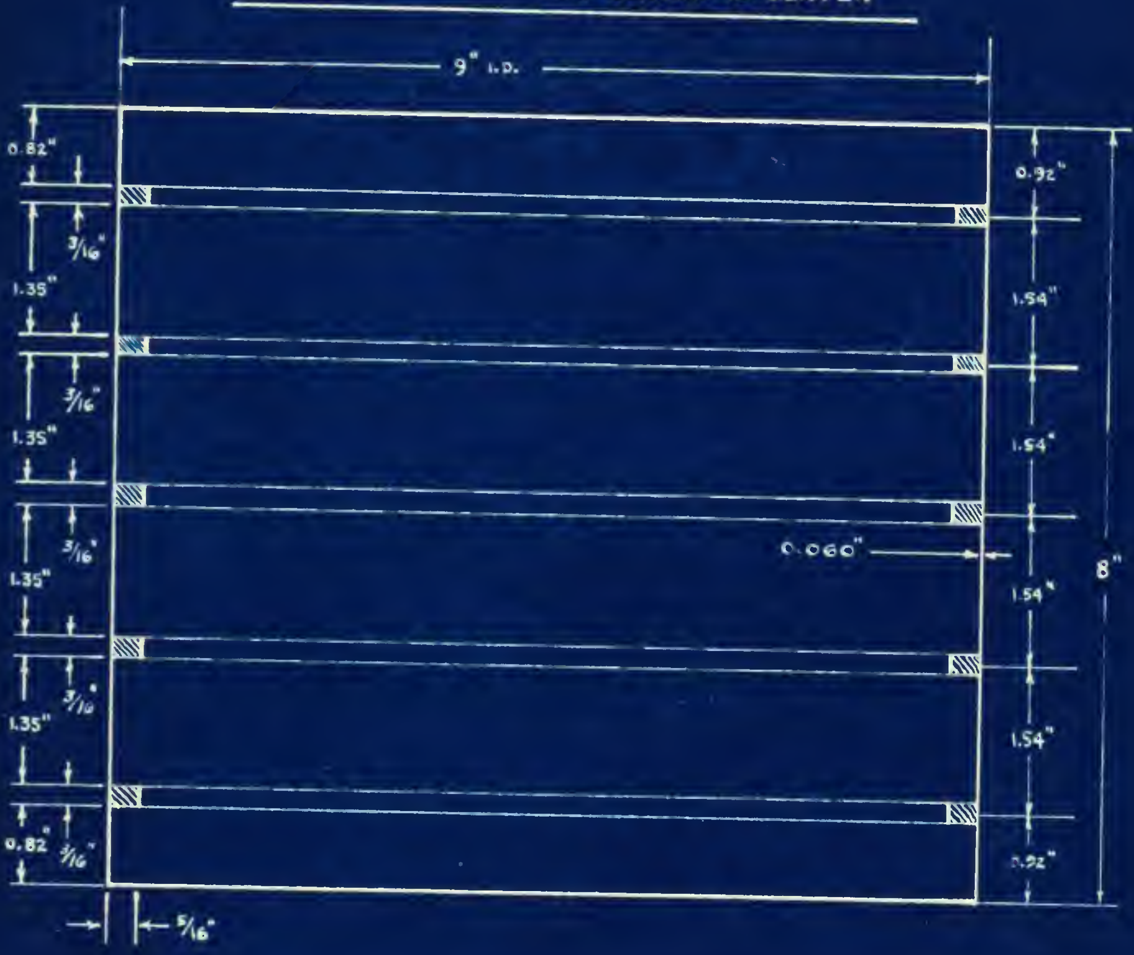

SCALE: 1" = 2"

3/17/51

fitted snug on the inside, and made with one butt. Shells, seam straps, and frames were permanently "welded" by use of ethylene dichloride solvent.

Model No. 52 maintains close geometric similarity with recent submarine practice, but the use of "Lucite" results in a λ value of 2.785 for Model No. 52 which is much higher than the λ for the steel prototype. Model No. 53 has the highest λ value of the quartet tested, 4.04; this value was as large as was felt practicable. Model No. 50 carries the minimum λ value of 1.73; the distance between frames is reduced in this model to 0.52".

Accordingly, the λ range covered by the four models tested is λ = 1.73 to λ = 4.04; this range is displaced in the direction of higher values of λ from the range which the authors would have liked to test.

All plastic submarine models were designed for use with one-piece "Lucite" end diaphragms which were to project into the shell for 3/8" and have a 1/8" x 9-1/8" integral end flange. The end diaphragms as built and used are shown in Figure VI.

Manufacture of Plastic Submarine Models

Four (4) "Lucite" submarine pressure hull sections were manufactured by Forest Products, Inc., Cambridge,

FIGURE VI

CONSTRUCTION, INSTALLATION & USE LUCITE CIRCULAR END DIAPHRAGMS

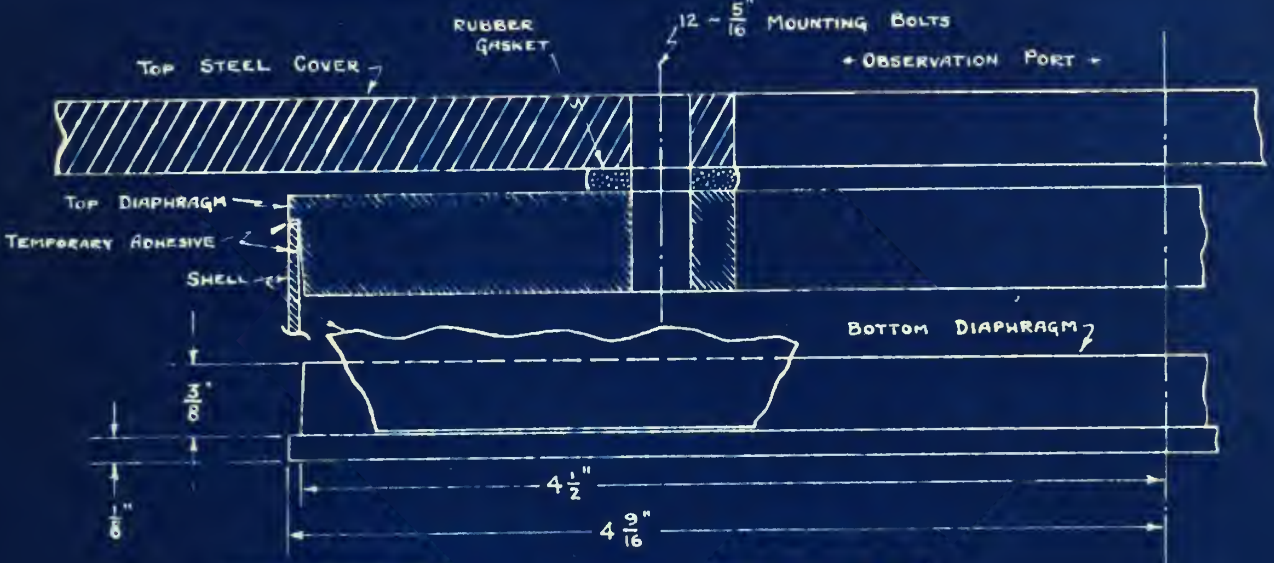

ARRANGEMENT ~ MODELS Nos 51-53

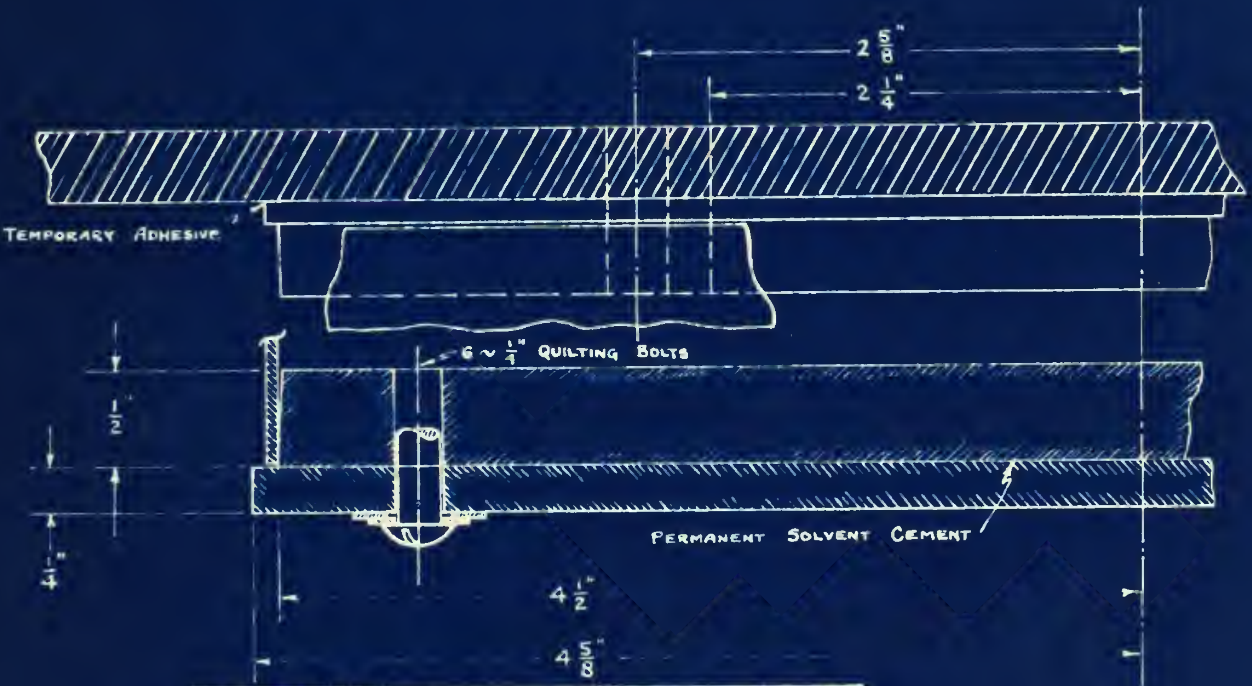

ARRANGEMENT ~ MODEL No 50

SCALE: FULL SIZE

JJ 4/24/51

Mass. The models were in accordance with Specification Sheets, Figures II-V, except as detailed on Figures XVII-XXII which show the diameters as built and the extra frames installed to suit the end diaphragms. The end diaphragms were built and used as detailed on Figure VI; note that, in order to save funds, one pair of end diaphragms was used on all models.

The model shells were formed from flat sheets which were heated, wrapped around a wooden mandrel, cooled, cut to size, and cemented. The frames were hot formed in a wooden jig to the size of the finished shell, and trimmed for a press fit. All frames were adjusted to size, positioned, and cemented in place by the authors.

Photograph No. 2 shows an exploded view of Model No. 53 as constructed prior to attachment to end diaphragms.

Appendix "B" contains further details concerning manufacture of the models, solvent, etc.

Design, Manufacture and Test of Steel Test Tank

The design of the testing tank and its attendant piping, vent, and valve arrangement can be readily understood from Figures VII and VIII, and Photograph No. 1. With the household main as the designed source of water pressure, the steel stresses were expected

Photograph No. 1

TEST APPARATUS

Test set-up showing tank used for submarine model tests, including piping, pump, recirculating line and connection to the water tap.

FIGURE VII

HYDROSTATIC TEST TANK ~ AS BUILT

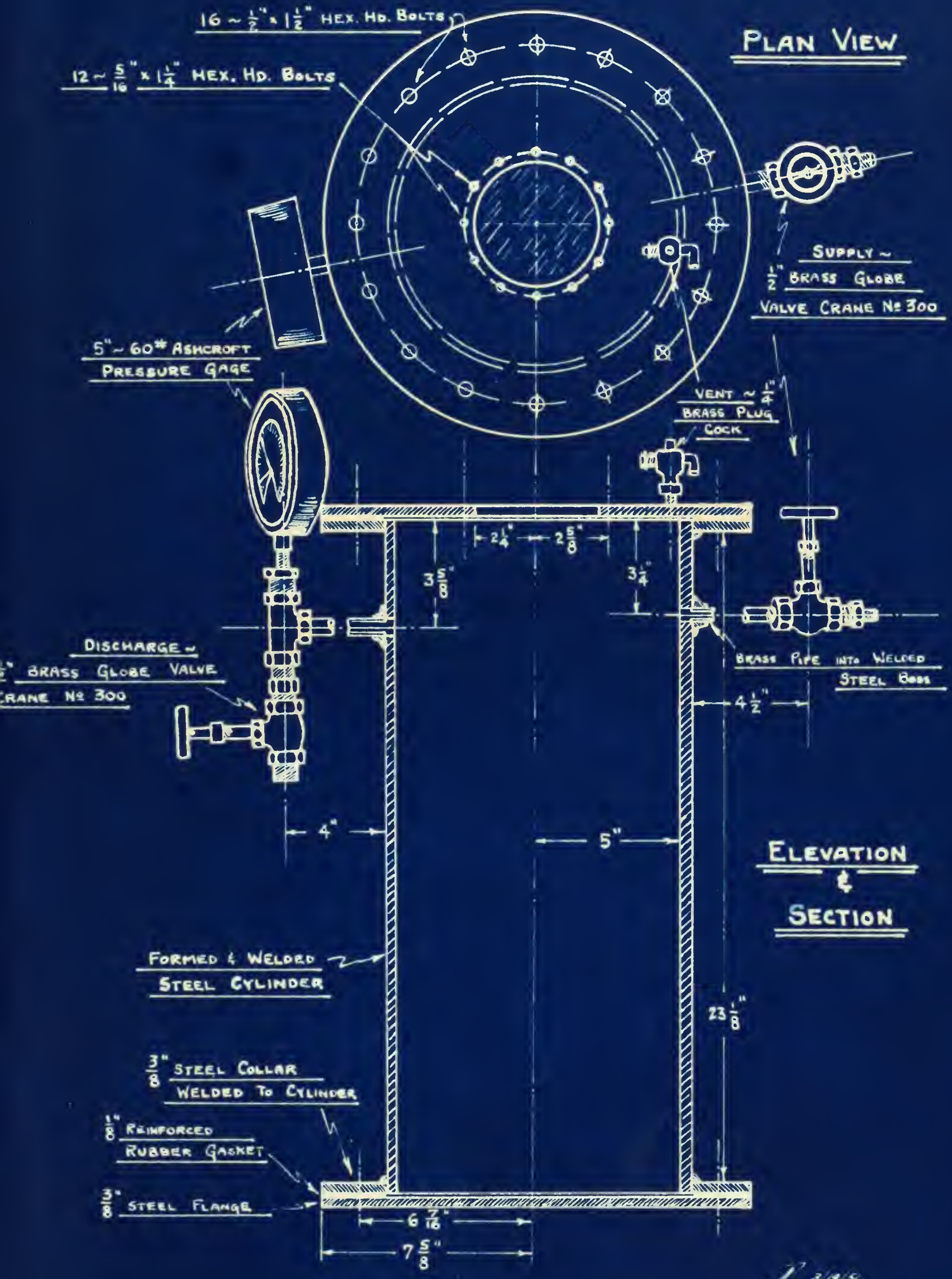

Photographs Nos. 2 & 3

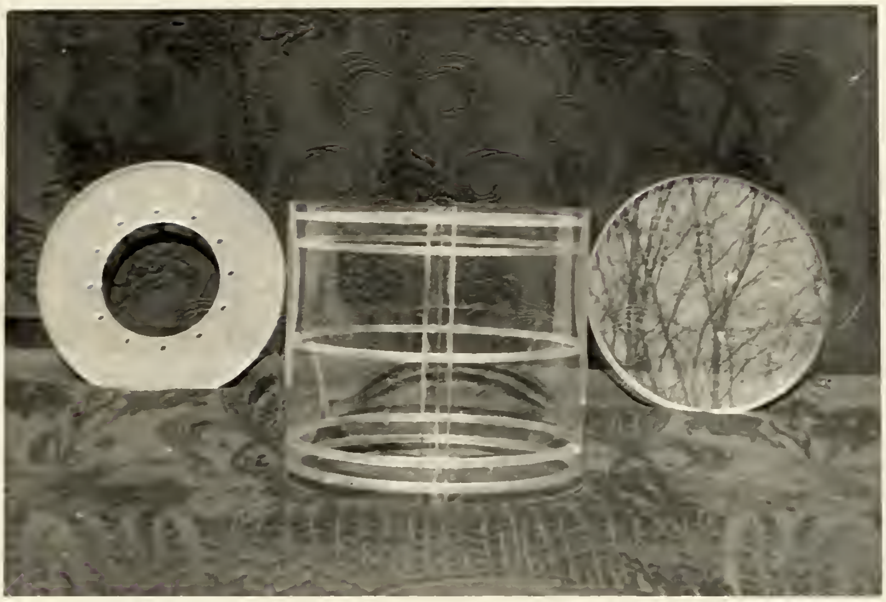

Model 53 before test showing end bulkheads before installation in model, and model frames including two extra frames used to help support end bulkheads in shear.

Model 53 after test showing dial gage set-up and model attached to end flange of test tank.

to be nominal. The tank was made by the Boston Naval Shipyard to a rough sketch furnished by the authors.

The Shipyard also furnished and calibrated the pressure gages used, and tested the assembled tank to 100 pounds per square inch gage.

Plastic Submarine Model Tests

The basic test set-up for hydrostatic test of plastic submarine models can be followed from Figures VII and VIII and Photograph No. 1. The initial step in the test of a model was to insert the end diaphragms into the reinforced shell; then mount the assembled model, complete with ends, upside down on the lower face of the upper steel flange of the test tank. The tank was next partially filled with water, the upper test tank flange together with model put in place, the tank filled with the vent open, and the upper tank flange securely bolted on (with the vent still open). The pressure control valve could then be opened wide, the guard valve cracked open, the supply valve opened, and the vent closed ready for test. Pressure on the model was controlled by gradual throttling of the pressure control valve.

During the tests of Models Nos. 50 and 53, two (2) diametrically mounted dial gages were mounted as

shown by Photograph No. 3 and by Figures VIII and IX. The normal test procedure was to build up the pressure at the rate of 2 pounds per square inch per minute, making continuous recordings of dial gage readings where mounted, and making continual examination of the model visually and by exploratory touch. In the event of minor leakage, a syphon tube was rigged, and the test continued without interruption. In the event of serious leakage, inexplicable cracking noises, etc., the pressure was dropped for careful examination of the model, including removal from the tank when appropriate.

Correlation and Evaluation of Plastic Submarine Model Test Data

The underlying basis chosen for attempting to correlate the plastic submarine model tests and experimental data from steel model tests is that of a non-dimensional plot such as the $\psi - \lambda$ plot of Figure XXXI.

No steel submarine model tests were contemplated under this thesis, and none were performed. In comparison with the case of steel columns, fewer steel submarine models have been tested, and - of those tested - not all test results are available in unclassified reports. The test spots shown on Figure XXXI represent the major portion of the results of scientific shown by Photographs 1a, 7 and in Figures VIII and IX. The normal test procedure was to [illegible] to the [illegible] at the rate of 2 passes per [illegible] per minute, making continuous recordings of tilt upon reaching [illegible], and making continual examination of the model visually and by exploratory touch. In the event of minor leakage, a [illegible] hole was [illegible], and the test continued without interruption. In the event of serious leakage, considerable spalling [illegible], etc., the pressure was dropped for careful examination of the model, including removal from the tank when appropriate.

Correlation and Comparison of Plastic Behavior Model Test Data

The underlying basis chosen for attempting to correlate the plastic behavior model tests and experimental data from steel model tests is that of a non-dimensional plot such as the ψ vs. [illegible] plot in Figure XXIII.

In other available model tests were standardized under this thesis, and were then performed. In conjunction with the work of [illegible], those other applicable models have been tested, and — at this writing — not all test results are available to the undersigned [illegible]. The test data shown in Figure XXIII represent the major portion of the [illegible] of [illegible]

FIGURE IX

MODELS 50 & 53 ~ DEFLECTION GAGES

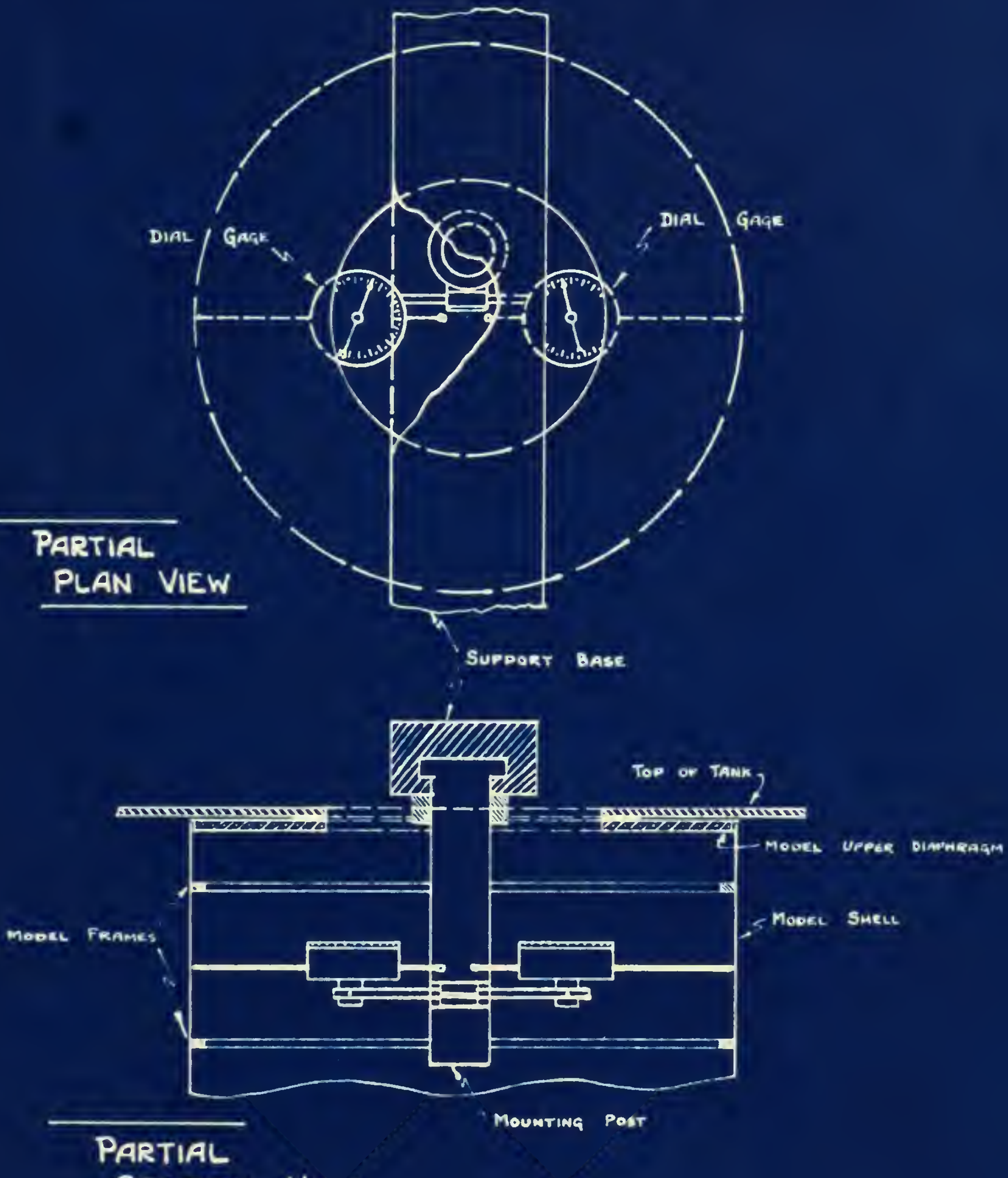

PARTIAL PLAN VIEW

PARTIAL SECTION VIEW

APPROXIMATE SCALE: 1" = 3"

DJ 4/24/51

steel submarine model tests to this date, and are considered to be the best available summary of steel model test data.

The major problem of correlation and evaluation, therefore, was to reduce the plastic submarine model data to a dimensionless form comparable to the steel data of Figure XXXI. In reducing and interpreting this data, the previous column data was drawn upon.

For further details concerning the correlation and evaluation of data, refer to "DISCUSSION OF RESULTS."

Evaluation of Thesis and Conclusions

The evaluation of the results of the thesis, and the conclusions, are justified by the "RESULTS" and are developed in the "DISCUSSION OF RESULTS." For such evaluation and conclusions, refer to "CONCLUSIONS" and "RECOMMENDATIONS."

IV.

RESULTS

All data presented in this section were obtained from tests conducted by the authors with the exception of the data on "Plexiglas" columns. The tests of "Plexiglas" columns recorded here were conducted by R.T. Miller during the summer of 1950 while at the David Taylor Model Basin. The data includes the results of over 23 column tests (10 by R.T. Miller) and 4 submarine model tests.

Figure X shows a comparison of the stress-strain curves of the various plastics tested in order to determine their relative merits for model tests.

Figures XI and XII give values of the tangent modulus and the reduced modulus for "Lucite," and the stress-strain curve upon which these values were based. Figures XIII and XIV give similar data for "Plexiglas."

Figure XV shows the buckling stresses for the "Lucite columns plotted against the length to gyradius ratio of the columns. Superimposed upon the test data and the curve of experimental data are two curves showing the buckling stress as calculated by Euler's column formulas. These curves will be discussed in detail in

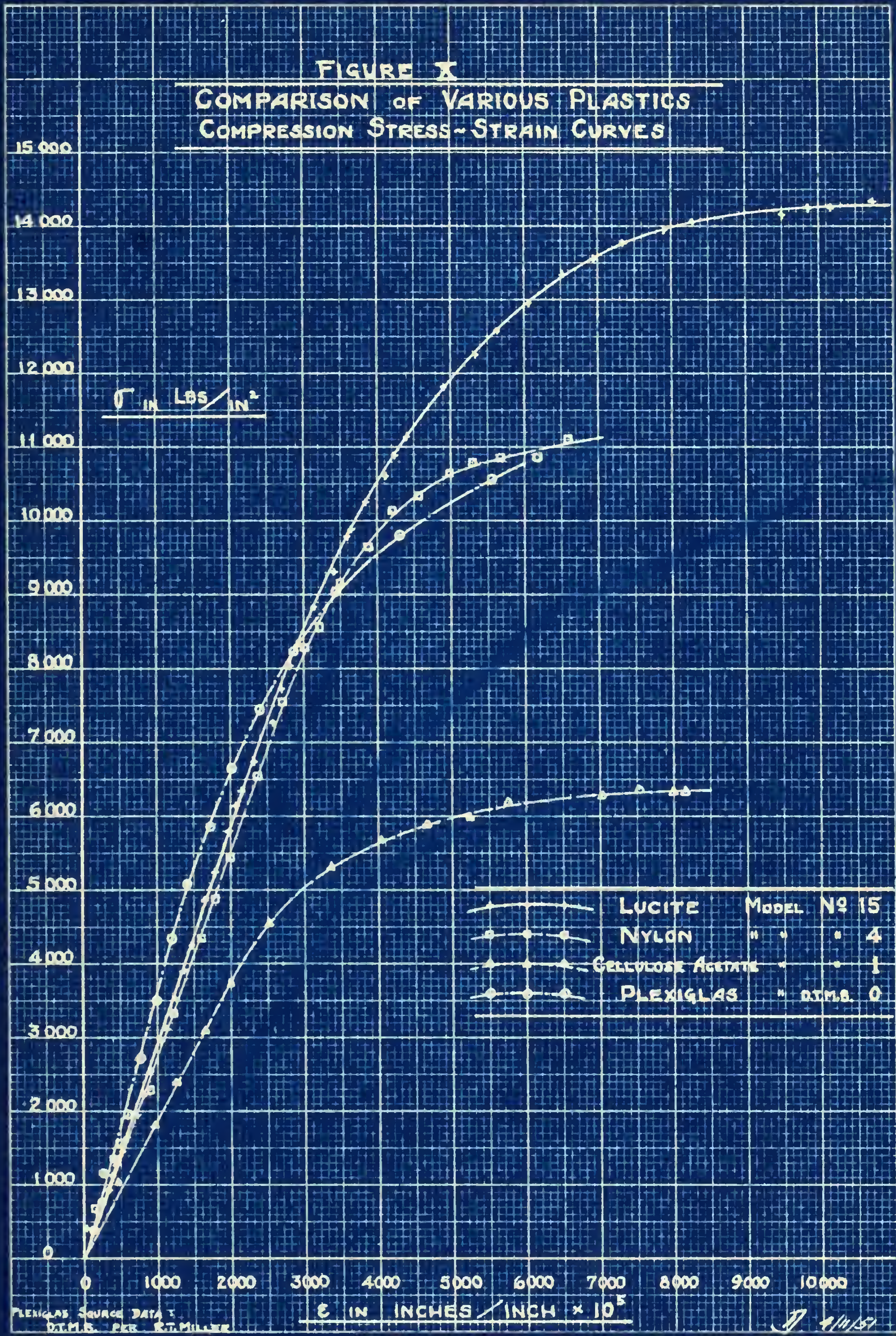

FIGURE X
COMPARISON OF VARIOUS PLASTICS
COMPRESSION STRESS-STRAIN CURVES
σ IN LBS/IN²
15 000
14 000
13 000
12 000
11 000
10 000
9 000
8 000
7 000
6 000
5 000
4 000
3 000
2 000
1 000
0
0
1000
2000
3000
4000
5000
6000
7000
8000
9000
10 000
ε IN INCHES/INCH × 10⁵
LUCITE MODEL Nº 15
NYLON " " " 4
CELLULOSE ACETATE " " 1
PLEXIGLAS " D.T.M.B. 0
PLEXIGLAS SOURCE DATA: D.T.M.B. PER R.T. MILLER
4/11/51

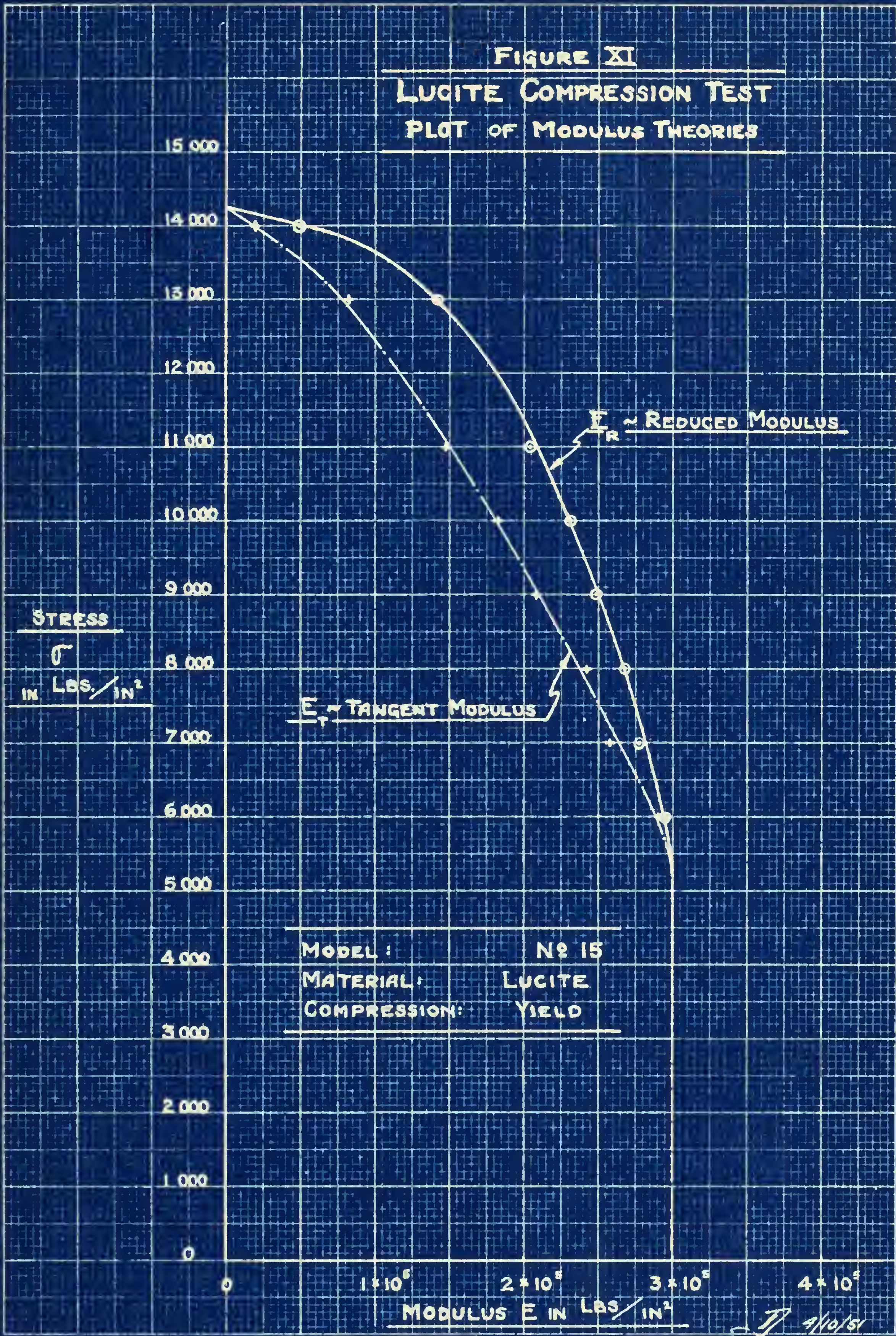

FIGURE XI
LUCITE COMPRESSION TEST
PLOT OF MODULUS THEORIES
15 000
14 000
13 000
12 000
11 000
10 000
9 000
8 000
7 000
6 000
5 000
4 000
3 000
2 000
1 000
0
STRESS
σ
IN LBS./IN²
E_R ~ REDUCED MODULUS
E_T ~ TANGENT MODULUS
MODEL: Nº 15
MATERIAL: LUCITE
COMPRESSION: YIELD
0
1×10⁵
2×10⁵
3×10⁵
4×10⁵
MODULUS E IN LBS/IN²
4/10/51

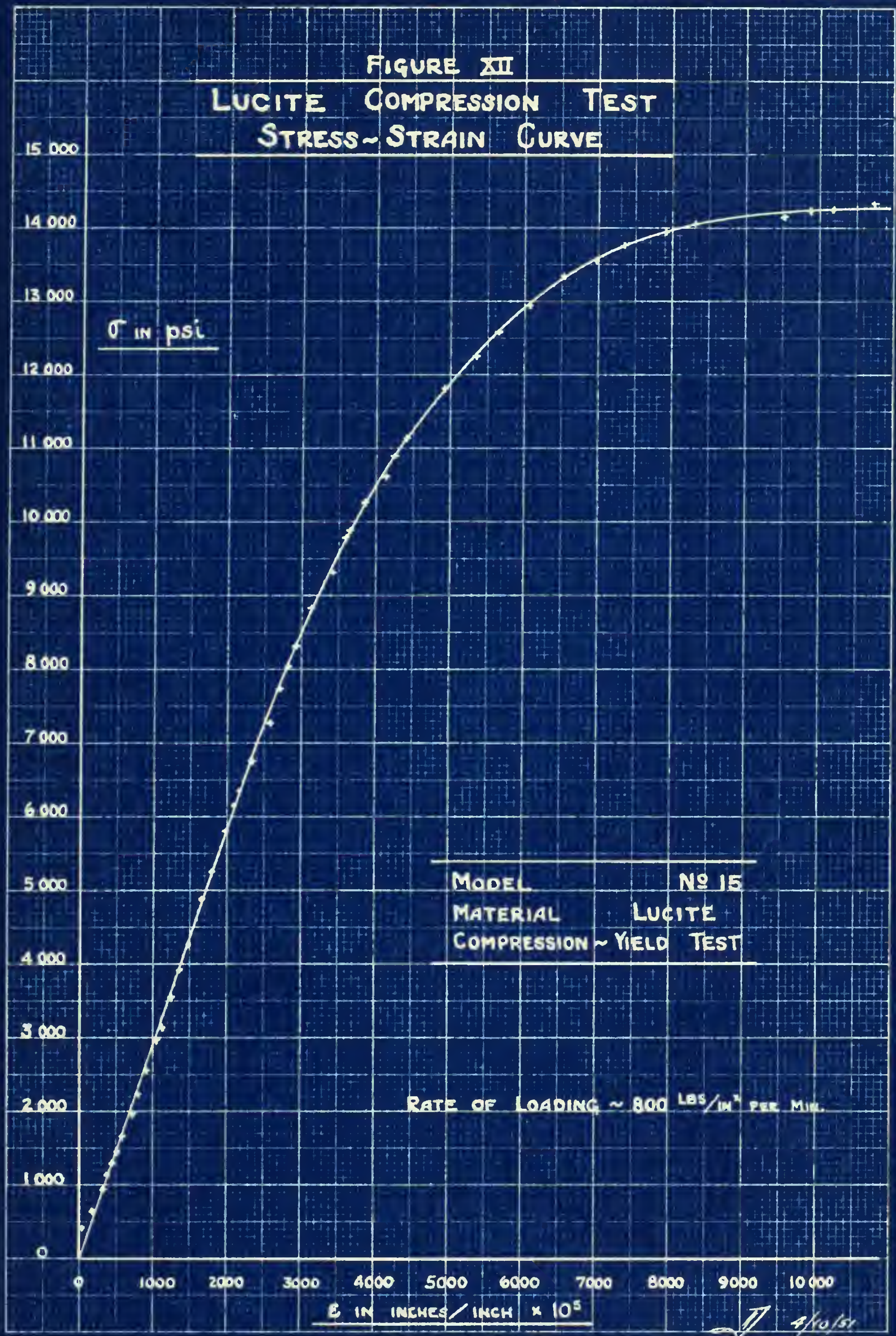
FIGURE XII
LUCITE COMPRESSION TEST
STRESS ~ STRAIN CURVE
σ IN psi
15 000
14 000
13 000
12 000
11 000
10 000
9 000
8 000
7 000
6 000
5 000
4 000
3 000
2 000
1 000
0
0
1000
2000
3000
4000
5000
6000
7000
8000
9000
10 000
ε IN INCHES / INCH × 10^5
MODEL Nº 15
MATERIAL LUCITE
COMPRESSION ~ YIELD TEST
RATE OF LOADING ~ 800 LBS/IN² PER MIN.
4/10/51

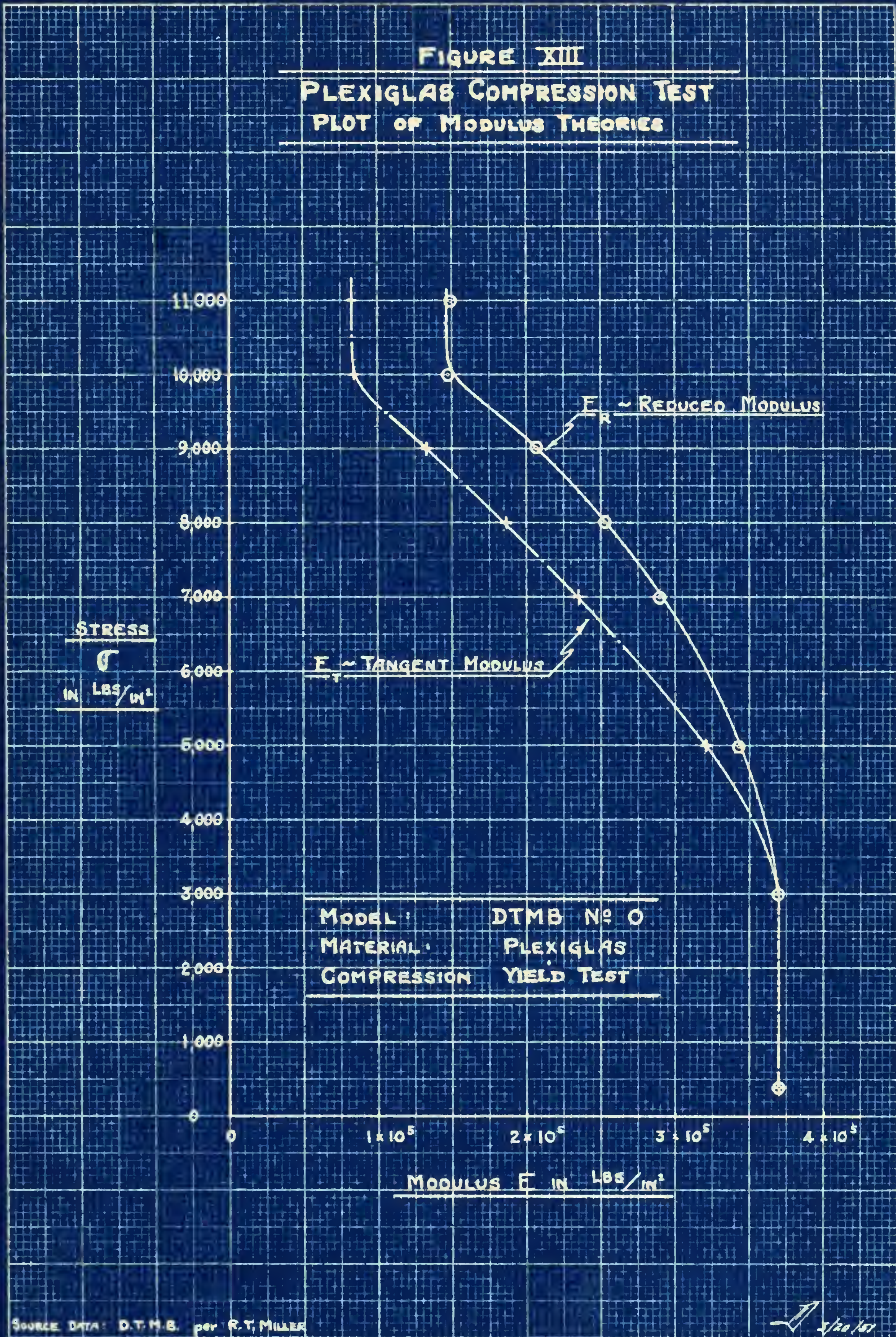
FIGURE XIII
PLEXIGLAS COMPRESSION TEST
PLOT OF MODULUS THEORIES
E_R ~ REDUCED MODULUS
E_T ~ TANGENT MODULUS
STRESS
σ
IN LBS/IN²
11,000
10,000
9,000
8,000
7,000
6,000
5,000
4,000
3,000
2,000
1,000
0
0
1×10⁵
2×10⁵
3×10⁵
4×10⁵
MODULUS E IN LBS/IN²
MODEL: DTMB Nº O
MATERIAL: PLEXIGLAS
COMPRESSION YIELD TEST
SOURCE DATA: D.T.M.B. per R.T. MILLER
3/20/57

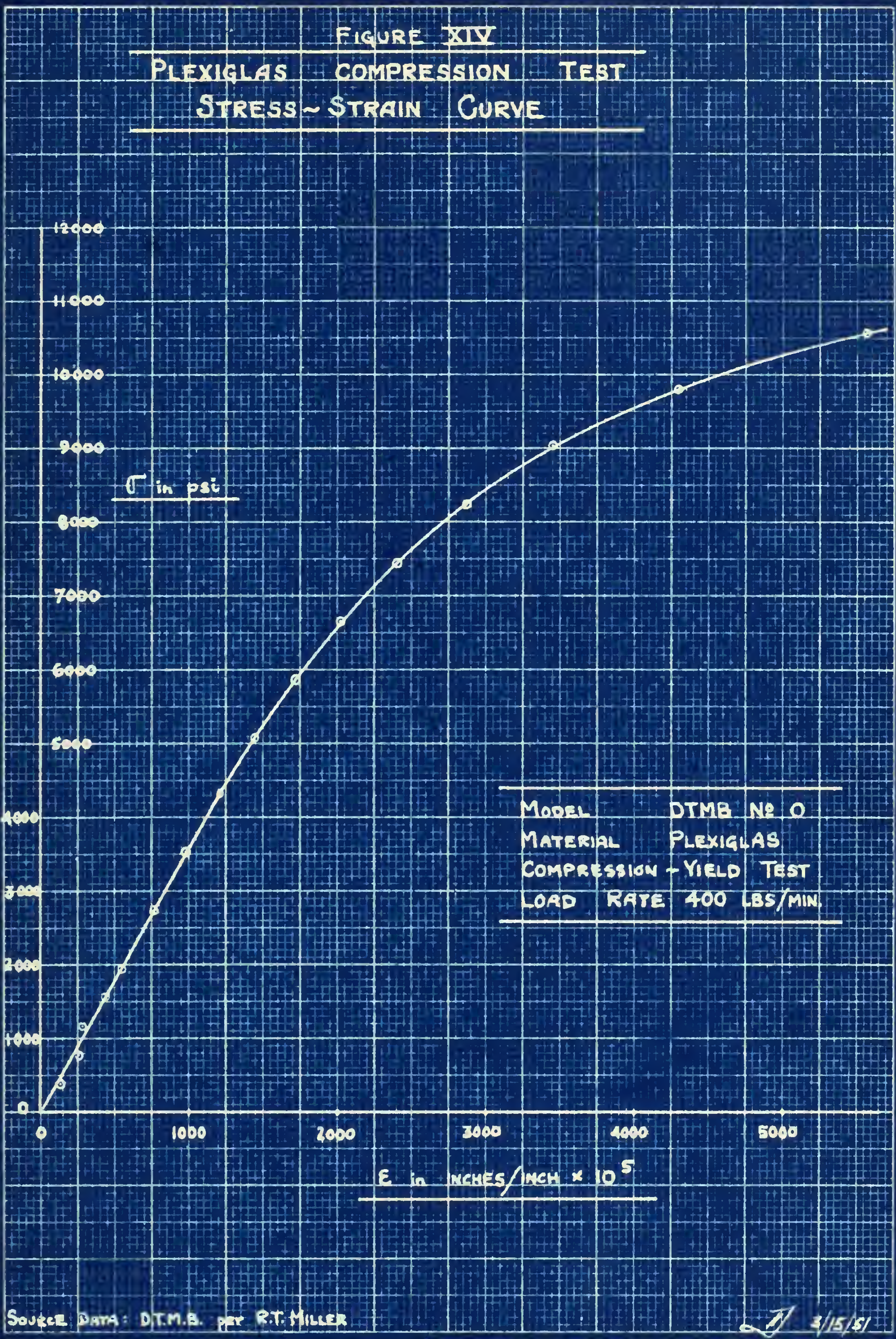

FIGURE XIV
PLEXIGLAS COMPRESSION TEST
STRESS ~ STRAIN CURVE
12000
11000
10000
9000
8000
7000
6000
5000
4000
3000
2000
1000
0
σ in psi
0
1000
2000
3000
4000
5000
ε in INCHES/INCH × 10^5
MODEL DTMB № 0
MATERIAL PLEXIGLAS
COMPRESSION - YIELD TEST
LOAD RATE 400 LBS/MIN.
SOURCE DATA: D.T.M.B. per R.T. MILLER
3/15/51

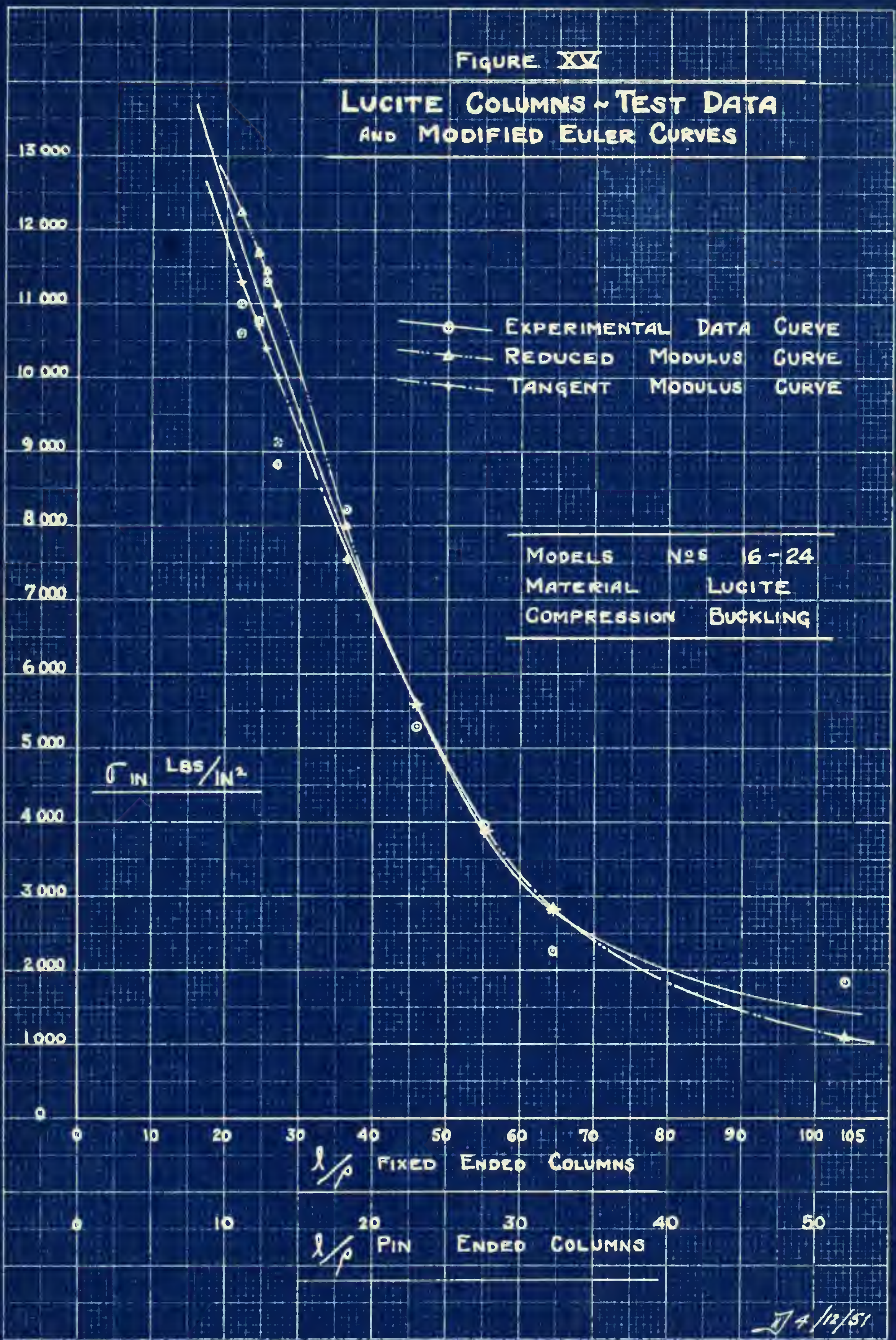

FIGURE XV
LUCITE COLUMNS ~ TEST DATA
AND MODIFIED EULER CURVES
13 000
12 000
11 000
10 000
9 000
8 000
7 000
6 000
5 000
4 000
3 000
2 000
1 000
0
EXPERIMENTAL DATA CURVE
REDUCED MODULUS CURVE
TANGENT MODULUS CURVE
MODELS Nos 16 - 24
MATERIAL LUCITE
COMPRESSION BUCKLING
σ IN LBS/IN²
0
10
20
30
40
50
60
70
80
90
100
105
l/ρ FIXED ENDED COLUMNS
0
10
20
30
40
50
l/ρ PIN ENDED COLUMNS
4/12/51

Section V, "DISCUSSION OF RESULTS." Figure XVI is a similar plot of the results of the "Plexiglas" column tests.

All data used to develop the plots shown in the Figures discussed above are tabulated in Appendix "C".

Figures XVII-XXIII, and Tables I-V give the results of the tests of four "Lucite" models of submarine pressure hulls. For each model tested there has been included a photograph of the model before and after test, a tabulation of the test data taken, and sketches showing details of the location, size, and shape of the failure. The sketches and tables are essentially self-explanatory.

The phenomenon of crazing which is detailed in Figure XIX, appeared as a maze of small scratches which were particularly noticeable when the model was held in certain positions under strong lighting. The crazing which was very apparent along the frame line immediately after the test, as shown in Figure XIX, completely disappeared after the model stood idle for several days. This phenomenon is discussed more fully in later sections of this thesis.

Test A of Model No. 52 was stopped due to excessive leakage from butt strap. When the model was removed from

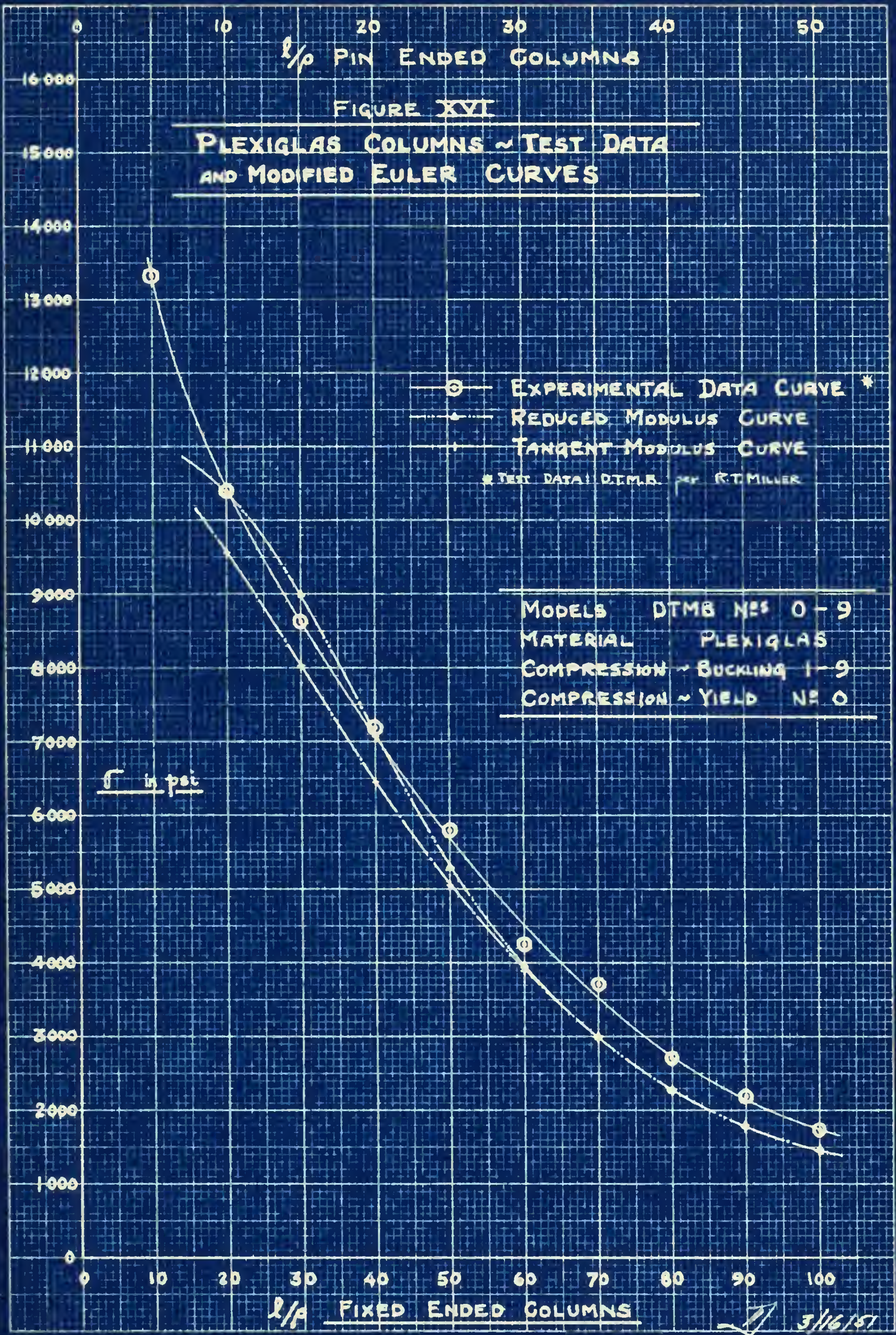

l/ρ PIN ENDED COLUMNS
FIGURE XVI
PLEXIGLAS COLUMNS ~ TEST DATA
AND MODIFIED EULER CURVES
EXPERIMENTAL DATA CURVE *
REDUCED MODULUS CURVE
TANGENT MODULUS CURVE
* TEST DATA: D.T.M.B. per R.T. MILLER
MODELS DTMB Nos 0 - 9
MATERIAL PLEXIGLAS
COMPRESSION ~ BUCKLING 1 - 9
COMPRESSION ~ YIELD No 0
σ in psi
l/ρ FIXED ENDED COLUMNS
3/16/51

Table No. I

Summary Of Tests Of Lucite Submarine Models

All Models 9" in Dia., 1/16" Thick

Model	Length Betw. Frames	Collapse Pressure	ψ	λ_1	λ_2
50	0.52"	58 psi	.417	1.73	1.66
51	0.93"	68 psi	.545	2.31	2.21
52	1.35"	37 psi	.297	2.785	2.66
53	2.84"	16 psi	.127	4.04	3.86

$\psi = \dfrac{P}{(h/R)\,\sigma_{y.p}}$

$R = 4.5''$

P = Column 3

$\sigma_{y.p.} = 9000$ psi

For λ_1, $E = 300{,}000$ psi

For λ_2, $E = 327{,}000$ psi

$\lambda = \sqrt[4]{\dfrac{(L/2R)^2}{(h/2R)^3}} \cdot \sqrt{\dfrac{\sigma_{y.p.}}{E}}$

$h = 1/16''$

L = Column 2

Model 50 Before Testing

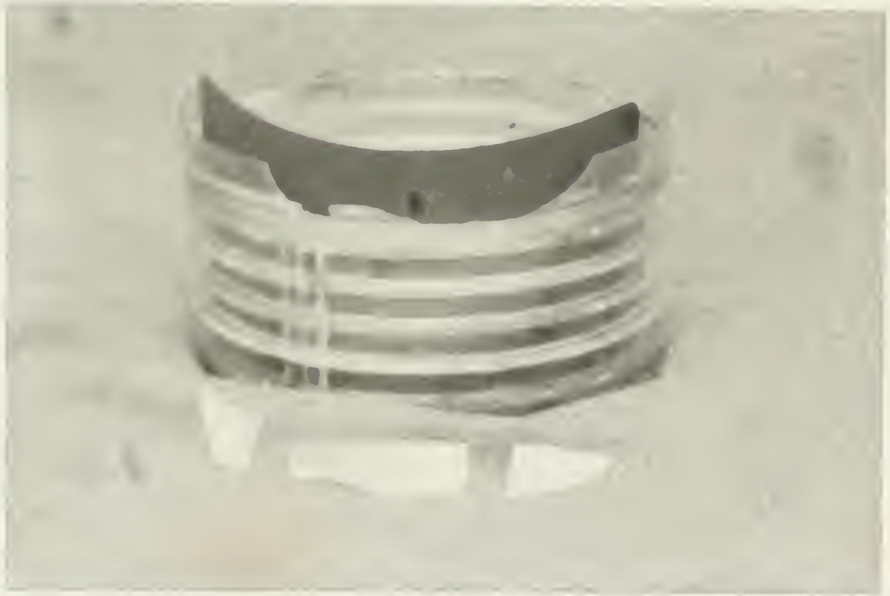

Model 50 After Testing - showing pieces of broken shell. Note: Picture shows butt strap construction used on all models.

Photographs Nos. 4 & 5

FIGURE XVII

MODEL Nº 50 ~ DETAIL OF FAILURE

PARTIAL EXPANSION SHOWING LOCATION OF FAILURE.

DIMENSIONS OF MODEL AS BUILT AND TESTED:

FRAMING – 3/16" × 5/16"

0.52" BETWEEN FRAMES

AVERAGE SHELL THICKNESS – 0.0625"

" INSIDE DIAMETER – 9.03"

" " " , TOP – 9.02"

" " " , BOTTOM – 9.05"

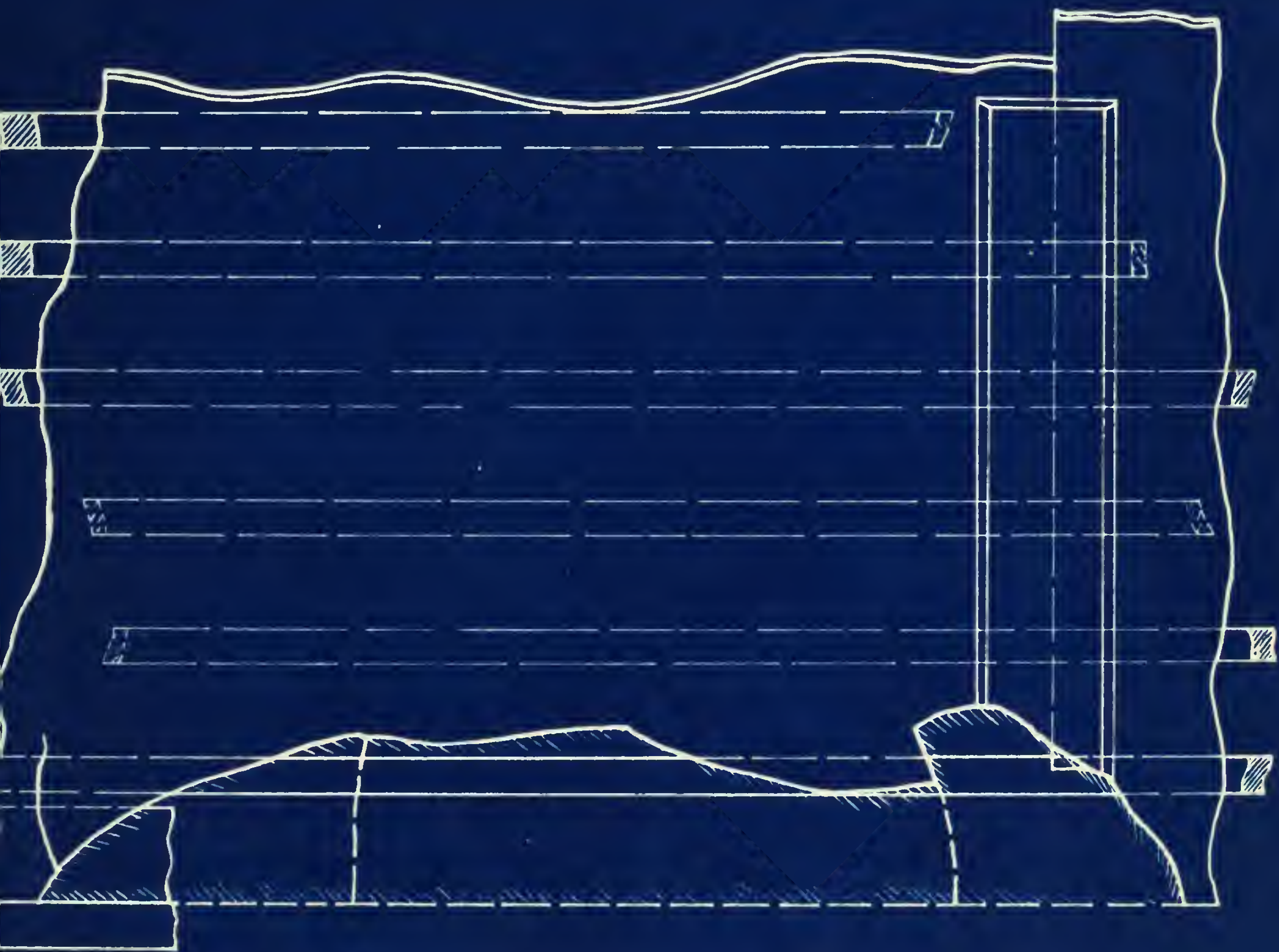

SCALE: FULL SIZE

JD 4/21/51

Table No. II

Test of Lucite Submarine Model No. 50

Tests By E. F. Durfee and V. D. Johnson

Length Between Frames – 0.52"

Diameter – 9.0"

Thickness – 1/16 inch

Rate of Loading – 2 psi/min

Temp of Water – 60°F (Both Tests)

Test A — 31 Mar. 1951 | Test D — 2 Apr. 1951

Hydro. Press.	Defl. Reading	Actual Defl.	Hydro. Press.	Defl. Reading	Actual Defl.
3 psi	1/2/+1.4	.12140"	3 psi	3/1/+2.95	.31295"
5	1/2/+2.7	.12270"	5	3/1/+2.95	.31295
7	1/2/+2.74	.12274"	7	3/1/+3.01	.31301
10	1/2/+2.90	.12290"	9	3/1/+3.46	.31346
14	1/3/-4.83	.12517"	11	3/1/+4.36	.31436
17	1/3/+0.56	.13056	13	3/1/-4.61	.31539
20.5	1/4/-4.13	.13587	15	3/1/-3.73	.31427
23	1/4/+0.57	.14057	18	3/1/-2.66	.31734
25	1/4/+4.30	.14430	20	3/1/-1.51	.31849
27	1/5/-2.41	.14769	22	3/1/-0.77	.31933
30	1/5/+3.56	.15356	24	3/2/+0.05	.32005
33	1/6/-0.40	.15960	26	3/2/+1.08	.32108
35	1/6/+1.46	.16146	28	3/2/+1.92	.32192
37	1/6/+2.02	.16202	30	3/2/+2.80	.32280
40	1/6/+2.28	.16228	32	3/2/+3.82	.32382
42	1/6/+2.63	.16263	34	3/2/+4.67	.32467
44	1/6/+2.66	.16266	36	3/2/-4.47	.32553
46	1/6/+2.67	.16267	38	3/2/-3.60	.32640
48	1/6/+2.82	.16282	40	3/2/-2.50	.32750
50	1/6/+2.82	.16282	42	3/2/-1.28	.32872
52	1/6/+3.17	.16317	44	3/3/+0.40	.33040
At 52 psi, Excessive Leakage at Upper Seam Stopped Test			46	3/3/+2.00	.33200
			46	3/3/+2.45	.33245
			48	3/3/+4.01	.33401
			50	3/3/+4.80	.33480
			52	3/3/-4.18	.33582
			54	3/3/+4.92	.33492
			56	3/3/+4.42	.33442
			58	Failure of Model See Following Page For Details	

Note: Tests "B" And "C" Were Terminated By Excessive Leakage From Seam On End Bulkhead. At End of Test "A", Examination Showed Lip On End Bulkhead Sheared Off. End Bulkhead Repaired Before Tests B, C And D.

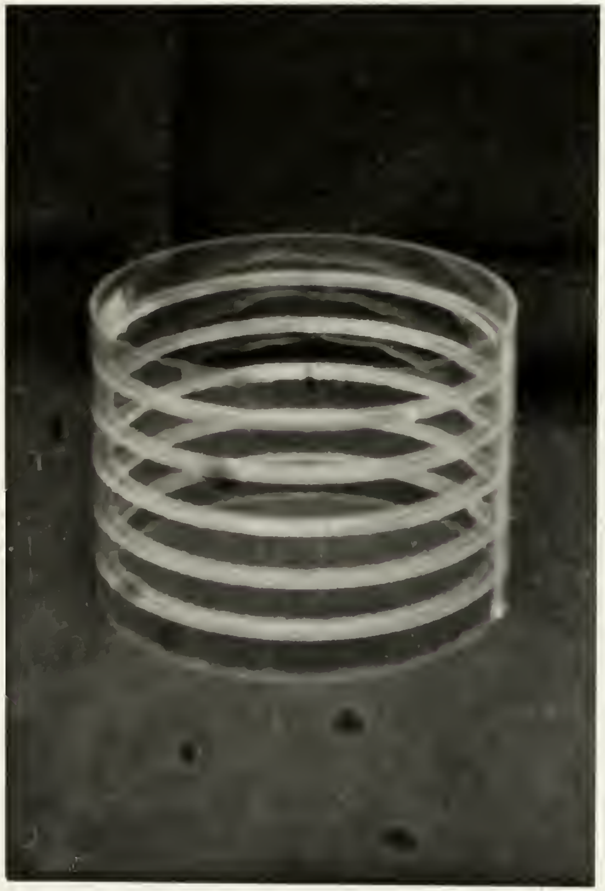

Model 51 Before Test

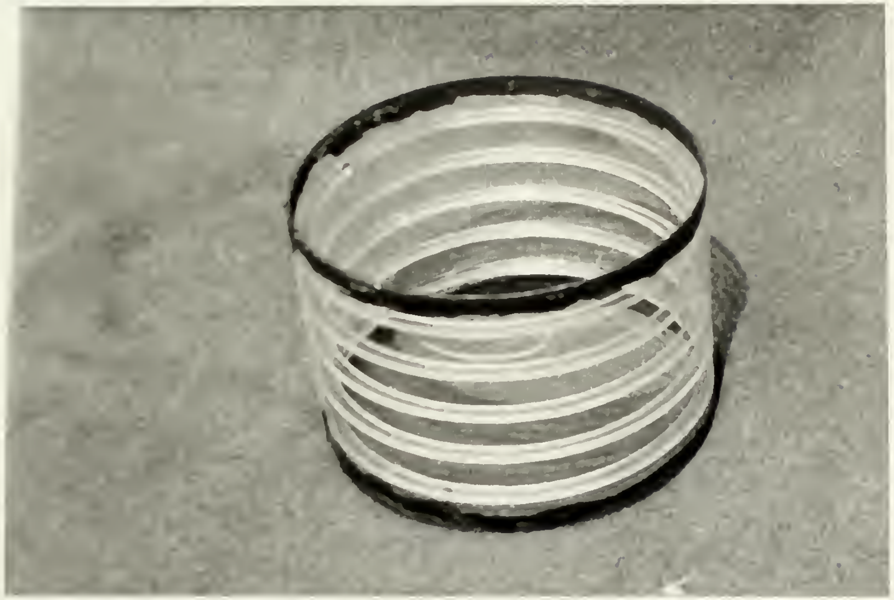

Model 51 After Test - showing fracture in first complete frame space from top and well clear of seam.

Photographs Nos. 6 & 7

Figure XVIII

Model № 51 ~ Detail of Failure

Partial Expansion Showing Location of Failure, and Approximate Shape of Critical Lobe.

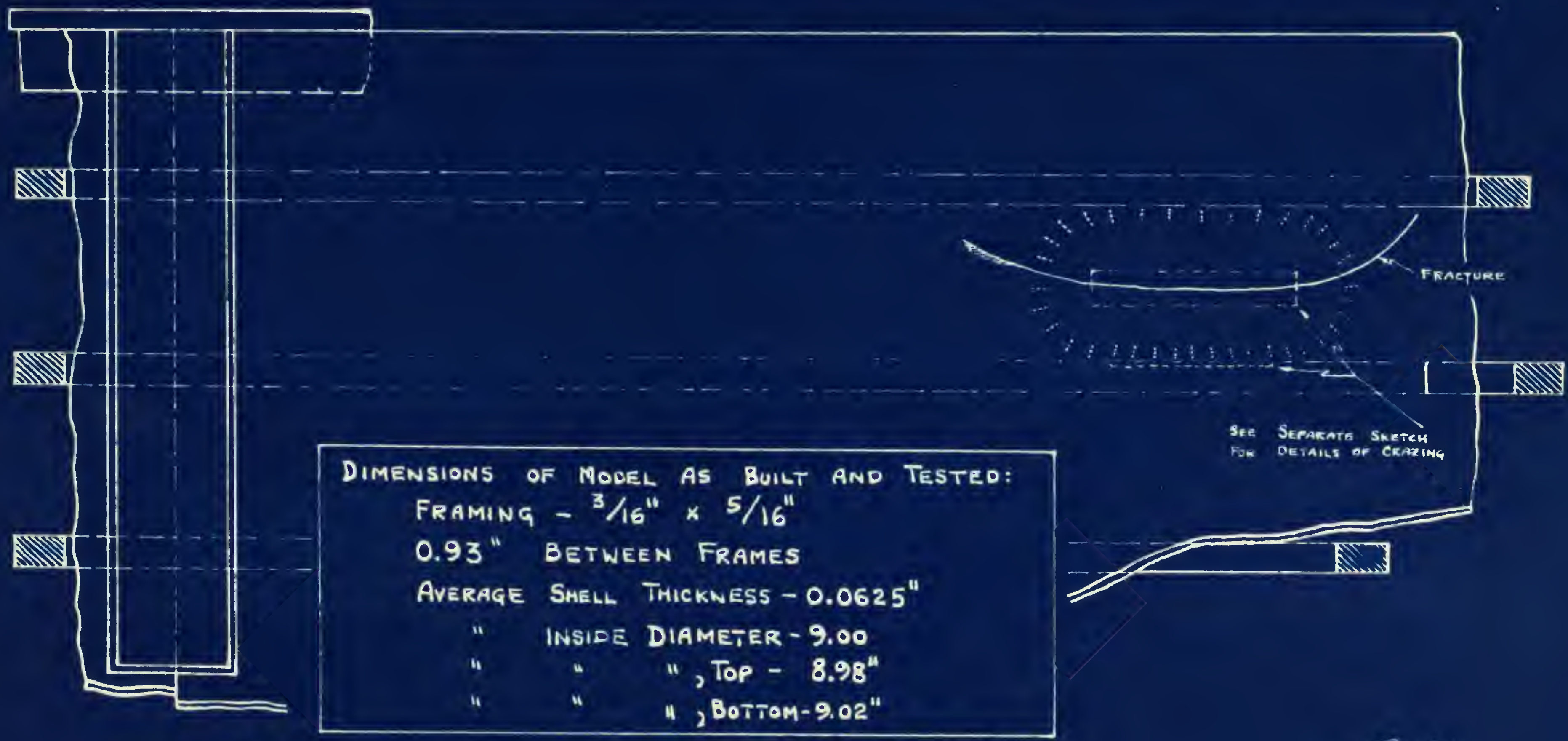

Scale : Full Size

FIGURE XIX

MODEL No 51 ~ DETAIL OF CRAZING

CRAZING ALONG FRACTURE IS ON INNER (TENSION) SIDE OF SHELL.

CRAZING ON EDGE OF FRAME SKETCHED AS OBSERVED IMMEDIATELY ON FINISH OF TEST ~ THIS CRAZING DISAPPEARED PRIOR TO DEFINITE LOCATION AS TO SIDE OF SHELL.

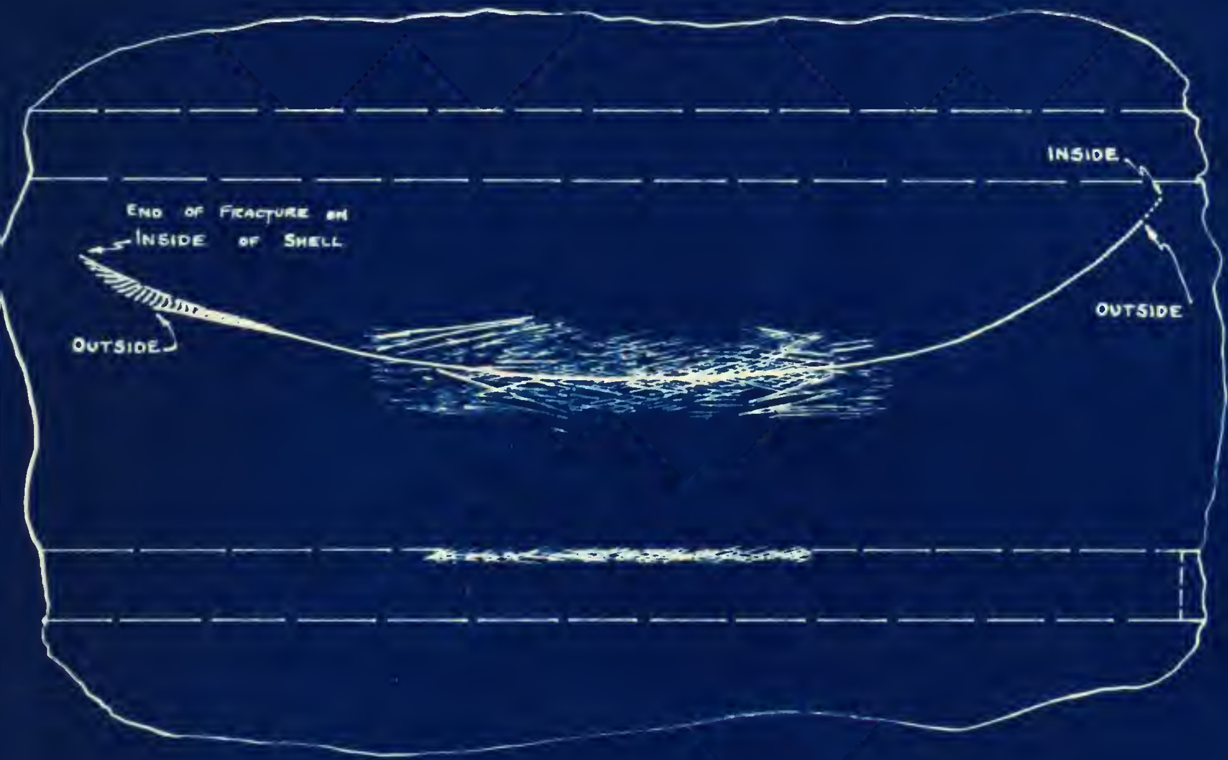

SCALE: $1'' = \frac{1}{2}''$

4/21/51

Table No. III

Test of

Lucite Submarine Model No. 51

Test By E. F. Durfee Jr. and V. D Johnson

30 Mar. 1951

Length Between Frames – 0.93"

Diameter – 9.0"

Thickness – 1/16 inch

Temp. of Water – 57.0°F

Test
Load Applied at Rate of 2 psi./min Hydrostatic Pressure
At 36 psi., Leak at Bottom Butt Strap
At 68 psi. Could Feel 1½" to 2" Lobes
At 68 psi, Failure See other Pages For Details

Model 52 Before Test - with
end bulkheads installed but
not secured with adhesive.

Model 52 After Test - showing
failure in second frame space
from bottom.

Photographs Nos. 8 & 9

Figure XX

Model № 52 ~ Detail of Failure

Partial Expansion Showing Location of Failure

Also Shown: Location of 2 Extra 3/16" x 5/16" Frames Cemented to Shell to Support End Diaphragms.

Dimensions of Model as Built and Tested:

Framing – 3/16" x 5/16"

1.35" Between Frames

Average Shell Thickness – 0.0625"

" Inside Diameter – 8.96"

" " " , Top – 8.97"

" " " , Bottom – 8.95"

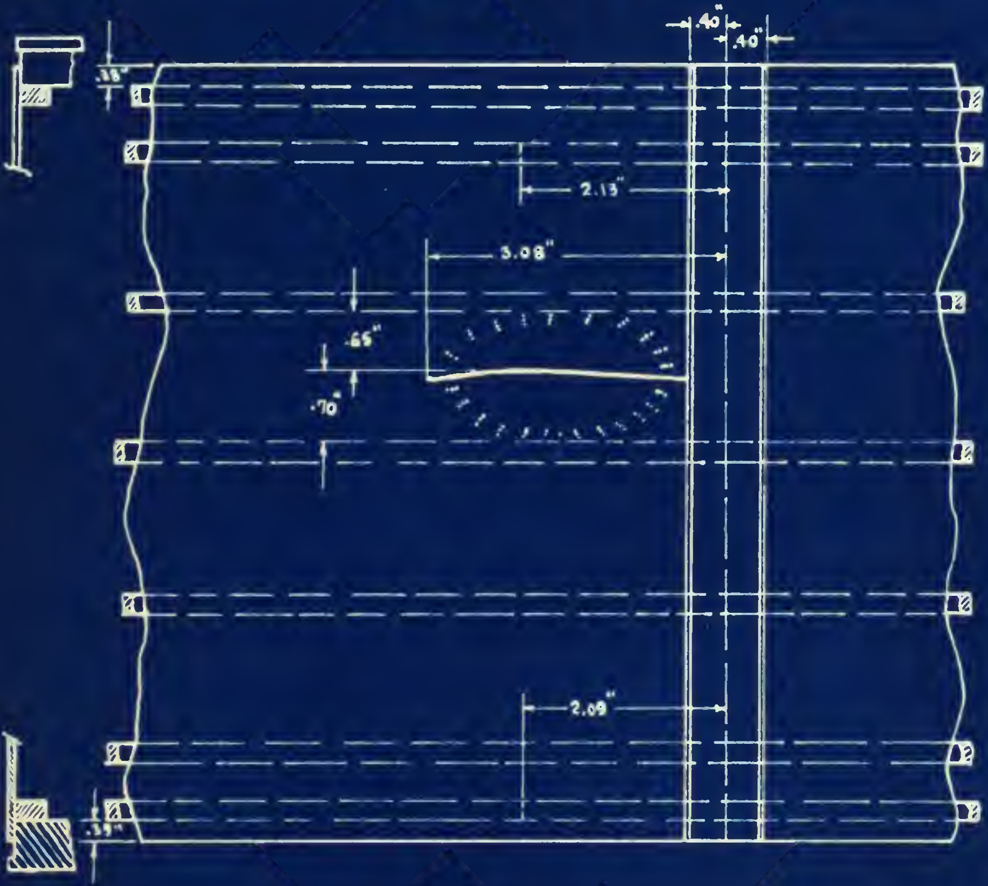

Scale : 1" = 2"

D 4/12/51

FIGURE XXI

MODEL № 52 ~ DETAIL OF FRACTURE

EXPANSION OF FRACTURE TO ACTUAL SIZE AND SHAPE

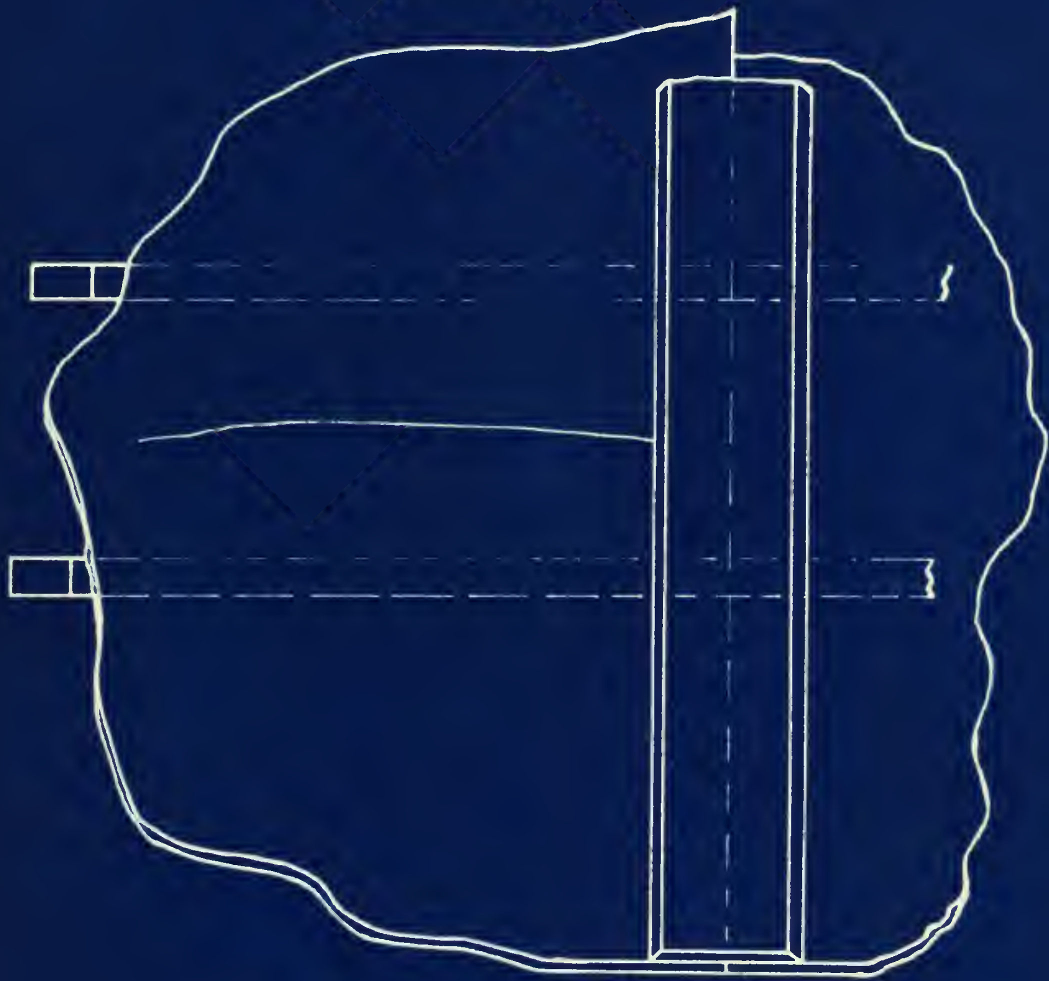

SCALE : FULL SIZE

4/12/51

Table No. IV

Test Of

Lucite Submarine Model No. 53

Test By E. F. Durfee Jr. and V. D. Johnson

30 Mar. 1951

Length Between Frames – 2.84"

Diameter – 9.0"

Rate of Loading – 1 psi/min

Thickness – 1/16 inch

Temp. of Water – 60.5°F

Hydro. Press.	Defl. Reading #1	Defl. Reading #2	Defl. Gage #1	Defl. Gage #2
0 psi	1/3/+0.50	-3.5	.13050"	-.0035"
1 1/4	1/2/-1.26	+8.5	.12874	+.0085
2 1/2	1/2/-3.85	+11.8	.12615	+.0115
3 3/4	1/1/+3.33	-14.5	.11333	+.0155
5	1/1/+3.31	-13.2	.11331	.0168
5 1/2	1/1/+3.30	-12.4	.11330	.0176
6	1/1/+3.72	-11.8	.11372	.0182
6 1/2	1/2/+4.18	-11.7	.12418	.0183
7	1/2/-4.80	-11.5	.12520	.0185
7 1/2	1/2/-4.00	-11.4	.12600	.0186
8	1/2/-3.10	-11.1	.12690	.0189
8 1/2	1/2/-2.50	-11.0	.12750	.0190
9	1/2/-1.20	-10.5	.12880	.0195
9 1/2	1/2/-0.40	-10.5	.12960	.0195
10	1/2/+0.86	-10.3	.13086	.0197
10 1/2	1/2/+2.10	-9.9	.13210	.0200
11	1/2/+3.08	-9.8	.13308	.0202
11 1/2	1/2/+3.09	-9.7	.13309	.0203
12	1/2/+4.92	-9.7	.13492	.0203
12 1/2	1/3/-1.80	-9.3	.13820	.0207
13	1/3/+2.00	-9.0	.14200	.0210
13 1/2	1/4/-3.90	-9.0	.14600	.0210
14	1/5/-5.00	-8.9	.15500	.0211
14 1/2	1/5/+4.04	-8.9	.15404	.0211
15	2/4/+2.80	-8.2	.24280	.0218
15 1/2	2/6/+2.50	-5.6	.26250	.0244
* 16	2/7/-1.00	-4.5	.27900	.0265

Columns 3 and 5, and 2 and 4 Above, Give The Dial Gage Readings and the Corresponding Actual Deflections in Inches Respectively

* Model Failed, See Other Pages For Details

Model 53 Before Testing - end bulkheads in place. Upper bulkhead shows bolt circle for attachment to test tank.

Model 53 After Testing - showing piece blown into model during test. Picture shows upper flange of test tank with model bolted in place.

Photographs Nos. 10 & 11

Figure XXII

Model № 53 ~ Detail of Failure

Partial Expansion Showing Location of Failure, And Shape of Critical Lobe Blown Into Cylinder. Also Shown: Location of 2 Extra $3/16" \times 5/16"$ Frames Cemented to Shell to Support End Diaphragms.

Dimensions of Model as Built and Tested:

Framing – $3/16" \times 5/16"$

2.84" Between Frames

Average Shell Thickness – 0.0625"

" Inside Diameter – 9.00"

" " " , Top – 8.98"

" " " , Bottom – 9.04"

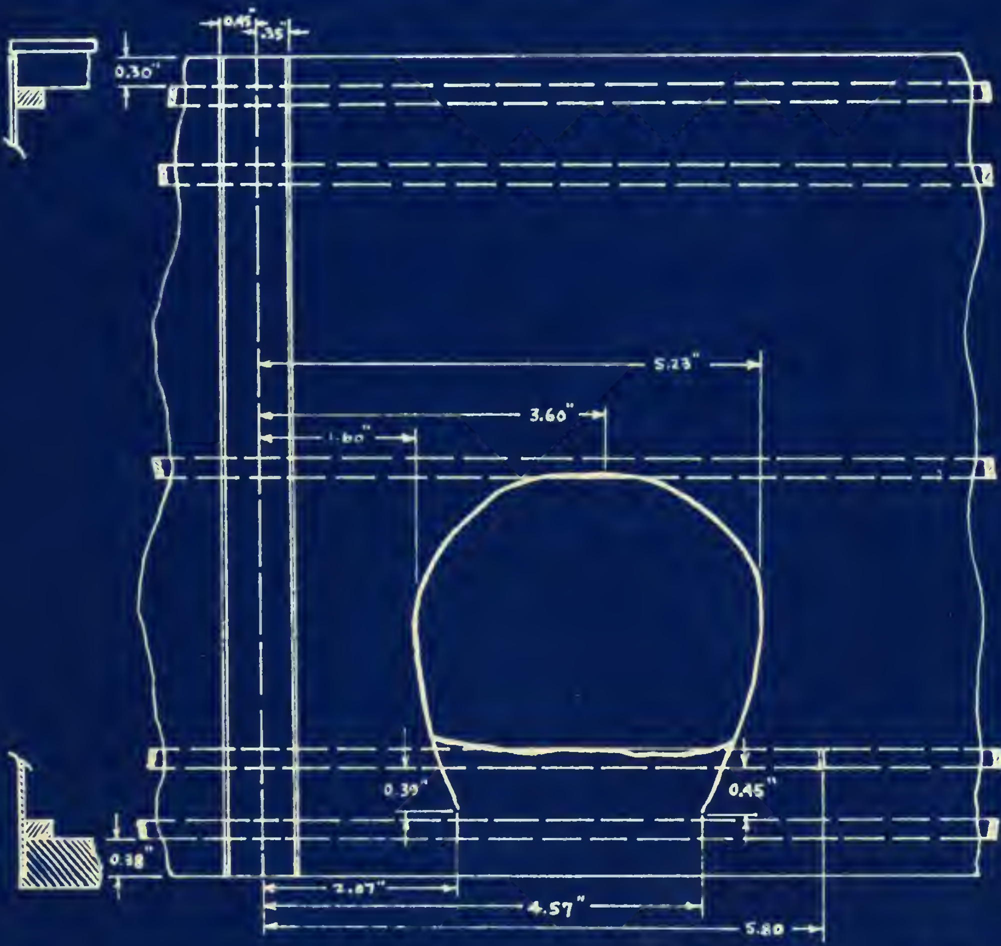

Scale : 1" = 2"

4/11/51

Figure XXIII

Model № 53 ~ Detail of Critical Lobe

Expansion of Fracture Lobe to Actual Size and Shape

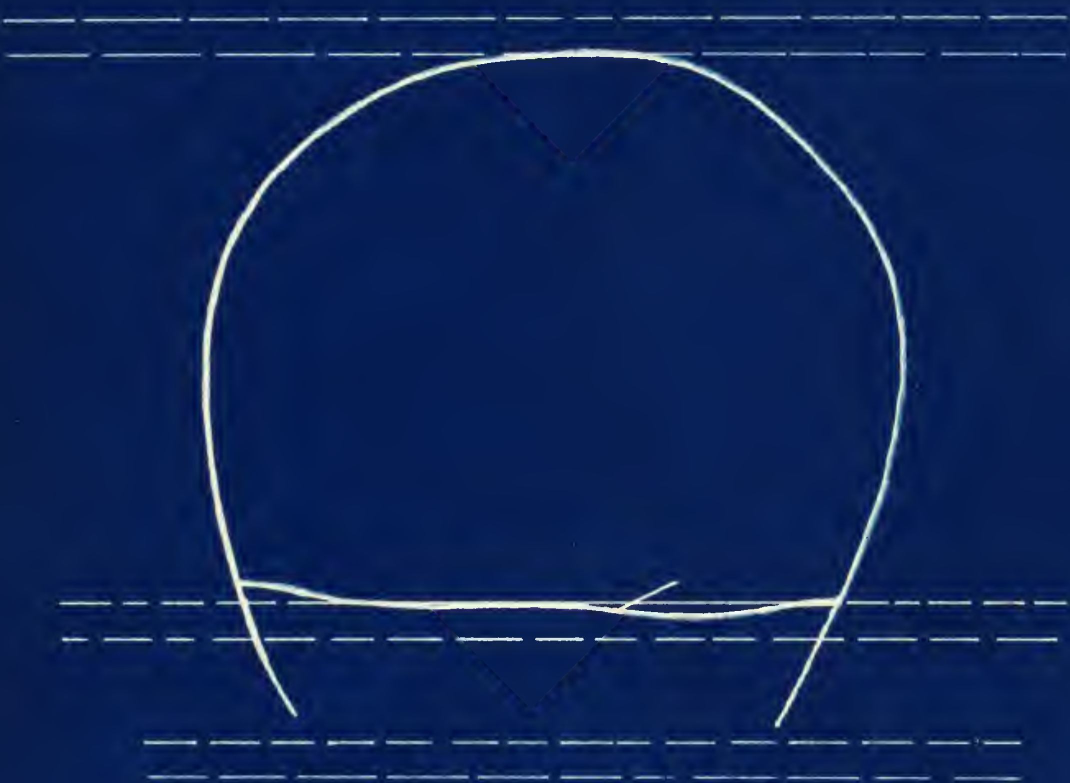

Scale : Full Size

4/11/51

Table No. V

Test of
Lucite Submarine Model No. 52

Test By E. F. Durfee Jr. and V. D. Johnson
30 Mar. 1951

Length Between Frames – 1.35"

Diameter – 9.0"

Thickness – 1/16 inch

Temp. of Water – 60.0°F

Test "A"
Load Applied at Rate of 1 psi./min Hydrostatic Pressure – At 12 ½ psi, cracking noise heard followed by extensive leaking from butt strap. See other pages for details

Test "B"
Load Applied at Rate of 2 psi/min Hydrostatic Pressure
At 15 psi, Violent Crackling Noise
At 23 ½ psi, " " "
At 26 psi, Leaking slightly at point where leakage occurred in test "A".
At 30 ½ psi, Violent Crackling Noise, Leakage at upper End
At 31 psi, Leakage at Upper End Reduced
At 37 psi, Failure. See other pages for details

Note: Examination of Model after test showed that End Pieces were pushed into model. Wedging action of taper of End Pieces distorted shell. Frame adjacent to end pieces broken loose from shell. It is believed that this caused leakage and noise at 30 ½ psi as noted above. Wedging action reduced leakage at 31 psi.

test tank, visual cracks were apparent in the butt strap. Liberal application of ethylene dichloride to the cracks stopped the leaks.

For both steel and plastics, in all calculations where μ occurs, the value 0.30 has been used where stresses are below the plastic flow range and the value 0.5 where stresses are above the plastic range. These values are consistent with the available data. Much less work has been done to verify these values for plastics than for steels, but a value of 0.30 to 0.35 is generally accepted for the plastic for the elastic region.

V.

DISCUSSION OF RESULTS

Introduction

As explained in Section III on Procedure, the investigation of the use of plastic models to study the behavior of steel submarine pressure hulls was conducted in two major steps. First, the performance of plastic columns was studied, and then the performance of the more complicated plastic submarine pressure hull models was investigated. This approach proved to be practical and profitable. The column is the simplest structure that exhibits an instability failure. The critical stress causing an instability failure of a column, whether determined by theoretical formulas or actual test, varies with the sturdiness of the column in much the same manner as does the collapse pressure of a submarine hull vary with its sturdiness.* Plastic column models are very inexpensive compared with plastic submarine models and are easily tested. Our study of the performance of plastic columns was therefore not limited by cost, and it was possible in the time available to run as many column tests as appeared

---

* Footnote: This similarity between columns and submarine hulls is discussed at greater length on page 6 of Reference (4).

necessary to adequately cover the full range of column dimensions required for this study.

From these results, general conclusions could be made on the practicability of using plastic models to predict the performance of steel prototypes. Because of the cost of the plastic submarine pressure hull models, the number of models tested was limited to four. While the dimensions of these models were selected to give as wide a range of sturdiness factor as possible, the number was rather limited. The conclusions obtained from the column tests proved valuable in interpreting the submarine model tests.

Examination of the stress-strain curves in Section IV and Figure XXIV shows that there is very little similarity between the stress-strain curves for steel and for plastics. The yield point for plastics is not definitely defined by the character of the stress-strain curve. For the purpose of this thesis the yield point has arbitrarily been defined as the point of 0.2% permanent set. The yield point stress of the plastic "Lucite" using this definition is approximately 1/5 the yield point stress of medium carbon steel. The modulus of elasticity (E) for "Lucite" is approximately 1/100 of the modulus of elasticity (E) for medium carbon steel. The shape of

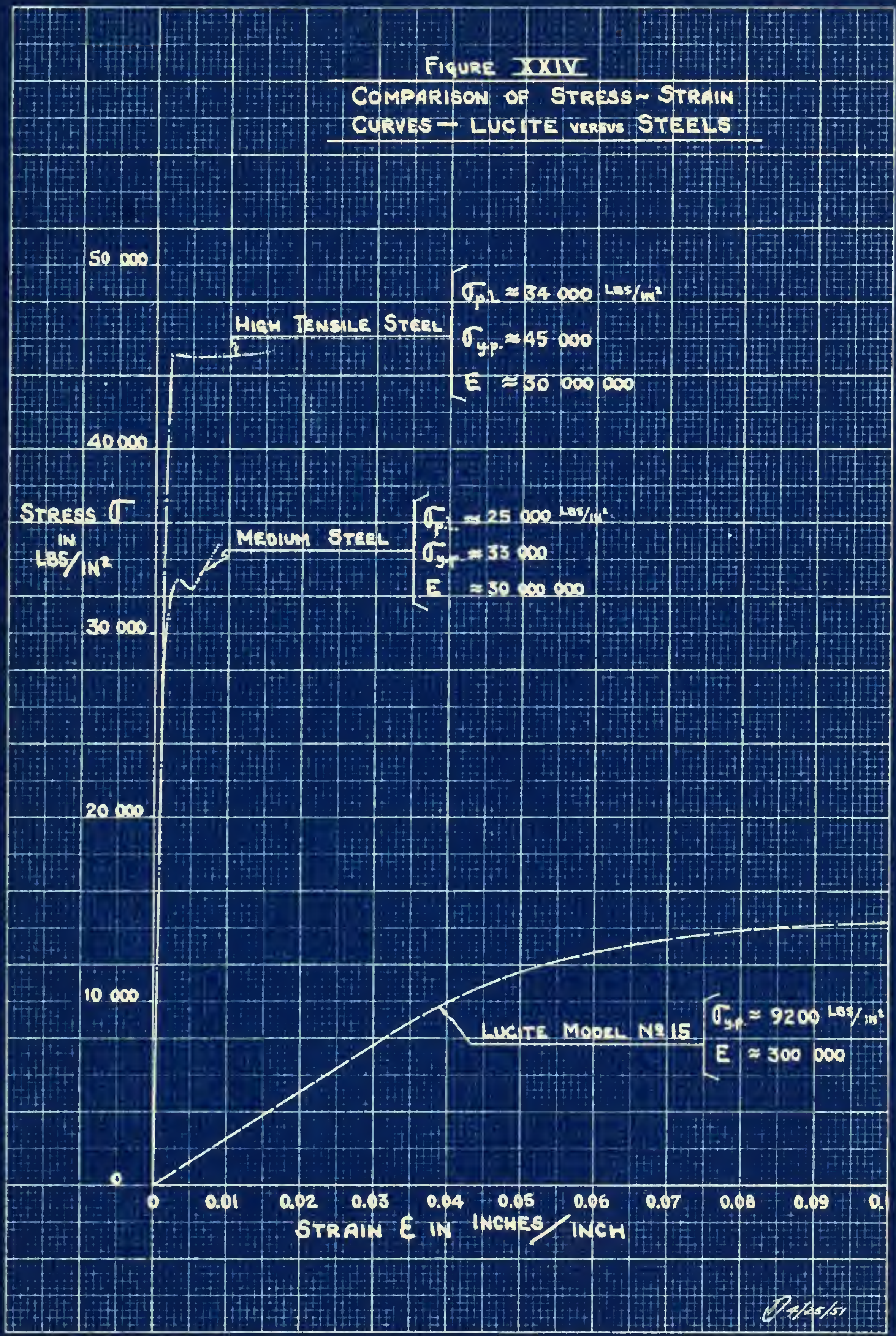

Figure XXIV
Comparison of Stress ~ Strain Curves — Lucite versus Steels
High Tensile Steel
$\sigma_{p.l.} \approx 34\ 000$ lbs/in²
$\sigma_{y.p.} \approx 45\ 000$
$E \approx 30\ 000\ 000$
Medium Steel
$\sigma_{p.l.} \approx 25\ 000$ lbs/in²
$\sigma_{y.p.} \approx 33\ 000$
$E \approx 30\ 000\ 000$
Lucite Model No. 15
$\sigma_{y.p.} \approx 9200$ lbs/in²
$E \approx 300\ 000$
Stress σ in lbs/in²
50 000
40 000
30 000
20 000
10 000
0
0
0.01
0.02
0.03
0.04
0.05
0.06
0.07
0.08
0.09
0.
Strain ϵ in inches/inch
4/25/51

the stress-strain curves are not the same since the steel curve has a well defined shoulder followed by a zero slope of the curve, while the plastic curves round over gently, and in many cases have no point of zero slope. In addition to all the above variations between plastic and steel stress-strain curves, the stress-strain curve of a given plastic will vary with rate of loading, humidity, temperature and other factors. Refer to Figures XXXIV and XXXV and to additional discussion in the Appendix.

When constructing a model to predict the performance of a prototype where such marked differences exist between the physical properties of the materials used for the prototype and the model, the question arises as to whether the model and the prototype should be geometrically similar or be similar based on some non-dimensional basis. The conventional non-dimensional parameters for submarine model work are $\psi = \frac{P}{(h/R)\ \sigma_{yp}}$, and $\lambda = \sqrt[4]{\frac{(L/2R)^2}{(h/2R)^3}} \cdot \sqrt{\frac{\sigma_{yp}}{E}}$. A similar set of non-dimensional parameters for columns would be $\psi' = \sigma_{crit}/\sigma_{yp}$ and $\lambda' = l/\rho\sqrt{\frac{\sigma_y}{E}}$. The type of similarity existing between model and prototype will have a marked effect upon the accuracy of the results, and it may also impose physical limits on the range the stress-strain curves are not the same since the steel curve has a well defined shoulder followed by a zero slope of the curve, while the plastic curves round over gently, and in many cases have no point of zero slope. In addition to all the above variations between plastic and steel stress-strain curves, the stress-strain curve of a given plastic will vary with rate of loading, humidity, temperature and other factors. Refer to Figures 30 and 31 and to additional discussion in the Appendix.

When constructing a model to predict the performance of a prototype where such strong differences exist between the physical properties of the materials used for the prototype and the model, the question arises as to whether the model and the prototype should be geometrically similar or be similar based on some non-dimensional basis. The geometrical non-dimensional parameters for collapse depth here are $\psi = \frac{1}{(R/h)\sqrt{l/R}}$ and $\lambda = \sqrt{[illegible]} = \sqrt{[illegible]}$. A similar set of non-dimensional parameters for collapse would be $\psi' = [illegible]$ and $\lambda' = [illegible]$. This type of similarity existing between model and prototype will make a direct solution from the analysis of the results, and it may also reveal physical limits of the analyof prototypes which can be model tested due to physical limitations of the models.

It may be noted again here that while the plastic materials used in these tests are called by their respective trade names of "Plexiglas" and "Lucite", both are cast Methyl Methacrylate resin and are considered as identical for the listing of physical properties in Reference (6).

Column Test Results

Figures XV and XVI and Table VI compare the results of tests by R.T. Miller and by the authors on "Plexiglas" and "Lucite" columns with the critical buckling stress predicted by Euler's column formula, $\sigma_{crit} = \frac{E' \pi^2}{(\ell/\rho)^2}$. The range of columns varied in sturdiness from Model O which crushed and did not buckle to Model 21 which had as large an ℓ/ρ value as appeared possible to secure in a plastic column and still have the column initially straight within the limits required for accurate test results.

The correct value to be used for E' in the Euler column formula has been the subject of much learned discussion since the formula was first suggested in 1757. All authorities seem to agree on using the value of E' = E, the initial slope of the stress-strain

Table No. VI

Actual Vs. Predicted Buckling Stress For Plexiglas And Lucite Columns Models

$\sigma_{ult.}$ = Buckling Stress From Column Tests

$$\sigma_{u} \quad 4\frac{\pi^2 E_T}{(L/\rho)^2} \qquad \sigma_R = 4\frac{\pi^2 E_R}{(L/\rho)^2}$$

Where E_T = Tangent Modulus

And $E_R = \dfrac{4EE_T}{(\sqrt{E}+\sqrt{E_T})^2}$

Model	L/ρ	σ_{ult}	σ_T	σ_R
1	20	10,400 psi	9,560 psi	10,350 psi
2	30	8 630	8,030	9,000
3	40	7 200	6,460	7,100
4	50	5800	5,050	5,300
5	60	4270	3,900	3,975
6	70	3720	3000	3,000
7	80	2710	2280	2 280
8	90	2200	1800	1800
9	100	1745	1460	1460
16	27	8 820	10,000	11,000
17	36.3	8220	7530	8,000
18	46	5 300	5600	5,600
19	55.1	3960	3900	3900
20	64.6	2280	2830	2830
21	104	1845	1100	1100
22	24.3	10,790	10,700	11,700
23	25.3	11,300	10,400	11,450
24	22	11,000	11,300	12,250
16 (Retest)	27	9,120	10,000	11,000

curve, for stresses below the proportional limit. Timoshenko in Reference (13) suggests that the so-called reduced modulus value developed by Von Karman be used for E' when stresses are above the proportional limit. By definition the reduced modulus is $E_R = \frac{4 E E_T}{(\sqrt{E} + \sqrt{E_T})^2}$. Shanley in References 2 and 3 suggests that the critical stress obtained using $E' = E_T$, as suggested by F. Engesser, is actually correct for predicting the load at which buckling of a perfect column will begin, and that the reduced modulus gives the upper limit for load as the bending increases. Practical tests seem to bear out this conclusion, test results generally following Euler's formula below the proportional limit and lying in the area bounded by the Euler formulas using E_T and E_R in the region above the proportional limit.

Figures XV and XVI show the actual buckling stress as determined by test, and the predicted buckling stress as determined by Euler's formula using both E_R and E_T where different. The E_R and E_T values for "Plexiglas" and "Lucite" were obtained graphically from Figures XII and XIV and are plotted in Figures XI and XIII.

Study of Figure XVI shows that the column tests conducted by R.T. Miller using "Plexiglas" columns give

values for critical buckling stresses which closely follow the shape of the Euler curves, but that the critical stress values are, in general, higher than those predicted by the Euler formula by about 15%. In these tests the critical buckling force was considered to be that force which produced a visual deformation. Determination of such a point depended on the judgment of, and careful observation by, the person conducting the test; in most cases this method did not permit determination of the exact moment of initial buckling covered by the Euler theory.

In the series of tests run by the authors, readings were taken of the lateral deflection of the midpoint of the column as the load was applied. The details of the arrangement of the dial gages used to record the deflections are described in Section III and Appendix "B". These dial gage readings were plotted against the load and buckling was defined as the point at which there ceased to be a small increase in lateral deflection with increasing load and instead there was a large non-linear variation in lateral deflection with increasing force. See Figures XXV-XXVII for these plots. Plotting the lateral deflections served an additional useful purpose in determining the values for critical buckling pressure which closely follow the shape of the Euler curves, but that the critical pressure values are, in general, higher than those predicted by the Euler formula by about 15%. In these tests the critical buckling force was considered to be that force which produced a visual deformation. Determination of such a point depended on the judgment of, and careful observation by, the person conducting the test; in most cases this method did not permit determination of the exact moment of critical buckling governed by the Euler theory.

In the series of tests run by the authors, readings were taken of the lateral deflection of the midpoint of the column as the load was applied. The details of the arrangement of the dial gage used to record the deflections are described in Section III and Appendix "D". These dial gage readings were plotted against the load and buckling was defined as the point at which there ceased to be a small increase in lateral deflection with increasing load and instead there was a large non-linear variation in lateral deflection with increasing load. See Figures XXX-XXXII for these plots. Plotting the lateral deflections served an additional useful purpose in determining the

Figure XXV

Lucite Column Compression Tests
Plots of Lateral Deflections

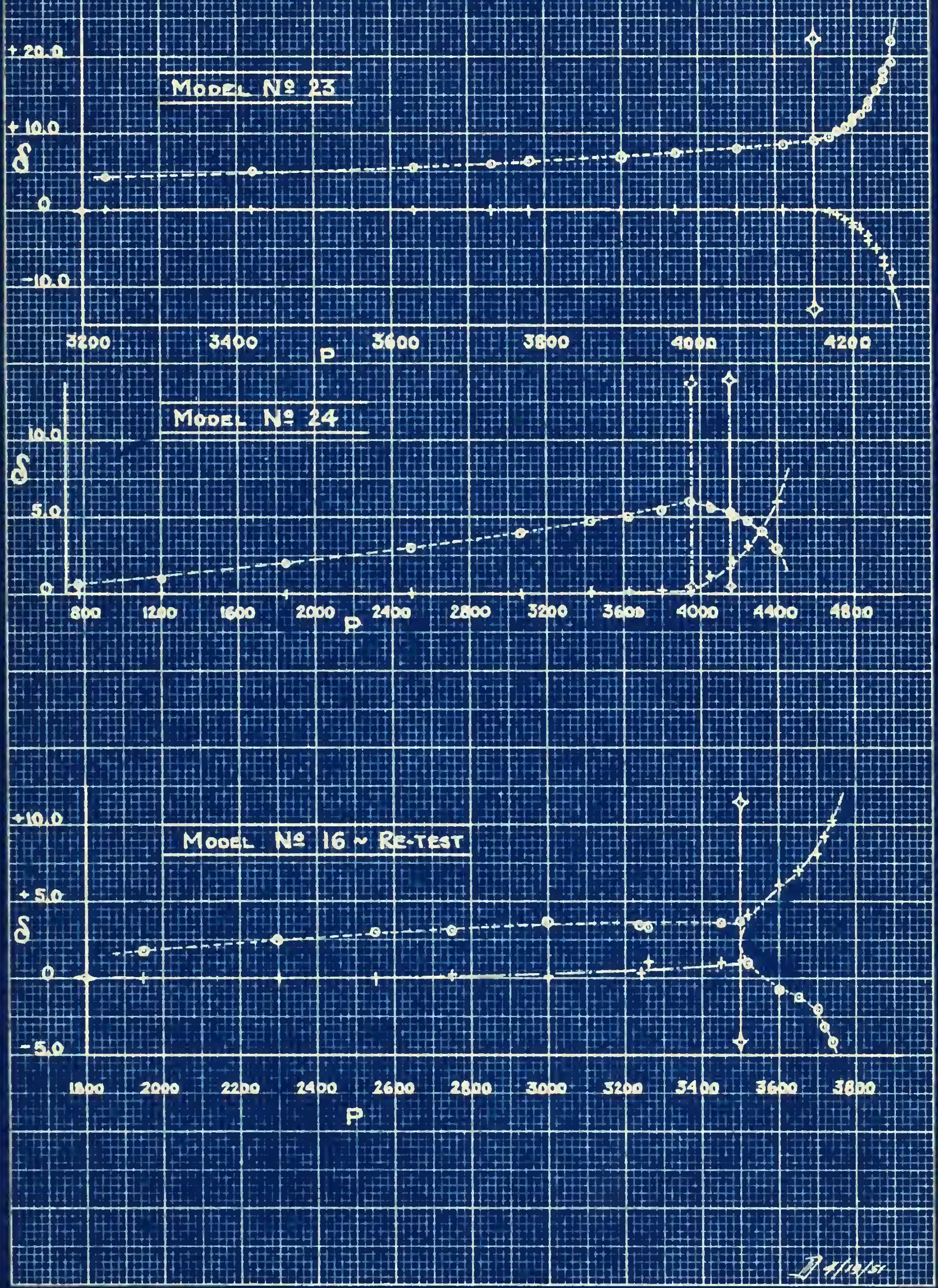

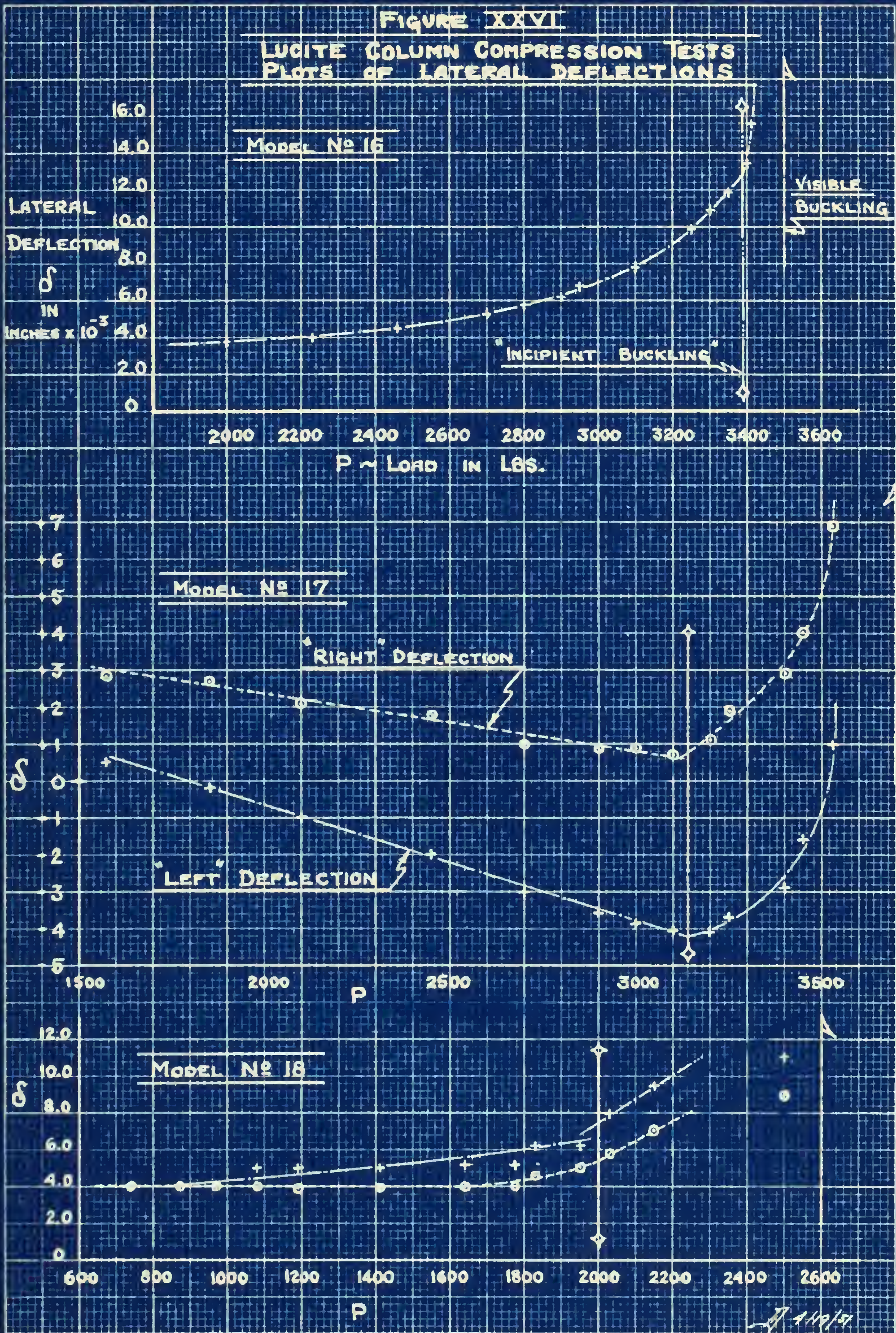

FIGURE XXVI
LUCITE COLUMN COMPRESSION TESTS
PLOTS OF LATERAL DEFLECTIONS
MODEL No 16
LATERAL DEFLECTION δ IN INCHES x 10^-3
16.0
14.0
12.0
10.0
8.0
6.0
4.0
2.0
0
VISIBLE BUCKLING
"INCIPIENT BUCKLING"
2000
2200
2400
2600
2800
3000
3200
3400
3600
P ~ LOAD IN LBS.
MODEL No 17
"RIGHT" DEFLECTION
"LEFT" DEFLECTION
δ
+7
+6
+5
+4
+3
+2
+1
0
-1
-2
-3
-4
-5
1500
2000
2500
3000
3500
P
MODEL No 18
δ
12.0
10.0
8.0
6.0
4.0
2.0
0
600
800
1000
1200
1400
1600
1800
2000
2200
2400
2600
P

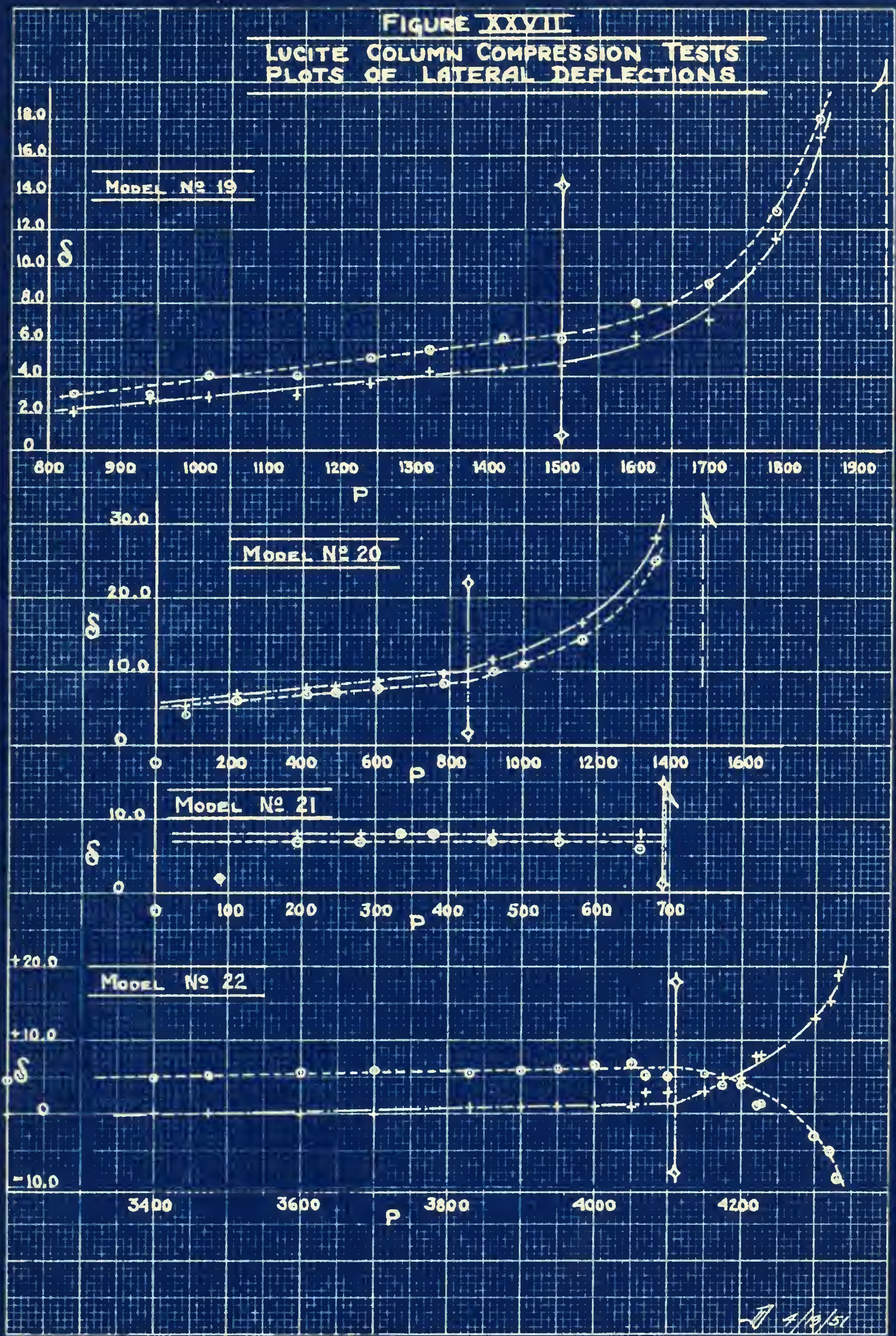
FIGURE XXVII
LUCITE COLUMN COMPRESSION TESTS
PLOTS OF LATERAL DEFLECTIONS
MODEL Nº 19
δ
0
2.0
4.0
6.0
8.0
10.0
12.0
14.0
16.0
18.0
800
900
1000
1100
1200
1300
1400
1500
1600
1700
1800
1900
P
MODEL Nº 20
δ
30.0
20.0
10.0
0
200
400
600
800
1000
1200
1400
1600
P
MODEL Nº 21
δ
10.0
0
100
200
300
400
500
600
700
P
MODEL Nº 22
δ
+20.0
+10.0
0
-10.0
3400
3600
3800
4000
4200
P
4/9/51

accuracy of the entire test. A reliable test should show a plot similar to that for Model No. 23, Figure XXV. The well defined buckling point indicates that the ends of the fixed-ended column were parallel within very close tolerances and that the faces of the testing machine were similarly parallel. In contrast, a plot of the type shown for Model 16, Figure XXVI, indicates that the column is bending in the initial phases of loading and that the column must either be bent when unloaded, have non-parallel faces, or that the faces of the testing machine are not parallel. In any case, such a plot shows that the results of the test are not very reliable.

A study of Figure XV shows that the column tests conducted by the authors using "Lucite" give results which again follow the general shape of the Euler formulas. In this set of tests, however, there appears to be a wider scatter of the points than in the "Plexiglas" set but the mean of the test results closely agrees with the values predicted by Euler. This closer general agreement with the Euler formula is believed to be due to the method of determining buckling (discussed above) which more accurately spots the point of initial buckling than is possible by visual observation. The wider scatter of points is more difficult to explain but may be due to

the method of manufacture of the columns. In manufacturing both the "Plexiglas" and the "Lucite" columns, extreme care was exercised to obtain end surfaces that were parallel within close tolerances in order to obtain a test with end fixity similar to that assumed in the theoretical derivation of the column formulas. However, in the case of the "Plexiglas" columns this was accomplished by milling the ends, while in the case of the "Lucite" columns the ends were sawed and then finished on a sanding machine. It would appear from the results that the milling of the ends produces a more uniform degree of parallelism and is the better method of the two.

The tests results in general are considered good, comparing rather closely with the Euler formulas and with the work of other investigators in the column field.

Fixed-ended columns were used in the tests because it is believed that with relatively simple testing equipment it is possible to more closely approximate the condition for perfect fixed-end columns than for perfect pin-ended columns. However, perfectly parallel ends on the column models cannot be obtained, nor are testing machine faces perfectly parallel, and the de-

gree of non-parallelism undoubtedly varies from model to model and test to test. Where extremely accurate results have been desired by other investigators, pin-ended columns using complicated roller bearing supports have been used. The use of such equipment would give slightly more accurate and consistent results than those herein obtained. The method used, however, was sufficiently accurate for the desired purpose, and not unduly time and money consuming.

From the above analysis we can conclude that plastic column models give accurate and consistent test results when compared to theoretical predictions. The next question is whether or not plastic column models can be used to predict the failure of steel column prototypes. The answer appears to be "yes, in some cases, but not all", as explained below.

First consider the possibility of using plastic column models geometrically similar to the steel prototypes. By Euler's equation, $\sigma_{crit} = \frac{E\pi^2}{(\ell/\rho)^2}$, we would expect the plastic model to failure at a $\sigma_{crit} = \frac{E \text{ plastic}}{E \text{ steel}}$ times the critical stress for the steel. Hence, a "Plexiglas" column would fail at approximately 1/100 the stress of a dimensionally similar steel column. Figure XXVIII shows this graphi-

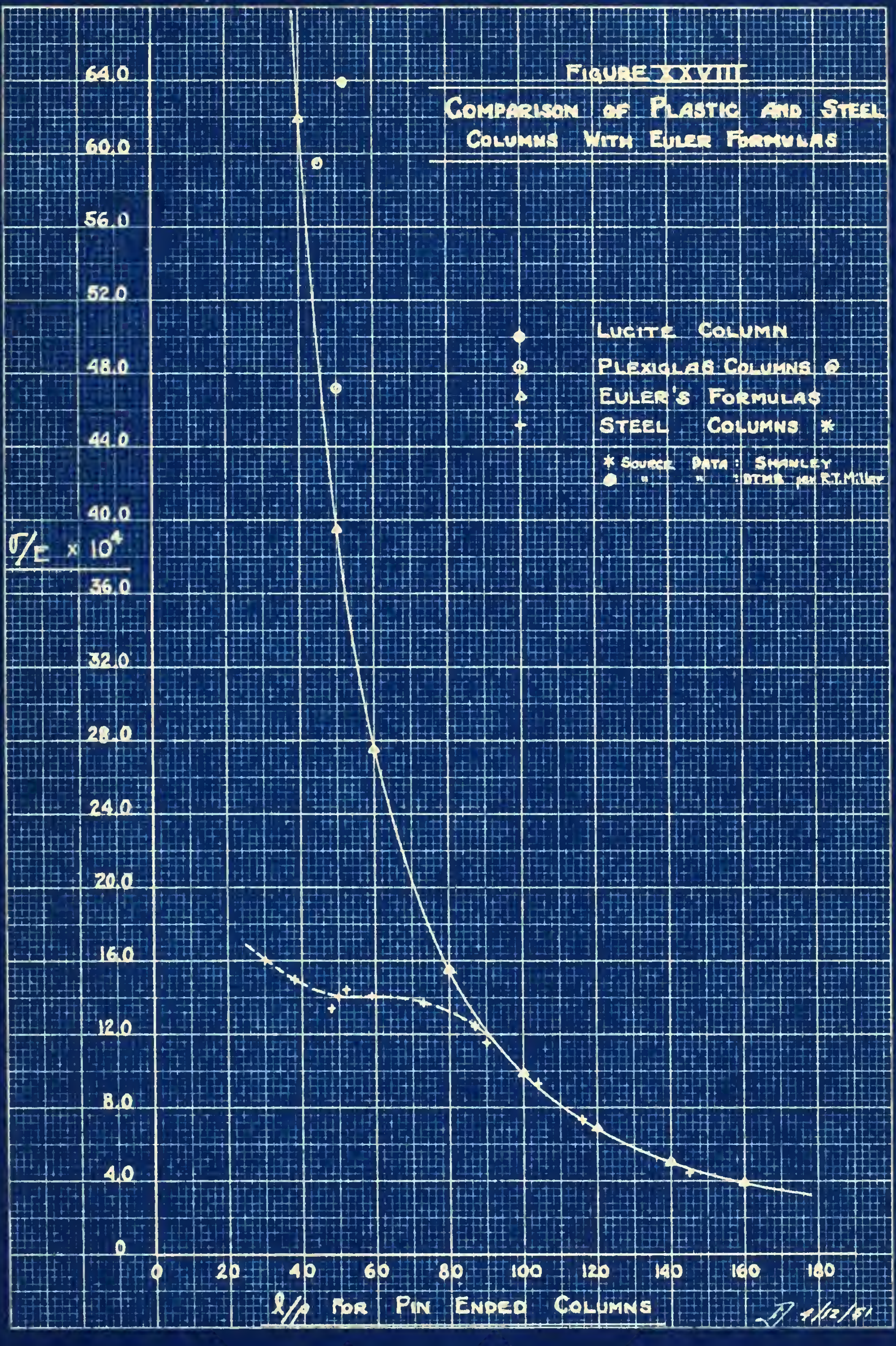
FIGURE XXVIII
COMPARISON OF PLASTIC AND STEEL COLUMNS WITH EULER FORMULAS
LUCITE COLUMN
PLEXIGLAS COLUMNS @
EULER'S FORMULAS
STEEL COLUMNS *
* SOURCE DATA : SHANLEY
" " : DTMB per R.T. Miller
64.0
60.0
56.0
52.0
48.0
44.0
40.0
$\sigma/E \times 10^4$
36.0
32.0
28.0
24.0
20.0
16.0
12.0
8.0
4.0
0
0
20
40
60
80
100
120
140
160
180
l/ρ FOR PIN ENDED COLUMNS
4/12/51

cally. The critical stress for a column of a given l/ρ can be obtained by taking the ordinate on the curve for the l/ρ value and multiplying the value of the ordinate by the applicable E.

In Figure XXVIII, data from both steel and plastic column tests are shown. The steel data are from Reference (2) while the "Plexiglas" and "Lucite" data are from this thesis. The steel curve is well defined by many points. Since plastic column models with an l/ρ of greater than 50 could not be manufactured without some initial curvature, no tests were run at l/ρ values greater than 52. However, the few experimental points shown for plastics lie along the line of the Euler formula using E equal to the initial modulus of elasticity. Although there is no experimental data for plastic column models at l/ρ greater than 52, such points if available would be expected to fall along the Euler column formula line as the critical stress in all such cases would be far below the yield stress of plastic.

Referring again to Figure XXVIII we see that for columns with a l/ρ value of greater than 90, the curve of data for plastic columns and steel columns coincides. Therefore, in this region dimensionally similar steel and plastic columns will have critical

stresses proportional to their respective moduli of elasticity and, hence, a plastic model theoretically can be used to predict the failure of a steel prototype.

The above is not true for values of l/ρ less than 90. Figure XXVIII shows graphically that the curves no longer coincide and that the error of using the plastic curve instead of the steel runs from 0% at $l/\rho = 90$ to approximately 1000% at $l/\rho = 23$. This is because of the difference in the ratio of $\frac{\sigma_{yp}}{E}$ for plastics and for steel. At $l/\rho = 90$ the steel columns reach a stress equal to the proportional limit and begin to enter the range where failure is determined by the reduced values of E_T and E_R which are fractions of the E value; hence the curve falls below the Euler curve for constant E. However, at this point of $l/\rho = 90$, the plastic column is stressed to but 1/13 of its proportional limit. In fact, it will not reach the proportional limit until the l/ρ equals approximately 23 and at this point the ordinate will be 189 for the plastic column compared to a value of 17.2 for the steel column. Therefore, if a plastic model were used to predict the failure of a steel column with an l/ρ value of 23 it would predict a failure at $\sigma_{crit} = 189 \times 10^{-4} \times 30 \times 10^{6} = 567,000$ psi, while

the steel column data predicts a failure at

$$\sigma_{crit} = 17.2 \times 10^{-4} \times 30 \times 10^{6} = 51,600 \text{ psi.}$$

Study of Figure XXVIII shows that any empirical correlation between the two curves is doubtful due to the fact that the two curves are entirely different in shape and have no functional relationship.

From the above discussion it is concluded that theoretically dimensionally similar plastic column models will predict the critical buckling stress of steel column prototypes when the steel columns are not stressed beyond the proportional limit. Actually it is extremely difficult, in fact nearly impossible, to construct plastic column models within this range of high l/ρ values that do not have some initial curvature. Therefore, for practical purposes the use of dimensionally similar plastic models to predict the buckling stress of steel prototypes is not feasible for any range of column dimensions.

In Figure XXIX the results of steel, "Lucite" and "Plexiglas" columns are plotted on the basis of the two dimensionless coefficients, $\sigma_{crit}/\sigma_{yield}$ and $l/\rho \sqrt{\frac{\sigma_Y}{E}}$, which take into account the physical properties of the specimen. This means that the plastic column model and its steel prototype would both have the same value of $l/\rho \sqrt{\frac{\sigma_Y}{E}}$. For values of $l/\rho \sqrt{\frac{\sigma_Y}{E}}$

the steel column data predicts a failure at

$\sigma_{crit} = 17.1 \times 10^{-4} \times 30 \times 10^{6} = 51,300$ psi.

Study of Figure XVIII shows that any semblance of correlation between the two curves is observed for λ/ρ 40. For less than 40 the two curves are entirely different in shape and keep no functional relationship.

From the above discussion it is concluded that theoretically dimensionally similar plastic column models will predict the critical buckling stress of steel column prototypes when the steel columns are not stressed beyond the proportional limit. Actually it is extremely difficult, in fact nearly impossible, to construct plastic column models within this range of high λ/ρ values when we do not have more rigid materials. Therefore, for practical purposes the use of dimensionally similar plastic models to predict the buckling stress of steel prototypes is not feasible for any range of column dimensions.

In Figure XXII the results of steel, "Lucite" and "Plexiglas" columns are plotted on the basis of the two dimensionless coefficients, $\sigma_{crit}/\sigma_{yield}$ and $\lambda/\rho\sqrt{\sigma/E}$, which take into account the physical properties of the materials. This shows that the plastic column model and its steel prototype would both have the same value of $\lambda/\rho\sqrt{\sigma/E}$. The values of $\lambda/\rho\sqrt{\sigma/E}$

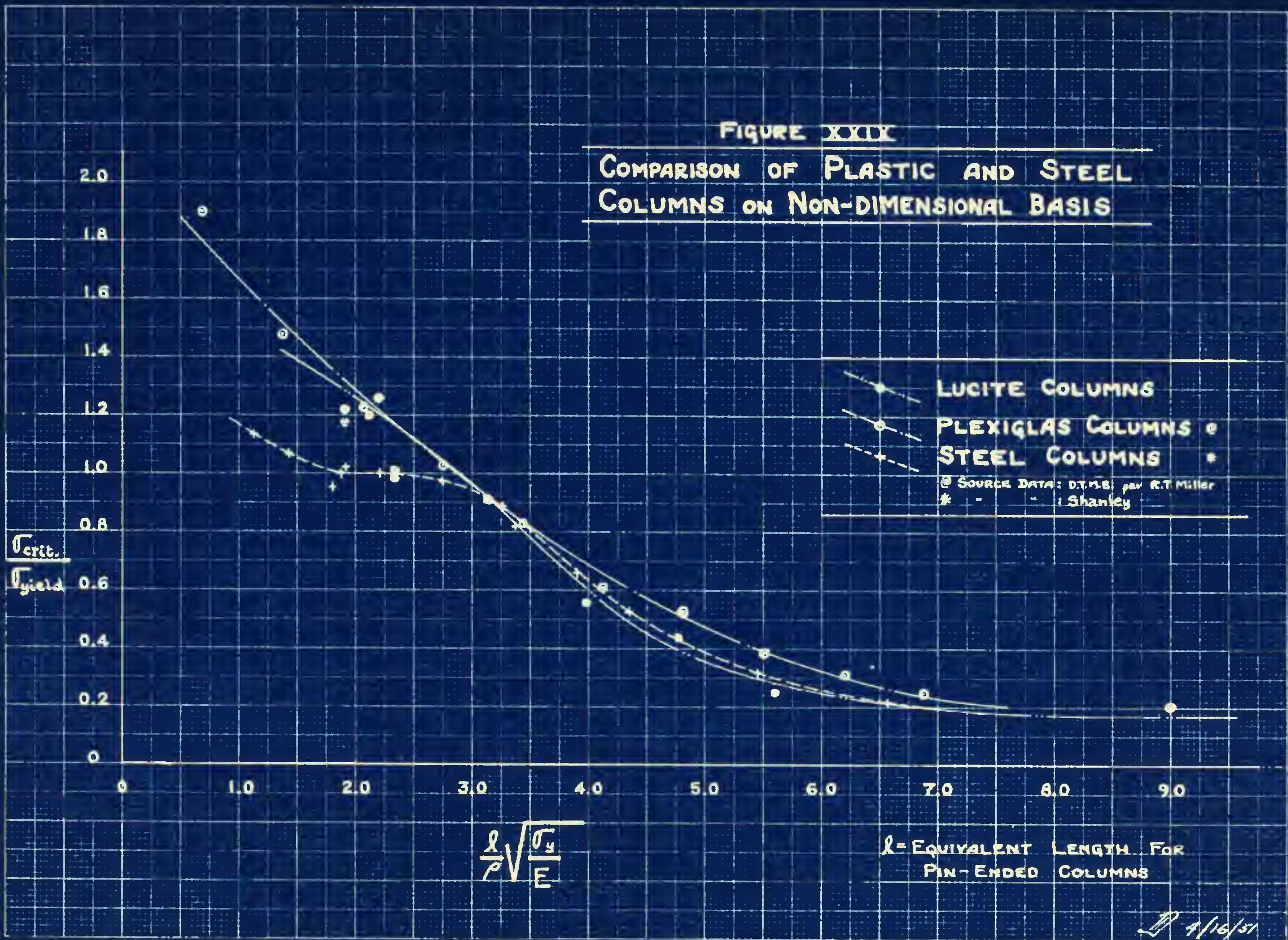

FIGURE XXIX
COMPARISON OF PLASTIC AND STEEL COLUMNS ON NON-DIMENSIONAL BASIS
LUCITE COLUMNS
PLEXIGLAS COLUMNS ⊙
STEEL COLUMNS *
⊙ SOURCE DATA: D.T.M.B. per R.T. Miller
* " " : Shanley
$\frac{\sigma_{crit.}}{\sigma_{yield}}$
2.0
1.8
1.6
1.4
1.2
1.0
0.8
0.6
0.4
0.2
0
0
1.0
2.0
3.0
4.0
5.0
6.0
7.0
8.0
9.0
$\frac{l}{\rho}\sqrt{\frac{\sigma_y}{E}}$
l = EQUIVALENT LENGTH FOR PIN-ENDED COLUMNS
4/16/51

of more than 3.25 the curves for "Lucite" column data and for steel column data practically coincide. The curve for "Plexiglas" data is slightly higher for reasons already discussed. This means that in this region plastic model columns can predict accurately the buckling stress of steel column models. Furthermore, there is no practical difficulty as the plastic columns are much shorter than steel columns which are non-dimensionally similar due to the difference in the ratio of σ_y/E for the two materials. The column tests run by the authors are equivalent to steel columns with an l/ρ ratio of as high as 240.

To the left of $\frac{l}{\rho}\sqrt{\frac{\sigma_y}{E}} = 3.25$, the plastic data curves again separate from the steel data curves, and again correlation of the two curves does not appear feasible. Therefore, it is believed that by using non-dimensional similarity between plastic column models and steel prototypes, the buckling stress of the steel columns can be accurately predicted by the plastic models if the corresponding steel prototype is not stressed beyond the proportional limit. If the steel prototype is stressed beyond the proportional limit, accurate predications cannot be made by using plastic models, and the error will increase with increasing stress.

of more than 0.35 the curves for "similar" column data and for steel column data practically coincide. The curve for "dissimilar" data is slightly higher than previous similarity discussed. This means that in this region plastic model columns can predict accurately the buckling stress of steel column models. Furthermore, there is no practical difficulty as the plastic columns are much stiffer than steel columns which are non-dimensionally similar due to the difference in the ratio of σ_y/E for the two materials. The column tests run by the author are equivalent to steel columns with an l/ρ ratio of as high as 150.

To the left of $\frac{1}{\pi}\frac{l}{\rho}\sqrt{\frac{\sigma}{E}} = 0.35$, the plastic data curves again separate from the steel data curves, and again correlation of the two curves does not appear feasible. Therefore, it is believed that in using non-dimensional similarity between plastic column models and steel prototypes, the buckling stress of the steel columns can be accurately predicted by the plastic models if the corresponding steel prototype is not stressed beyond the proportional limit. If the steel prototype is stressed beyond the proportional limit, accurate predictions cannot be made by using plastic models, and the error will increase with increasing stress.

Submarine Model Test Results

As noted in the Introduction, there has been very little work done in the field of testing plastic models for structural strength. The tests conducted by the authors on plastic submarine pressure hull models, therefore, involved not only the actual conducting and analyzing of the tests but, in addition, the use of techniques of manufacture which were of an unproven and experimental nature.

An examination of the mode of failure of each of the four models tested shows that three of the models failed in a manner which indicates that the results of these tests should furnish reliable data. Models Nos. 51, 52, and 53 appear to have had lobe type failures which were not materially influenced by the butt strap on the models nor by the end bulkheads of the models. Model 50 appears to have failed prematurely due to a local failure near an end bulkhead.

Figure XVII shows the nature of the failure of Model No. 50. The failure is confined to the area between the last frame of the model and the end bulkhead. From Figure XVII it can be seen that there is very little space between the frame and the portion of the bulkhead which overlaps the shell. This distance is so much smaller than the distance between frames that

a lobe type of failure in this area appears unlikely. The shape of the fractured area seems to indicate that it was caused by some local stress raiser.

Model No. 50 had the greatest inside end diameter of any of the four models tested. While this was less than 1/10 of an inch greater than the smallest diameter at the corresponding end, it was sufficient to make the common solid end piece used on all the models fit somewhat loosely into the model. As a result, the usual method of sealing the end joint with "Miracle Adhesive," which proved successful in the tests of the three other models, failed to make the joint sufficiently tight to prevent excessive leakage in three successive trys. To help prevent this leakage, a cloth gasket was placed in between the model shell and the rabbetted part of the end bulkhead along with cotton wicking and "Miracle Adhesive." It is believed that forcing this end in place with the sealing agents mentioned probably cracked the shell or butt and caused a premature failure.

Figures XVIII and XIX show the location and type of failure which occurred in Model No. 51. The failure is at a distance of a quarter of the circumference of the model from the butt strap and one frame space from the end bulkhead. The fracture appears to have started in the middle of the frame space. Such a location a new type of failure in this area appears unlikely; the shape of the fractured area seems to indicate that it was caused by some local stress raiser.

Shell 84, is that the greatest radial bell diameter of any of the four shells tested. While this was less than 1/10 of an inch greater than the smallest diameter at the corresponding end, it was sufficient to make the grommet rolls and plates used to fit the shells fit rather loosely into the barrel. As a result, the usual method of sealing the end joint with "Minnesota Adhesive," which proved successful in the tests of the three other shells, failed to seal the joint sufficiently tight to prevent excessive leakage at later successive firing. To help prevent this leakage, a rubber gasket was placed between the barrel shell and the machined part of the end bulkhead along with copious quantities of Minnesota Adhesive." It is believed that forcing this end in place with the sealing clamps mechanism probably crushed the shell or bent and caused a premature failure.

Figures XVIII and XIX show the location and type of failure which occurred in Shell No. 84. The failure is at a distance of a quarter of the circumference of the shell from the weld seam and the fracture extends from the end bulkhead. The fracture appears to have started in the middle of the frame space. Such a location indicates that the butt strap and the end bulkheads had a negligible influence on the failure. The fracture appears to be ideally located. Before the failure, half lobes of 1½" to 2" could be felt. Formula 24 from Reference (4) gives a half-lobe length of 1.28" for this model. One peculiarity of the failure was the presence of so-called "crazing" on the specimen after failure. This appeared as a network of scratches as shown in Figure XIX both at the point of rupture and along the frame line. A more detailed discussion of "crazing" is contained in Appendix "D", but the type found in this model is believed due to tension yielding above the proportional limit. Hence, the shell at the frame was apparently near the yield point as was the shell at the middle of the frame space where the lobes reached the maximum which resulted in the shell fracture.

Figures XX and XXI show the details of the failure of Model 52. While the crack which was the ultimate method of failure of the model extends just to the butt strap, the shape of the crack and its length indicates that a lobe failure occurred which was not materially affected by the presence of the butt strap. The failure is also well clear of the end bulkhead influence. This model had the smallest diameter of the indicates that the [illegible] and the [illegible] had a negligible influence on the failure. The fracture appears to be [illegible], however, the failure, [illegible] at [illegible]. Formula of [illegible] (1) gives a [illegible]-type length of [illegible] for this panel. The peculiarity of the failure was the presence of [illegible] on the specimen after failure. This appeared as a network of scratches as shown in Figure [illegible] both at the point of rupture and along the [illegible] lines. A more detailed discussion of "crazing" is presented in Appendix [illegible], but the type found in this panel is believed due to tension yielding above the conventional limit. Hence, the shell at the fracture was apparently under [illegible] yield [illegible] at the [illegible] of the [illegible] where the [illegible] reached the maximum which resulted in the shell fracture.

Figures [illegible] and [illegible] show the details of the failure of model [illegible]. [illegible] was the ultimate pattern of failure of the [illegible] to the test [illegible], the [illegible] of the [illegible] and the length indicates that a [illegible] failure occurred which was not materially affected by the presence of the [illegible]. The failure is also [illegible] of [illegible] influence. This model had the smallest [illegible] of the four models, and as a result the tapered end pieces extended into the shell for only a short distance and were supported by two auxiliary frames, as shown in Figure XX, to take the shear forces. This arrangement proved undesirable but did not prevent a satisfactory test. Six and one-half psi below the final collapse pressure, the solvent fastening the frames to the shell failed in shear causing a loud cracking noise and some leakage, but the wedge-shaped piece sealed itself and did not adversely influence the test.

Figures XXII and XXIII show the failure of Model 53. The failure is clear of the influence of the butt strap and the end bulkheads. The fracture appears to have started at one of the frames bounding the failure. The piece of shell which was blown into the cylinder is of the size and shape to indicate a lobe type failure. The piece of shell is 3.62" long and extends from frame to frame. Formula 24 of Reference (4) gives a half-lobe length of 1.77 for this model.

Dial gages were used to record deflections during tests of Models 50 and 53. These gages were installed as shown in Figures VIII and XIX and were intended to determine the collapse pressure by indicating the pressure at which shell deflections no longer increased linearly with pressure. It was thought this might be

more reliable than visual signs of failure since the lateral deflection readings had proven to be more reliable than visual indications in the column tests. The readings taken are plotted in Figure XXX. It will be noted that the maximum variation in readings for Dial Gage "A" in the test of Model No. 58 is .036" while Dial Gage "B" opposite has a variation of .162". It is believed that this was caused by some lack of rigidity in the dial gage set-up; and that the deflection indicated by each gage was actually a function of the total deflection of both sides of the model, the spring constants of the dial gages, and the rigidity of the dial gage support. The plots of the readings of these two gages, however, both indicate a point of rapid change in deflection readings 1 psi below the failure point.

The dial gage arrangement made visual observation of the model under test difficult and precluded any examination of the model by running ones hand along the surface to spot the exact location of leaks or lobe formations. Since the readings taken on Model No. 58 had not proven much more accurate than visual means for discovering buckling, it appeared that a good visual inspection was more important than the gage readings.

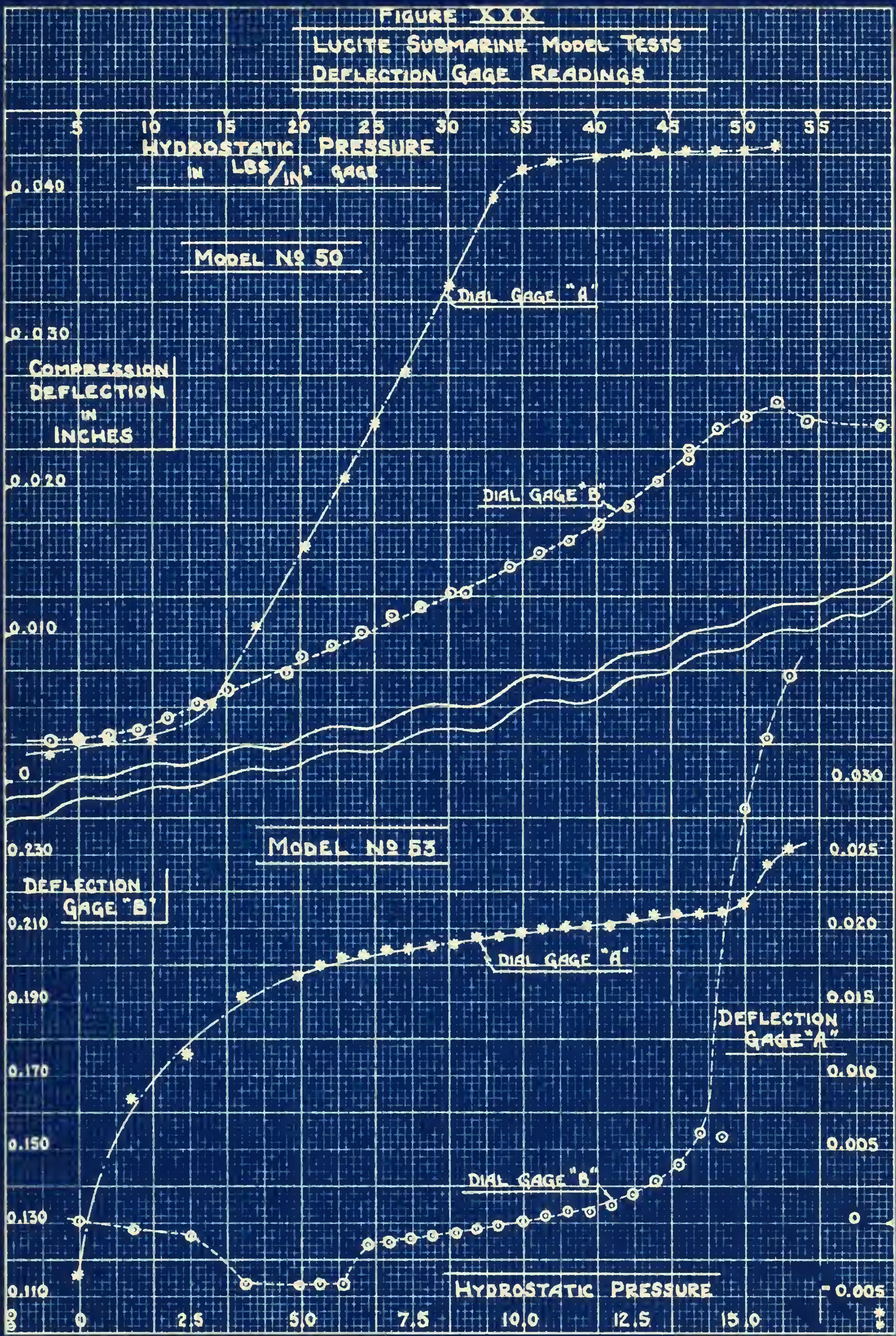

FIGURE XXX
LUCITE SUBMARINE MODEL TESTS
DEFLECTION GAGE READINGS
HYDROSTATIC PRESSURE IN LBS/IN² GAGE
MODEL Nº 50
DIAL GAGE "A"
DIAL GAGE "B"
COMPRESSION DEFLECTION IN INCHES
MODEL Nº 53
DEFLECTION GAGE "B"
DIAL GAGE "A"
DEFLECTION GAGE "A"
DIAL GAGE "B"
HYDROSTATIC PRESSURE
5
10
15
20
25
30
35
40
45
50
55
0.040
0.030
0.020
0.010
0
0.230
0.210
0.190
0.170
0.150
0.130
0.110
0.030
0.025
0.020
0.015
0.010
0.005
0
-0.005
0
2.5
5.0
7.5
10.0
12.5
15.0

Therefore, gages were not used for the tests of Models Nos. 51 and 52. For test No. 53 a more simple dial gage arrangement was devised which still permitted visual examination of the model under test. The readings taken during the tests run on Model No. 53 are shown in Figure XXX but have little significance as the model failed prematurely.

The conventional basis for plotting submarine model test results is on a ψ vs λ graph where, as mentioned before, $\psi = \frac{P}{(h/R)\sigma_{yp}}$ and $\lambda = \sqrt[4]{\frac{(L/2R)^2}{(h/2R)^3}} \cdot \sqrt{\frac{\sigma_{yp}}{E}}$.

Figure XXXI is a plot of steel data from David Taylor Model Basin tests. Included on this plot is DTMB formula "9" for the collapse of thin-walled steel pressure vessels with stiffening rings and the curve $\psi = \frac{1.20}{\lambda^2}$ which closely approximates experimental data.

DTMB Formula "9" was developed by the David Taylor Model Basin for predicting the collapse by instability of thin cylindrical shells under external pressure.

$$P(\text{the collapse pressure}) = \frac{2.42E}{(1-\mu^2)} \frac{(h/2R)^{5/2}}{\left[\frac{L}{2R} - 0.45(h/2R)^{\frac{1}{2}}\right]}$$

While this formula is independent of $\sigma_{y.p.}$ it can be rewritten as $\psi = \frac{1.30}{\lambda^2 - \varepsilon}$ for plotting on a ψ vs λ plot, where $\varepsilon = 0.045 \frac{1000\ \sigma_{yp}}{E}\left(\frac{1-\mu^2}{0.91}\right)^{3/4} \cdot \frac{1}{(100h/2R)}$ *

* Footnote: For further discussion of this formula see Reference (4).

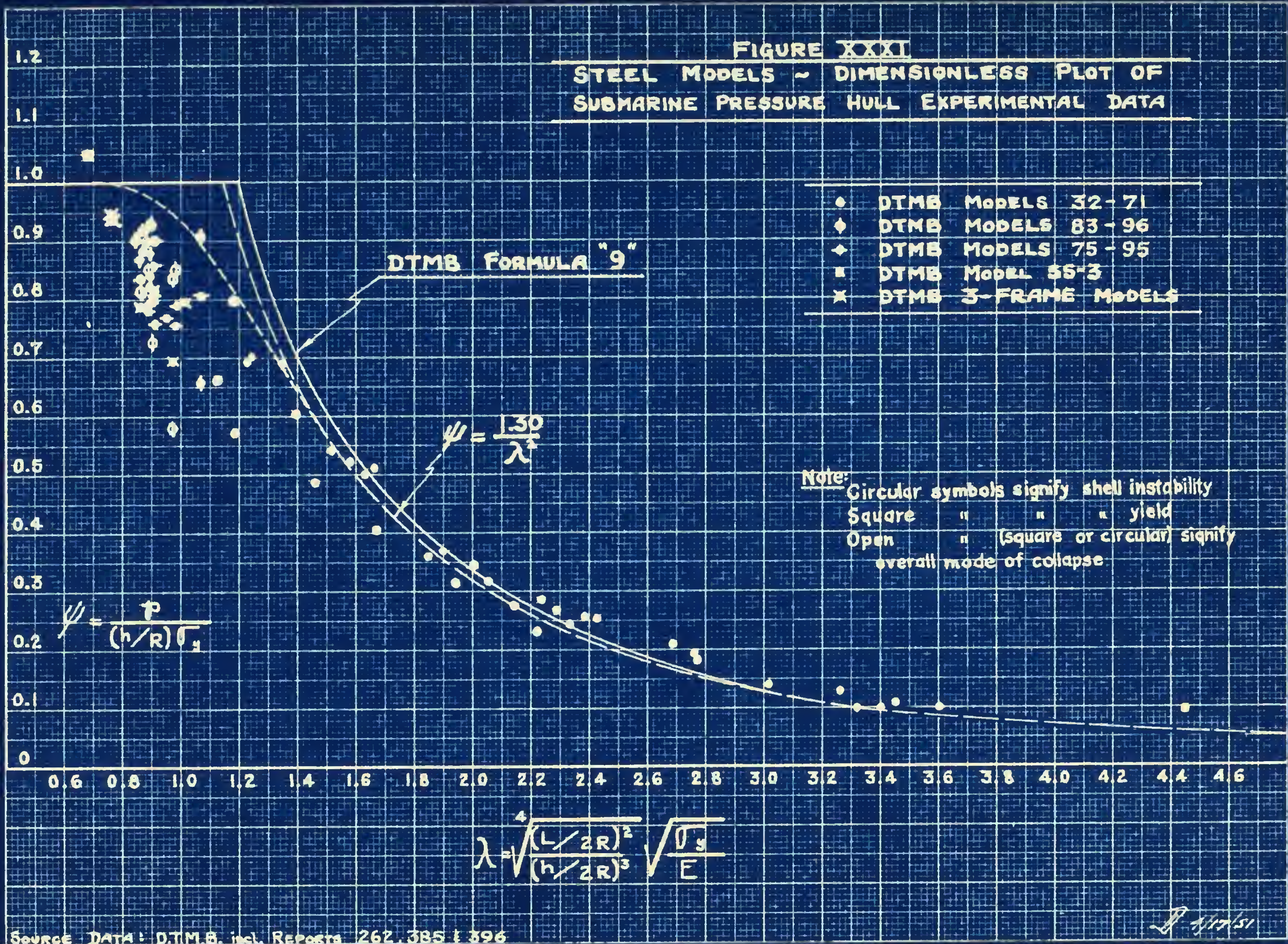
FIGURE XXXI
STEEL MODELS ~ DIMENSIONLESS PLOT OF
SUBMARINE PRESSURE HULL EXPERIMENTAL DATA
DTMB MODELS 32-71
DTMB MODELS 83-96
DTMB MODELS 75-95
DTMB MODEL 55-3
DTMB 3-FRAME MODELS
DTMB FORMULA "9"
$\psi = \frac{1.30}{\lambda^2}$
$\psi = \frac{p}{(h/R)\sigma_y}$
Note: Circular symbols signify shell instability
Square " " " yield
Open " (square or circular) signify overall mode of collapse
$\lambda = \sqrt[4]{\frac{(L/2R)^2}{(h/2R)^3}}\sqrt{\frac{\sigma_y}{E}}$
0.6 0.8 1.0 1.2 1.4 1.6 1.8 2.0 2.2 2.4 2.6 2.8 3.0 3.2 3.4 3.6 3.8 4.0 4.2 4.4 4.6
0 0.1 0.2 0.3 0.4 0.5 0.6 0.7 0.8 0.9 1.0 1.1 1.2
SOURCE DATA: D.T.M.B. incl. REPORTS 262, 385 & 396

It will be noted that ε is a function of the ratio of σ_y to E and will be different for steel and plastic. Figure XXXII shows the curves for Formula "9" for steel and "Lucite" assuming the E and σ_y values shown on the plot. The experimental model results are also shown on this plot. Figure XXXIII shows a similar plot except in Figure XXXIII, E for "Lucite" is taken as 327,000 psi; while in Figure XXXII, it is taken as 300,000 psi, the value determined by compressive tests conducted by the authors at a temperature of 69°F.

The experimental points in Figure XXXII, lie in a curve parallel to Formula "9" but somewhat higher. In Figure XXXIII the experimental points agree more closely with the theoretical Formula "9".

From Reference (6), for methyl methacrylate cast resin which includes "Lucite" and "Plexiglas" sheets, E for compression is 300,000 psi at 72°F. (no rate of loading specified) and is 350,000 psi at 55°F. The compression test conducted by the authors which gave E = 300,000 psi was conducted at 69°F. The tests of the submarine models were at temperatures ranging from 57 to 60.5°F. Interpolation of data in Reference (6) suggests that a modified value for E of 327,000 psi should be used for the submarine model tests.

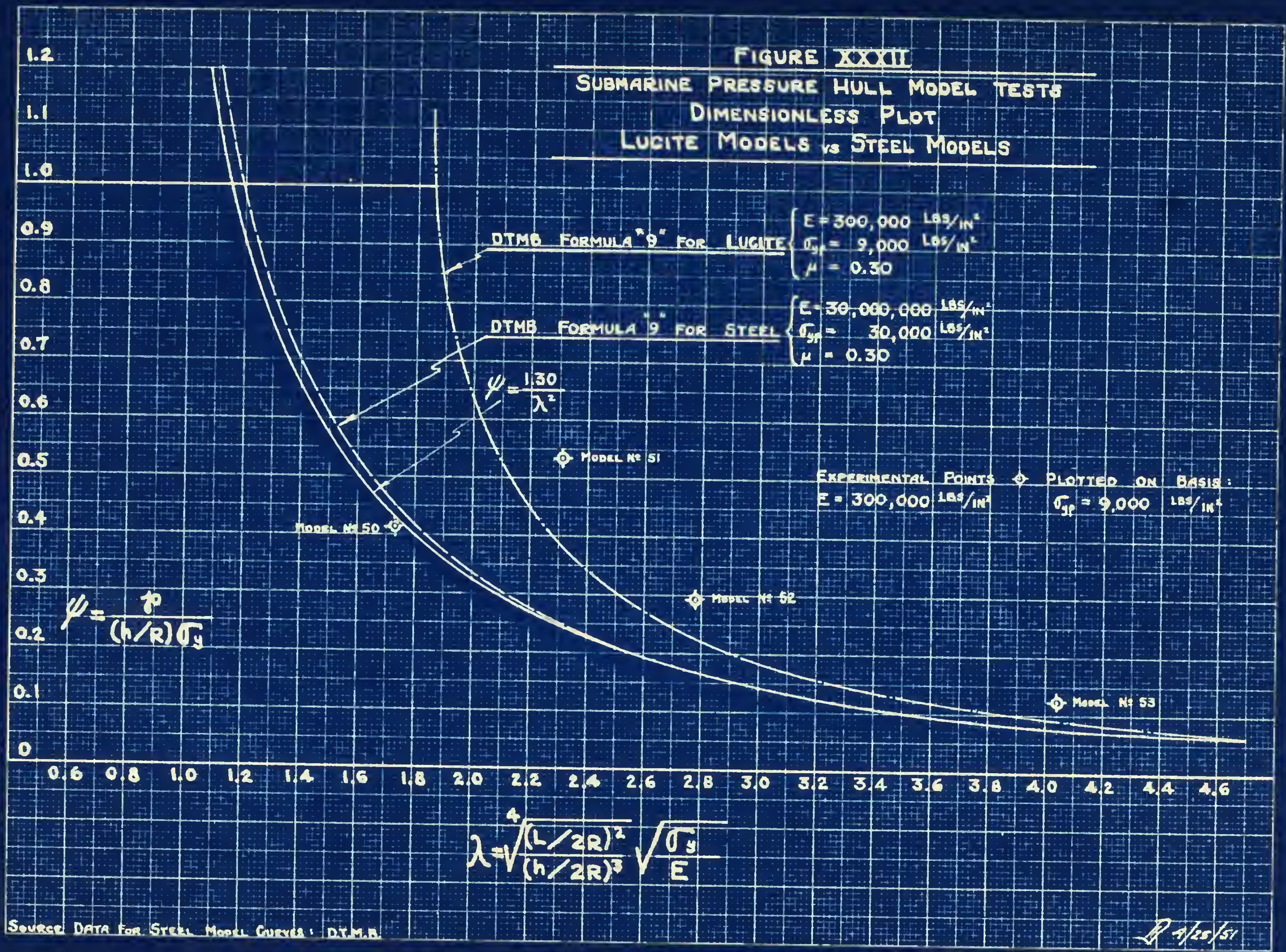

FIGURE XXXII
SUBMARINE PRESSURE HULL MODEL TESTS
DIMENSIONLESS PLOT
LUCITE MODELS vs STEEL MODELS
DTMB FORMULA "9" FOR LUCITE
E = 300,000 LBS/IN²
σ_{yp} = 9,000 LBS/IN²
μ = 0.30
DTMB FORMULA "9" FOR STEEL
E = 30,000,000 LBS/IN²
σ_{yp} = 30,000 LBS/IN²
μ = 0.30
$\psi = \frac{1.30}{\lambda^2}$
MODEL Nº 50
MODEL Nº 51
MODEL Nº 52
MODEL Nº 53
EXPERIMENTAL POINTS ⌖ PLOTTED ON BASIS:
E = 300,000 LBS/IN²
σ_{yp} = 9,000 LBS/IN²
$\psi = \frac{p}{(h/R)\sigma_y}$
$\lambda = \sqrt[4]{\frac{(L/2R)^2}{(h/2R)^3}}\sqrt{\frac{\sigma_y}{E}}$
0
0.1
0.2
0.3
0.4
0.5
0.6
0.7
0.8
0.9
1.0
1.1
1.2
0.6
0.8
1.0
1.2
1.4
1.6
1.8
2.0
2.2
2.4
2.6
2.8
3.0
3.2
3.4
3.6
3.8
4.0
4.2
4.4
4.6
SOURCE DATA FOR STEEL MODEL CURVES: D.T.M.B.
4/25/51

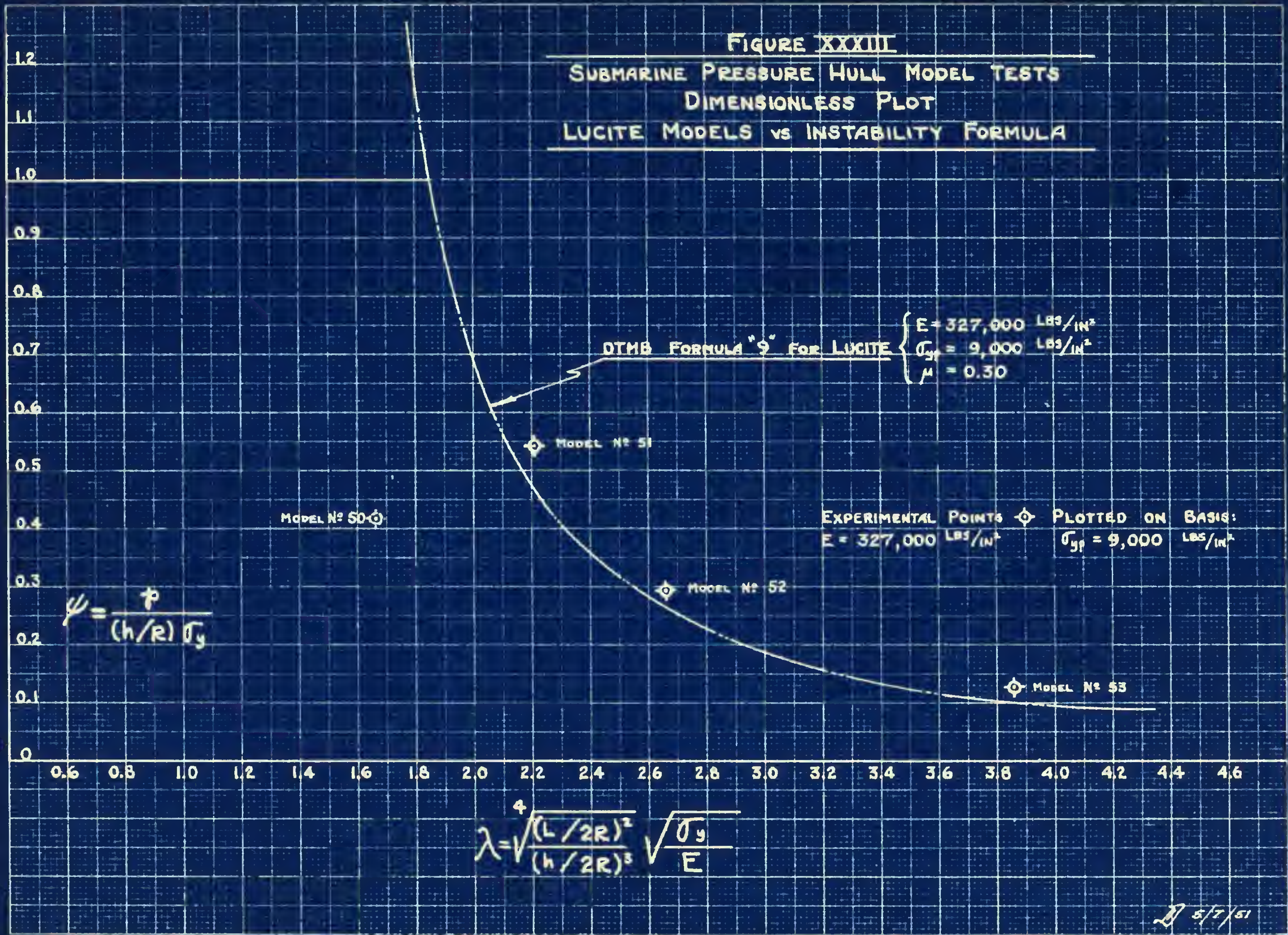
FIGURE XXXIII
SUBMARINE PRESSURE HULL MODEL TESTS
DIMENSIONLESS PLOT
LUCITE MODELS vs INSTABILITY FORMULA
DTMB FORMULA "9" FOR LUCITE
E = 327,000 LBS/IN²
σ_{yp} = 9,000 LBS/IN²
μ = 0.30
MODEL Nº 50
MODEL Nº 51
MODEL Nº 52
MODEL Nº 53
EXPERIMENTAL POINTS PLOTTED ON BASIS:
E = 327,000 LBS/IN²
σ_{yp} = 9,000 LBS/IN²
$\psi = \frac{p}{(h/R)\,\sigma_y}$
$\lambda = \sqrt[4]{\frac{(L/2R)^2}{(h/2R)^3}}\sqrt{\frac{\sigma_y}{E}}$
0
0.1
0.2
0.3
0.4
0.5
0.6
0.7
0.8
0.9
1.0
1.1
1.2
0.6
0.8
1.0
1.2
1.4
1.6
1.8
2.0
2.2
2.4
2.6
2.8
3.0
3.2
3.4
3.6
3.8
4.0
4.2
4.4
4.6
5/7/51

Reference books in the field of plastic give physical properties in very general figures such as $E = 3\text{-}5 \times 10^5$ psi and, hence, are not much help when a question arises as to whether to use E = 300,000 psi or 327,000 psi. This is apparently due in part to the lack of demand for such detailed information because of the manner in which these materials are normally used, and to the considerable variation in these properties with humidity, rate of loading, and temperature. It will be noted that for the methyl methacrylate resin "Plexiglas", R.T. Miller, using the same rate of loading in pounds per square inch as the authors and approximately the same temperature, determined E to be 370,000 psi.

From the foregoing, it may be concluded that the failures of the plastic models follow a general curve which has the same shape as the curve of Formula "9", and that the experimental data check with the formula results within the accuracy with which it is possible to determine E.

As in the case of the column tests, the submarine models tested represent as wide a range of sturdiness, measured by l/ρ for columns and by λ for submarine models, as could be incorporated in the models without introducing large secondary effects due to mechanical

imperfections. Also, as in the case of the column models, any given model tested can be considered as either geometrically similar to a certain steel prototype, or non-dimensionally similar to some other steel prototype based on having a common λ value. For instance:

Model	λ for "Lucite" model and non-dimensionally similar steel model	λ of steel model geometrically similar to "Lucite" model
50	1.73	.389
51	2.31	.528
52	2.785	.636
53	4.04	.925

Geometric Similarity Basis

Tests of the "Lucite" model give experimental results in agreement with Formula "9" which is a function of E and the model dimensions. Therefore, geometrically similar steel prototypes and plastic models should fail at pressures in proportion to their respective E values. Eliminating Model 50 data which are considered unreliable, the predicted collapse for geometrically similar steel models would be:

Model	Collapse Pressure for Plastic Model	Collapse of Steel Model from Fig. XXXI*	Predicted Steel Collapse
51	68 psi	651 psi	5820 psi
52	37 psi	651 psi	3170 psi
53	16 psi	651 psi	1370 psi

The models tested represent geometrically similar steel prototypes with λ values from .389 to .925. In this range steel prototypes are stressed beyond the proportional limit before the collapse pressure is reached. Paralleling the experience with columns and for similar reasons, the plastic models predict failure values for steel prototypes which are too high. Theoretically, as in the case of columns, reliable data concerning the collapse pressure of geometrically similar steel prototypes can be obtained from plastic models in the range where the steel prototypes are stressed below the proportional limit at collapse. However, the largest frame spacing used in our tests was on Model 53 and is about the maximum frame spacing which can be used on plastic models and maintain close out-of-roundness tolerances. Still, this spacing is less than the minimum required to be in the range where geometrically similar plastic models give reliable predicts.

* Very little exact data available. Figures given are approximately correct.

Therefore, as in the case of columns, there appears to be practical and theoretical considerations which make the use of geometrically similar plastic models unsuitable for predicting the collapse of steel prototypes.

<u>Non-Dimensional Similarity Basis</u>

Plastic models appear in a somewhat more favorable light when used to study the collapse of steel prototypes having common λ values.

Studying Figures XXXI-XXXIII, we see that the plastic model test data as plotted in Figure XXXIII and the steel model test data each vary from their respective theoretical curves of Formula "9" by about the same percentage of the ψ value for a given λ value. Hence, it should be possible to test a plastic model, compare the results percentage wise with Formula "9" for the plastic, and conclude that the steel prototype would fail at the same proportional relationship to Formula "9" for steel.

However, the results of such predictions using the method proposed are sensitive to variations in the E value used. This is especially true at low values of λ; say, less than 2.5. Figures XXXII and XXXIII illustrate this. Due to the steepness of the Formula "9" curve at low λ values, small variations in the relative

Therefore, as in the case of columns, close agreement in the practical and theoretical considerations which make the use of geometrically similar plastic models unsuitable for predicting the collapse of steel prototypes.

Non-Dimensional Similarity Basis

Plastic models appear in a somewhat more favorable light when used to study the collapse of steel prototypes having common λ values.

Comparing Figures XXVI-XXXIII, we see that the plastic model test data as plotted in Figure XXXIII and the steel model test data each vary from their respective theoretical curves of Formula VII by about the same percentage of the ψ value for a given λ value. Hence, it should be possible to test a plastic model, compare the results obtained with both Formula VII for the plastic, and conclude that the steel prototype would fail at the same proportional relationship to Formula VII for steel.

However, the results of both investigations using this method produced the inability to extrapolate to the ψ λ values used. This is especially true at low values of λ, less than 1.5. Figures XXXII and XXXIII illustrate this. Due to the asymmetry of the Formula VII curve at low λ values, small variations in the relative position of the experimental points and the Formula "9" curve mean large variations in the percentage difference between theoretical and experimental results. For this reason, it appears that plastic models should be used where a qualitative comparison is desired such as when conducting a research program investigating the effect of variation of some parameter, rather than for prediction of the collapse depth of a specific submarine design.

All models tested are in the region where the steel prototypes collapse before reaching the proportional limit. Beyond the proportional limit E in Formula "9" should be replaced by E_T or other modified E value. Since for steel models E_T approaches zero as the stress approaches the yield point, an instability failure occurs as the stress reaches the yield point. This is also evidenced by the fact that DTMB Formulas "92" and "92a" from Reference (5) include only σ_y and not E since they are for failure in this area.

In plastic models such as "Lucite", the E_T value at the "yield point" has only decreased some 20% below the initial value. Therefore, collapse by instability will not occur just because the material has reached the "yield point". As shown in Figure XXIX for columns,

the curves of data for steel models and plastic models no longer coincide after the proportional limit is reached. Had it been possible to conduct tests of plastic submarine models in this region, the results would undoubtedly have been similar to the column results, and the plastic model collapse pressures would have been higher than the steel results in this region.

A possible means of getting around the difficulty could be to take deflection readings of a plastic model with a low λ value, in the neighborhood of .70 to .80, and plot these readings so as to determine when a yield point was reached. Since reaching the yield point in a steel model would result in collapse, this point where the plastic model reached a yield point could be considered the collapse pressure. This approach appeared very encouraging until the dimensions of the "Lucite" models that would have the necessary low λ values were calculated. See table below:

Model Dimensions	λ	Distance Between Frames	Estimated Collapse Pressure ("Lucite")
9" dia. x 1/16"	.90	.282"	200 psi
"	.80	.222"	275 psi
"	.60	.125"	400 psi
16" dia. x 1/16"	.90	.245"	120 psi
6" dia. x 1/8"	.90	.675"	625 psi

The above table shows that it is not practical to construct "Lucite" submarine pressure hull models having low λ values. The first four models listed in the table above have h/2R ratios corresponding to the usual submarine practice. It can be seen that for such dimensions the spacing between frames becomes of the same order of magnitude as the width of the frame, and that secondary effects which are not present in the steel prototype (since it will not have this close spacing even though it has the same λ value), become large and make the results unreliable. The last model listed has a more acceptable distance between frames, but here the h/2R ratio for the model is three times the values commonly used for submarine design. Also, the test pressure becomes very high and therefore eliminates one of the advantages of plastic models. While the table is based on "Lucite", the distance between frame values would not change appreciably for any of the other common plastics including Cellulose Acetate, "Nylon" and "Plexiglas".

General Considerations

A general conclusion from the results of the "Lucite" submarine model tests and the column tests follows.

Models made of methyl methacrylate and other plastics readily available (such as cellulose acetate) are practical for studying the performance of steel prototypes in the region where the steel model collapses before the steel reaches the proportional limit. Such models should be constructed so as to have λ similarity to the prototype. Plastic models are neither practical nor reliable for predicting the collapse pressure of submarine pressure hulls when the steel prototype is stressed beyond the proportional limit at the time of failure. Unfortunately, this is the region in which modern submarines are designed.

While three or four tests are not sufficient evidence upon which to base a conclusion, it is believed that, in general, the construction of plastic submarine models - while more simple than the construction of steel models - is more susceptible to small errors such as local out-of-roundness. Hence, the test results of a series of plastic models would probably show more "scatter" than a series of similar steel model tests.

The frames used for all tests were 3/16" x 5/16" and withstood a maximum pressure of 69 psi. By DTMB Formula "88", from Reference (5) this frame should be good for a pressure of 68.2 psi. However, usual

practice is to consider that this formula is over-optimistic, and the usual working value is considered to be one-half the derived value. The frames in these tests, though tested to the full value of the formula rather than one-half as is standard practice, showed no signs of weakness.

The details of construction of the models tested proved very satisfactory. The use of a butt strap to make the longitudinal seam did not appear to introduce any difficulties or inaccuracies into the tests. The few leaks which developed in the longitudinal seam during the tests were stopped by removing the model from the test tank and putting a few drops of ethylene dichloride under the butt strap in the vicinity of the leak.

In order to save money, the same end bulkheads were used on every model. There was some difficulty here due to the variation in the inside diameters of the models from model to model and from end to end. The taper that was given to the rabbetted part of the bulkhead did not entirely solve this problem. On the model with the smallest diameter, the taper tended to wedge open the cylinder and slit the butt strap seam. On the largest diameter model, it was difficult to get the joint tight and this was probably the reason for

the premature failure. Using the bulkheads over again in successive tests presented the problem of securing watertight joints and still being able to remove the bulkheads after the test. "Miracle Adhesive" manufactured by the Miracle Adhesive Corporation was used for this purpose and worked very well.

The highest pressure on the circular bulkheads of the models was 60 psi. By Reference (14) the maximum stress in the 1/2-inch plastic end bulkheads at this pressure was:

σ = 6,800 psi if fixed ended support was considered to exist.

σ = 10,920 psi if simple support was considered to exist.

Compared to the physical properties of:

$\sigma_{\text{yield point}}$ = 9.000 psi. $\sigma_{ult.}$ = 14,800 psi.

The testing tank arrangement used was very satisfactory. Regulation of the pressure in the tank by throttling the recirculating line gave a very simple, smooth and accurate means of pressure control. The ease of using the water pressure from the tap instead of a pump as required for high pressure tests was particularly noticeable.

One of the most important features of this investigation of the use of plastic models is the relative cost of steel vs. plastic models. The four models tested cost a total of approximately $100. Of this cost, about one-quarter was fixed charges which could be spread over any number of models, reducing the cost per model to below $25 if more than four models were tested. To reproduce these models in steel models of the same size and simplified form would cost apporximately $125 per model. This is one of the important advantages of using plastic models for a series of tests involving many models.

The "time-edge effect" noted in photoelastic work with some plastics seems to indicate that plastics might change in physical properties with time, which would mean that models made of older stock would react differently than models made from newer material. However, examination of the literature and discussion with Professor A.G.H. Dietz and Dr. S. Yurenka of the M.I.T. staff indicate that no noticeable effect would occur unless the material was at least several years old.

The use of plastic submarine models offers many attractive possibilities. These include photoelastic study of the stresses around stress raisers such as

One of the most important features of this in-vestigation of the use of plastic models is the relative ease of [illegible] models. The four models tested cost a total of approximately $200. Of this only about one-quarter was direct charges which could be charged directly to models [illegible], the [illegible] more than four models were tested. [illegible] models of the same size and complexity would cost approximately $125 per model. This is one of the important advantages of using plastic models for a series of tests involving many models.

The "[illegible]" effect [illegible] work with [illegible] tend to indicate that plastics [illegible] which would mean that models made of these [illegible] react differently than models made from other materials. [illegible] of the [illegible] with Professor [illegible] and Dr. [illegible] of the [illegible] indicate that no [illegible] effect would [illegible] for material one at least several years old.

The use of plastic [illegible] models offers some interesting possibilities. These include photoelastic study of the [illegible] hatches, valves, frames, etc. There is relatively little known about the effect of these on submarine strength.

This thesis limited itself principally to models of plastics commercially available, and shows that these are limited in their usefulness, but that the field has great possibilities. The next step appears to be to overcome the difficulties pointed out in this thesis by developing a plastic with a stress strain curve of similar shape to that of the steel to be used for pressure hulls. This may be feasible, but is more in the realm of metallurgy and chemistry than Naval Engineering.

VI.
CONCLUSIONS

1. Simplified submarine pressure hull models constructed of commercially available plastics can be used to predict the collapse of steel prototypes subjected to hydrostatic pressure. Reliable results can be expected, however, only in the rather limited range where the prototype is not stressed above the proportional limit, and where λ -similarity is maintained between plastic model and steel prototype.

2. Conventional submarine designs do not fall in the above specified range.

3. Plastic models are recommended for qualitative evaluation of the effect of varying a given parameter, rather than for quantitative prediction of the collapse depth of one specific design.

4. Plastic models can be constructed in accordance with good commercial standards of workmanship and give reliable, consistent data.

5. Plastic models cost approximately one-fifth the cost of comparable small, simplified steel models, and may be tested satisfactorily with simple, inexpensive test apparatus.

VII.

RECOMMENDATIONS

Inasmuch as plastic submarine models do offer some definite advantages, particularly for research programs involving large numbers of models, it is recommended that efforts be made to expand their present limited range of applicability. Since this range is restricted, primarily, by the physical performance characteristics of commercially available plastics (specifically, the shape and nature of the stress-strain curve, and the yield stress-modulus of elasticity ratio), it is suggested that attention be given to the development of a plastic having a stress-strain curve similar in shape and nature to that of submarine hull steel but with lower absolute values. Use of such plastics would offer an extension of the range of model-prototype correlation to include conventional submarine designs.

VIII.

A P P E N D I X

APPENDIX "A"

Supplementary Introduction

Formulas and Theories of Failure

It is not the object of this thesis to attempt to evaluate existing theories for failures in steel submarine pressure hulls, nor the corresponding formulas for critical pressures and critical design parameters. Detailed discussions of such theories and formulas may be found in References (4) and (5). These formulas and theories must be referred to, however, for the insight they give as to the probable actual mode of failure of the steel model or prototype in order that the failure of the plastic models can be critically compared. In the range of large ratios of frame spacing to diameter, and low ratios of shell thickness to diameter, the shell will fail through instability; Von Mises and Windenburg have developed theoretical formulas for this range of failure. For excessively weak or flexible frames, the frames may collapse even though supported by contiguous shell; Tokugawa and Von Sanden and Gunther have formulated this type failure. For adequate strength of frames

and proper minimum spacing of frames, the plating may reach the yield point either in longitudinal stress at a point of local bending over the frame, or in transverse stress at mid-panel between frames; Von Sanden and Gunther have attempted to formulate these types of yield failure.

Design Parameters

From the above, and study of the references, it is apparent that the relative values of the various design parameters are of paramount importance: i.e., shell thickness (h), versus shell diameter (2R), versus frame spacing (L'), versus distance between frames (L), versus frame stiffness (I), etc.

Importance of E, σ_p, and σ_y:

One very important consideration in submarine design is that of weight; an acceptable design must produce the greatest collapse depth for a given weight of pressure hull structure. Within the limitations of the least weight solution, the several design parameters may be varied and adjusted so that the resultant structure may fail with what the literature commonly terms an "elastic instability" failure, or with what is referred to as a "yield" failure, or with an intermediate mode of failure which is often called failure

by "plastic instability." The meaning of these terms will be briefly outlined; for a more comprehensive treatise on the theory involved see References (4) and (5).

By an "elastic instability" failure is meant a failure (evidenced by bulging of the shell between frames) in which the combination of a relatively low value of h/2R and a relatively high value of L/2R permits the shell to evade the load before the shell is stressed above its $_{p}$; this situation is analogous to the behavior of a long and slender column which may buckle at a very low nominal stress.

By a "yield" failure is meant a failure in which the combination of a high value of h/2R and a low value of L/2R results in the shell being held up to the load and stressed to, or almost to, its yield point; at this high stress the instantaneous modulus E_T is so reduced that the actual form of collapse is through instability. Accordingly, a more proper description of this type of failure might be "instability at yield stress."

By failure by "plastic instability" is meant that type of failure that occurs when the composite effect of the h/2R and L/2R parameters is such that the shell is stressed beyond the proportional limit, but is not stressed to the yield point. (For example, each of the

two ratios, h/2R and L/2R, might have a value intermediate between its two values in the extreme cases of "elastic instability" and "yield"). Again, the value of the instantaneous modulus E_T decreases as the proportional limit is passed, and the actual form of failure is one of instability. Similarly, a more proper description of this type of failure might well be "instability between proportional and yield stresses."

For purposes of brevity, and in order to conform to the literature, the terms "yield failure", "failure by plastic instability", and "elastic instability failure" will be employed.

From the above, the significance of E, E_T, σ_p, σ_{yp} - ie., the shape and magnitudes of the stress-strain curve - for the submarine pressure hull steel is apparent. The stress-strain curve for such a steel is readily obtainable, and is essentially fixed and constant for the encountered ranges of temperature and rates of hydrostatic loading.

For most plastics, however, including the methyl methacrylates, the shape and magnitudes of the stress-strain curve may vary significantly according to the type of test (tension versus compression versus bending), the temperature, the rate of loading, etc. Note Figures XXXIV and XXXV.

FIGURE XXXIV

TRUE STRESS TRUE STRAIN CURVES (COMPRESSION)
METHYL METHACRYLATE (B285-1) VARYING MOL. WEIGHTS
TESTS AT VARIOUS CONSTANT RATES OF STRAIN

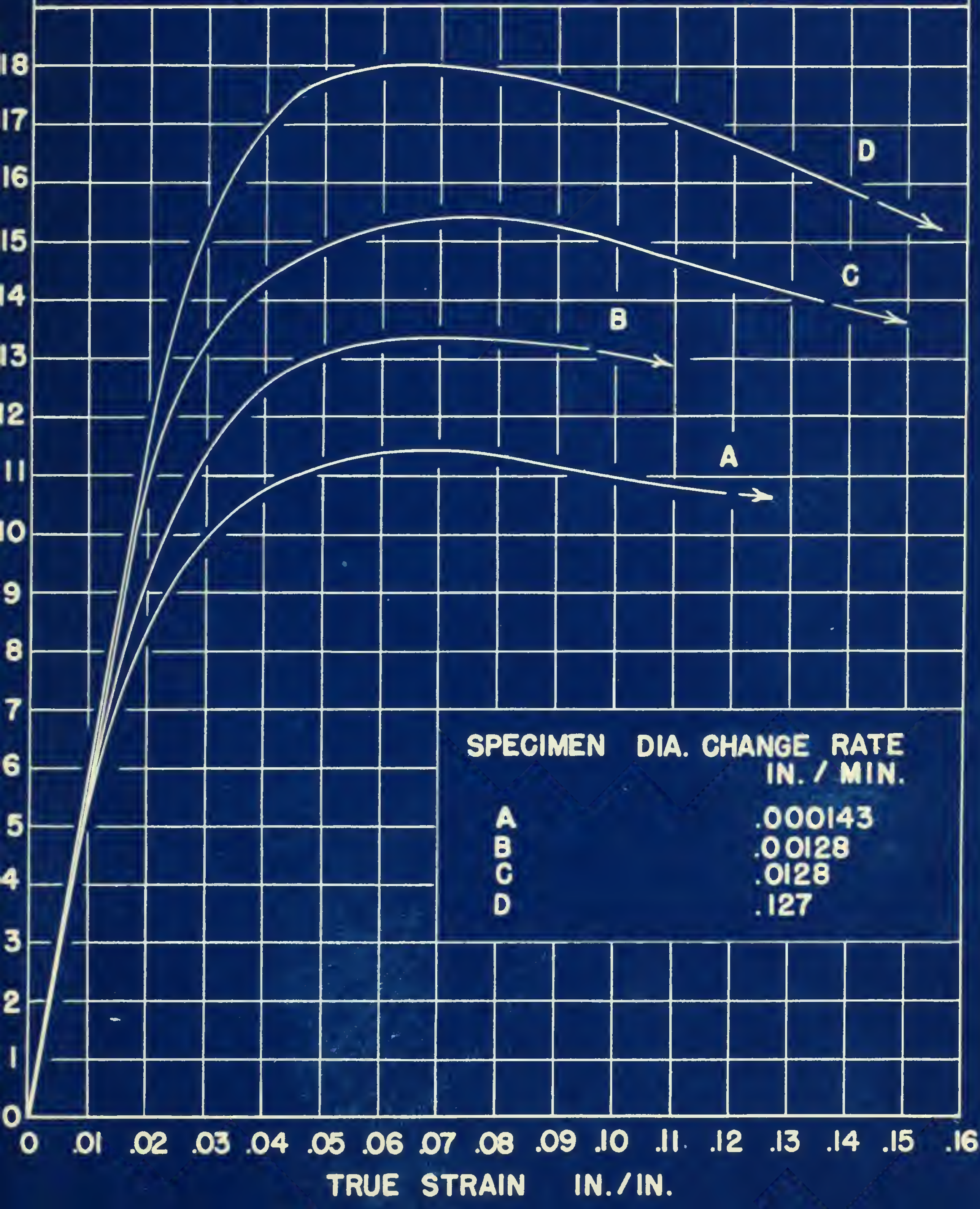

FIGURE XXXV

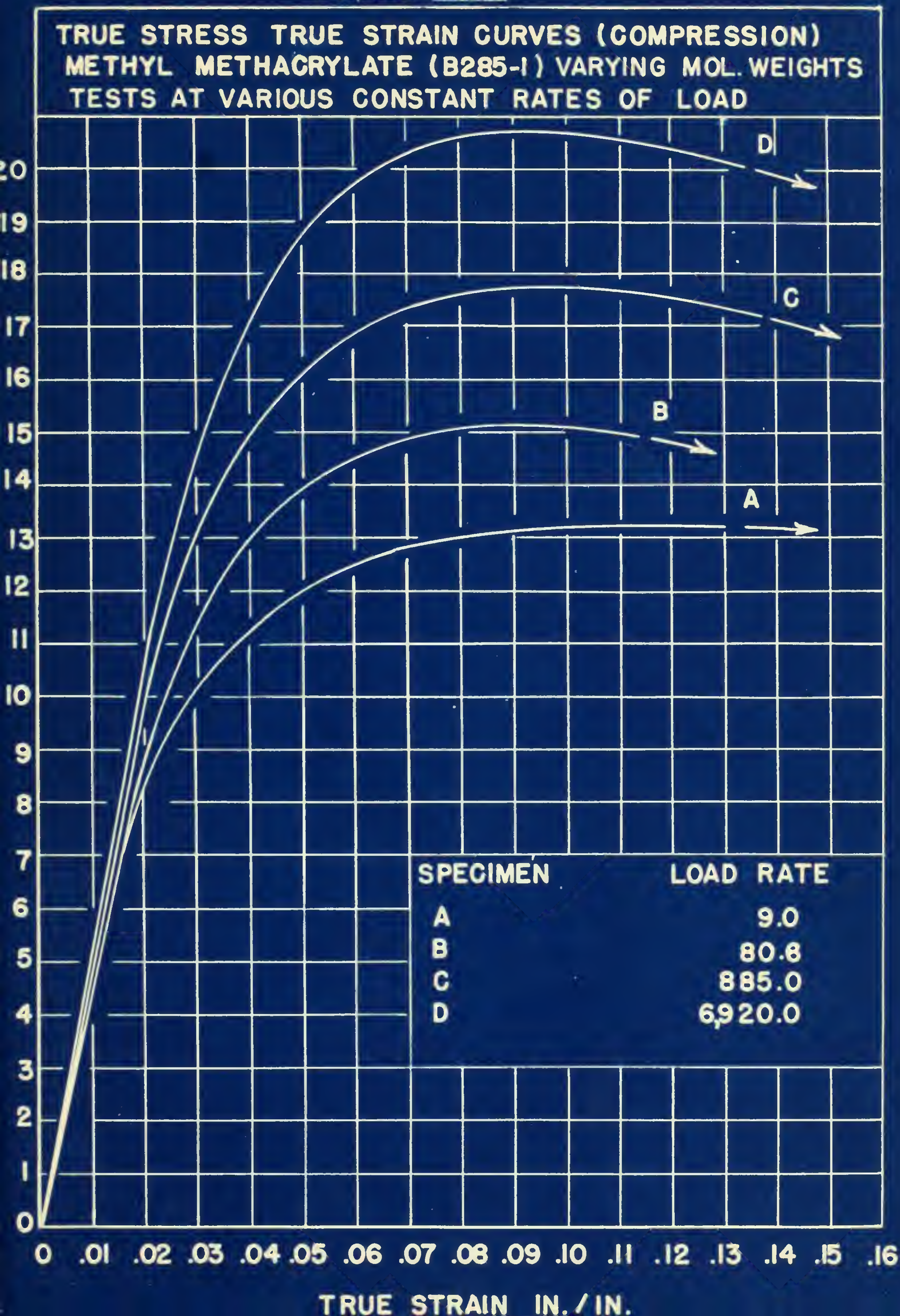
TRUE STRESS TRUE STRAIN CURVES (COMPRESSION)
METHYL METHACRYLATE (B285-1) VARYING MOL. WEIGHTS
TESTS AT VARIOUS CONSTANT RATES OF LOAD
D
C
B
A
SPECIMEN LOAD RATE
A 9.0
B 80.6
C 885.0
D 6,920.0
0 1 2 3 4 5 6 7 8 9 10 11 12 13 14 15 16 17 18 19 20
0 .01 .02 .03 .04 .05 .06 .07 .08 .09 .10 .11 .12 .13 .14 .15 .16
TRUE STRAIN IN./IN.

Basis of Steel-Plastic Comparison

The foregoing brief and oversimplified summary of some of the differences between steel and plastic presents one of the most important problems that confronted the authors: Upon what basis could steel and plastic submarine models be compared? Which design parameters or parameter ratios should be held constant? Could the respective sets of models, steel versus plastic, be reduced to a truly comparable set of dimensionless parameters in which the effect of variables such as σ_y, E and μ are eliminated or reduced to an insignificant degree? What variables between steel and plastic are relatively fixed, what are controlled to some degree (as by rate of loading), and what are essentially independent - and, perhaps, unpredictable?

Brief History of DTMB Work on Plastic Models

During the period June through August, 1950, one of the authors, Cdr. E.F. Durfee, had the opportunity to observe the preliminary work done by the David Taylor Model Basin upon plastic submarine models. The work by DTMB has been periodically reviewed by the authors to this date, and is briefly summarized. DTMB has not as yet completed any programs involving the use of plastic submarine models, nor reported any results thus far.

Initial experimental tests by DTMB upon plastic submarine models involved cellulose acetate models. The models were about 16 inches in diameter, about the same length, and approximately 1/8 inch shell thickness. The shell was formed from flat sheets with a longitudinal seam reinforced by a butt strap on the inside of the shell. Rectangular frames, machined from flat sheets, were fitted inside the shell, and were suitably notched for the shell seam strap. This type model gave trouble through weakness and non-circularity at the shell seam, and the frames demonstrated a tendency to fracture where notched. Preliminary tests with these models employed stress-coat, and whitewash, as devices to attempt to indicate the advent of incipient failure or collapse. Verbal reports from DTMB representatives indicate these first models gave inconclusive indications of results.

Another set of three (3) methyl methacrylate models has been manufactured by DTMB, and is ready for test. These models are also of approximately 16 inch length and diameter and 1/8 inch shell thickness, and are of constant total weight of frame material. One model is intended to fail by shell instability, and has all frame material concentrated in four (4) $\frac{1}{2}$" x $\frac{1}{2}$" well separated frames. In another model, it is expected

that the frames will fail: this model has eight (8) 1/4" x 1/2" frames, with the frame space approximately one-half that of the model first described. The third model has an intermediate arrangement of frames, six (6) 3/8" x 1/2" frames. In this series of models, the main variable has been the number and spacing of constant depth frames of a constant total frame weight. For this group of models, the shell strap is run longitudinally on the exterior of the model, and the individually machined one-piece rectangular frames are fitted inside the shell, thus avoiding any notches or other discontinuities in the frames.

The experience of DTMB in manufacturing plastic models was drawn upon by the authors in designing and constructing their models in regard to techniques of shaping the shell mandrel, heating the shell sheet, forming the shell, designing frame rings, choice and use of solvents, etc.

Work by Cdr. R.T. Miller at DTMB

During August, 1950, Cdr. R.T. Miller, of the M.I.T. group at DTMB, began a series of column compression tests on "Plexiglas," a methyl methacrylate, in order to initiate an investigation of the behavior of "Plexiglas" columns. Cdr. Miller ran a series of

columns in compression buckling tests and compared his results with Euler's Column Curve. The specimens, dimensions of which are detailed in appropriate tabulations in Appendix "C", were accurately sawed to breadth and width, and the ends carefully milled to true and parallel planes. The columns were tested as "fixed ended" columns. After some unsatisfactory attempts with plaster-embedded base plates, the tests were run similar to those later conducted on "Lucite" by the authors, with no special mounting plates other than those furnished with the testing machine. The tests were run at fixed rates of loading. Points of buckling, or "visible buckling," were noted by careful visual observation. A compressive stress-strain plot was prepared from crush test of one short specimen.

When Cdr. Miller dropped preliminary plans to work with the authors on this thesis, he generously furnished the authors with his data, which has been used by the authors to supplement and corroborate the data obtained by the authors in their tests of "Lucite" columns.

APPENDIX "B"

Details of Procedure

Choice of Plastic

Prior to choice of the plastic to be utilized, a variety of materials were investigated, and consultations held with, among other authorities, Dr. Edward Wenk, Jr., of DTMB, Dr. A.G.H. Dietz and Dr. S. Yurenka of the Department of Building Engineering and Construction, M.I.T., Dr.C.H. Norris of the Department of Civil and Sanitary Engineering, M.I.T., and Dr. J.P. Den Hartog and Dr. E. Orowan of the Department of Mechanical Engineering, M.I.T. Much of the study centered upon the search for a plastic with a stress-strain curve similar in shape to that of steel, with a distinct yield point, and with a ratio between stress and initial modulus of elasticity approximating that of steel.

Among the materials studied to the point of conducting stress-strain compression tests were methyl methacrylate, cellulose acetate, and nylon; see Figure X and Tables VIII-XVII. Another material investigated was neoprene ebonite. A consideration in connection

with all materials was the question of the availability of the sheets and stock required for construction of column models and of submarine models.

Extensive study indicated to the authors the necessity for choosing an acceptable and available material, even though the selected material might not be the optimum, on a theoretical basis, as regards stress-strain curve and yield-modulus ratio.

Accordingly, "Lucite", a methyl methacrylate, was chosen. In addition to the advantages listed in the body of the thesis, this material - in the almost exact thickness desired - was found to be available at the Forest Products, Inc., Cambridge, Mass., a concern capable of manufacturing the desired column and submarine models, and possessed of the required experience in heating and forming the "Lucite" shell and frames.

Detailed disadvantages of the "Lucite" material are developed elsewhere in this thesis, and will merely be listed here. The primary disadvantage is the stress-strain curve shape, and the discrepancy between Lucite's yield-modulus ratio and that of steel. As with most plastics, "Lucite" exhibits a greater degree of non-uniformity of material scantlings, chemical composition, and physical characteristics than does steel. Other

"Lucite" disadvantages characteristic of most plastics include: the change in stress-strain behavior, modulus value, ultimate strength, and "creep characteristics" with change in rate of loading; susceptibility to humidity; possible dessicating effects of prolonged periods of time;"crazing"; and weakening effects of solvents; and uncertainties as to behavior under different conditions of, and rates of, tension, compression, and bending.

It is of interest to note that the published literature concerning plastics, or even the unpublished data compiled by the M.I.T. plastics group, appears quite meager in regard to determination of physical performance characteristics for plastics such as values for yield stress, modulus of elasticity, Poisson's ratio, etc., under specified conditions of loading and rates of loading. This is due in great part, no doubt, to the sensitivity of these physical characteristics to the chemical composition and conditions of manufacture of each lot of plastic. Another factor is probably the relatively small emphasis on physical characteristics for many uses, and the greater concern with molding behavior, dielectric properties, etc.

<u>Plastic Column Tests</u>

"Lucite" columns, Models Nos. 15 to 21, were made by Forest Products, Inc., from commercial grade one-half inch "Lucite" cut to width by a circular saw. The ends were cut by saw, and then finished to exact length, planeness, and parallelism by continuous belt wet sander. Models Nos. 22 to 24 were cut by the authors from Model No. 21, using a band saw and a continuous belt dry sander.

Column Models Nos. 16 to 21 were chosen to check, and to expand, the range covered by Models DTMB No. 0-9, and, in particular, to secure points to be used to compare with steel column data when plotted on a non-dimensional basis such as on Figure XXIX.

The test apparatus utilized in the column tests is that located in the M.I.T. Plastics Laboratory, Building 20. Column tests were performed by the authors under the guidance of Dr. Steven Yurenka. A 1/10,000" dial gage was first used to check the rate of automatic cross head travel which was adjusted for each specimen. Concurrently, a test weight was used to check and calibrate the continuous and automatically ink-trace-recording load cell. For the actual test, one 1/10,000" and one 1/1,000" dial gages were used at mid-height and mid-breadth of the model to record transverse deflections in the plane of minimum

moment of inertia, while a second 1/1000" dial gage was used to check the rate of travel which was automatically recorded by proper gear setting in the ink trace. Periodic readings of travel versus load were recorded to check the automatically recorded data.

Particular care was given to the transverse deflection dial gages in order to determine the point of incipient buckling, or non-linearity of deflection, by these dial gages, rather than by reliance on visible buckling. (As noted in the "DISCUSSION," the "Plexiglas" column data of August, 1950, tended to show excessively high values of critical loads; the authors suspected that buckling had actually started a finite load increment before the "visible buckling" could be detected).

Upper and lower loading anvils were treated with silicon oil in an effort to avoid "binding" and distortion of the loaded ends as the (shorter)columns attempted to conform to Poisson's ratio.

Design of Plastic Submarine Models

From purely theoretical considerations, the authors would have preferred to have tested plastic models in sufficient number and of proper characteristics to define

by test spots the entire $\lambda - \psi$ curve from $\lambda = 0.4$ to about $\lambda = 3.0$. There were, however, several impediments.

Among the non-theoretical considerations were those of available money and time, and the selected interrelated physical limitations as to maximum diameter of model and maximum pressure of the test tank, the design and procurement of which had to go forward fairly early in the thesis work. Considerations of desired tank pressure and model size led to choice of a design inside diameter of models of nine inches. Although the tank was built and tested to 100 pounds per square inch, available water main pressure indicated a desirable pressure limit of about 70 pounds per square inch gage.

One feature of the plastic submarine model design that gave the authors cause for anxiety concerned the problem of "out-of-roundness." Lack of true circularity, particularly at a longitudinal seam, has been observed as a point of potential and probable weakness in steel submarine models, and in the preliminary plastic submarine model tests conducted by DTMB. Accordingly, the authors endeavored to find a commercial source of plastic seamless tubing of a practicable h/2R ratio. The largest diameter tubing which the authors could find on the

commercial market is six inches, with a wall thickness of one-eighth inch; thus, a $h/2R$ value of 0.0104. As developed in more detail under "DISCUSSION OF RESULTS," so great a $h/2R$ ratio would lead to a low λ value, heavy and closely spaced frames, and high pressures. Accordingly, the design was developed employing a longitudinal seam in a thin shell of large diameter, with circularity maintained by external butt strap and snugly fitted internal frames.

A study of conventional submarine designs indicated that, for geometric similarity, a model shell thickness of approximately 0.055 inch for an inside diameter of nine inches was desirable. With "Lucite" available in nominal thicknesses of 0.040 inch, 0.050 inch and 0.060 inch, the design was premised upon 0.060 inch shell thickness. For geometric similarity to modern submarine design the resultant distance between frames on Model No. 52 was estimated to 1.35 inches. The intended λ value was 1.93; the actual λ value of the completed model was approximately 2.79, the difference resulting from variations in h, σ_y and E of the actual "Lucite" from which constructed.

In order to limit to the greatest practicable extent the number of variables involved, and in order to keep the cost and time of manufacture within bounds, all four (4) submarine models were designed for constant

diameter and shell thickness (as well as frame size), with the frame spacing used as the prime variable. Model No. 53, with a designed λ value of 2.8 and an actual λ of 4.04 as built, was designed as the largest λ value desired. At the design stage, the authors hoped that this model could be tested to "failure" without destruction, and be unloaded without damage to permit subsequent re-testing; this hope was not fulfilled.

Model No. 50, with a λ value of 1.2 as designed, and 1.73 as built, had a distance between frames of 0.52". This was the closest frame spacing used, a minimum adopted for the following reasons: (1) anticipated difficulties in building a model with closer frame spacing, and, (2) belief that the resultant structure could not possibly fail in the lobe pattern of a steel model, but would have a failure significantly influenced by secondary effects at the frames. (At the design stage, the authors expected this model to fail in an overall mode including fracture of the frames.)

Model No. 51, with a designed λ of 1.6 and a λ of 2.31 as built, was intended to fill in the λ range between Models 50 and 52.

ciency and small distance (as well as those also);

Since the frame spacing used is the prime variable, Model No. 92, with a designed λ value of 2.0 and an actual λ of 1.84 as built, was designed as the largest λ value studied. At the design stage, the authors hoped that this model would be tested to failure without destruction, and in advance without damage to permit subsequent re-testing; this hope was not fulfilled.

Model No. 95, with a λ value of 1.0 as designed, and 1.78 as built, has a distance between frames of 9.35". This was the closest frame spacing used, a distance adopted for the following reasons: (1) anticipated difficulties in building a model with closer frame spacing, and (2) belief that the resulting structure would not possibly fail in the mode typical of a long model, but would have a failure significantly influenced by secondary effects of the frames. (In the British study, the authors expected this model to fail in an overall mode including fracture of the frames.)

Model No. 91, with a designed λ of 1.5 and a λ of 1.71 as built, was intended to fail in the λ range between models 92 and 95.

Note is made that to design a plastic model (of the chosen thickness and diameter) for λ similarity to a conventional submarine design would have required a frame spacing smaller than Model No. 50. See "DISCUSSION" for further details. Thus, the resulting series of four (4) plastic models, while covering the maximum feasible range of λ values, does not go to as low λ values as would be desirable for λ-similarity to existing design nor to the even lower λ values desirable for full coverage of the entire contemplated λ range.

The problem of frame size was approached in the following manner. A steel H-beam consistent with current submarine practice was taken as the datum, to accompany Model No. 52. On the basis of approximating the faying flange, to suitable scale, a frame width of 3/16" was chosen for the plastic models. The actual H-frame was then replaced by a rectangular frame having a faying flange of width corresponding to the 3/16" dimension suitably scaled up. The depth of the steel rectangular frame was calculated on the basis of maintaining the I of the combined section, frame plus faying portion of shell, about its own neutral axis. Additional calculations were made on the basis of moment of inertia

of the frame plus entire frame spacing of shell, and of the frame alone, in order to avoid any possible unusual disparity in any one of these criteria. The range of rectangular frame depths obtained from the above calculations were then scaled down to the plastic model size - a nominal depth of 5/16" was selected as satisfying the requirements for I on the various bases outlined above, as well as providing a definite "directional stability" to the frame. That is, the 5/16" depth gave the model frame a definitely greater I about one axis than about the other, and avoided the equality of stiffness that, for example, a square frame would provide.

Once the frame spacings and frame size were determined, the model lengths could be chosen. Several criteria were applied: the model length should approximate the model diameter, but the number of frames need not exceed six (6); the spacing between the end diaphragm and the first frame was to be less than the normal frame spacing; and the minimum number of uniformly strong frame spaces was to be two (2). The model lengths specified on Figures II-V result from application of the above criteria.

End diaphragms for use with the plastic submarine models were designed to consist of a 9" x 3/8" disc

with an integral 9-1/8" x 1/8" flange. The 1/8 disc was designed to support the end panel of the shell, permit a tight end joint, and minimize the possibility of longitudinal bending in the shell at or near the end. The integral 1/8" x 9" flange was designed to withstand the end loading, and was calculated to carry, in shear, an end pressure of approximately 100 pounds per square inch gage.

Manufacture of Plastic Submarine Models

The material used for all parts of the plastic submarine models was "Lucite", acrylic resin cast sheeting, U.S. Army-Navy Specification AN-P-44. The shell material was 1/16" flat sheet heated to approximately 240-300°F. and wrapped upon a rubber covered wooden mandrel, with surplus material for a butt strap, and held until the temperature dropped to about 150°F. The shell then trimmed to size, a butt strap applied on the outside, and "welded" with ethylene dichloride solvent.

A wooden jig for molding frames to the nine inch inside diameter of the cooled shell was then constructed, and the frames were heated as above and formed to shape, with excess length, from 3/16" x 5/16" flat rods cut by table saw from 3/16" sheet.

The final tubes were not perfect cylinders in all cases, but had slight variations in diameter as listed on Figures XVII-XXII. Frames were individually fitted and cut to length for a press fit. Where necessary in final fitting, additional filler pieces were pressed into place and cemented into the frames.

All final fitting and cementing of frames was done by the authors. In all cases, frame butts were carefully staggered and in no event were frame butts permitted to fall near the shell seam in the middle frame spaces. The procedure in setting frames was as follows. First, the length of the tube was carefully checked, and any deviation from specified length adjusted for in setting the frame ring nearest the truest end of the tube. Three gage blocks, approximately $3\frac{1}{2}$" long x 1/2" wide were then carefully filed and sanded to the exact spacing between frames at the three points of contact on each block, ends and center. With the butt steadied over the center of one of the three equi-spaced gage blocks, the next frame was carefully located and "tack welded" with a fine syringe containing solvent. More and more points were so secured, and the gage blocks slid around the periphery, until the entire ring was located properly, at which point the entire frame was

The final tubes were not checked optically in all cases, but had slight corrections in alignment as listed in Figures XVII-XXII. Frames were individually fitted and sawed to length for a press fit, where necessary to final fitting, individual friction pieces were pressed into place and cemented into the tubes.

All final fitting and assembling of frames was done by the authors. In all cases, frame ends were carefully chamfered and, if so fitted, were frame mounts permitted to fall down the tube to the middle frame spacer. The procedure in fitting frames was as follows. First, the length of the tube was carefully checked, and any deviation from specified length allowed for in setting the frame ring against the thrust end of the tube. Three cork blocks, approximately 1/4" long x 1/4" wide were then carefully fitted and cemented to the exact spacing between frames at the three points of contact on each block, each set. With the tube standing over the center of one of the three cork-capped cage blocks, the next frame was carefully lowered and "tacked" with a fine spruce containing solvent, and more points were so cemented, and the cage blocks slid around the periphery, until the entire ring was located properly, at which point the other frame was cemented in place and the butt cemented, caution being exercised to prevent any solvent from running over the shell surface except in way of the frame. All frames were so located and cemented, the gage blocks being progressively cut down in size from Model No. 53 to Model No. 50.

Plastic Submarine Model Tests

For all models the end diaphragms were temporarily glued on by generous use of Miracle Black Magic Adhesive, a heavy-bodied, fast drying, waterproof (when dry), self-bonding adhesive manufactured by Miracle Adhesives Corporation, New York, N.Y. This adhesive was selected after extensive preliminary tests involving such varied materials as Duco Household Cement, Weldwood, etc. Experience showed an optimum time for test of the model after affixing ends: after about 15 minutes the surface of the adhesive was tough enough to resist penetration, while the main body of the adhesive was pliable enough to keep tight under local bending and compression. When too dry the adhesive tended to be too brittle; when too wet, it flowed out under water pressure. The adhesive did not harden under water, and readily permitted removal of the end diaphragms on completion of a test.

cemented in place and the bolt inserted, caution being exercised to prevent any solvent from running down the shell surface except in way of the frame. All frames were so treated and [illegible], the [illegible] being progressively [illegible] from 1/4 inch from Model No. 3 to Model No. 5.

<u>Elastic Deflection Model Tests</u>

For all models the SR-4 [illegible] were temporarily fixed on by excessive use of [illegible] adhesive; a heavy-bodied, fast drying, waterproof (when dry), self-sealing adhesive manufactured by Minnesota [illegible] Corporation, New York, N.Y. This adhesive was selected after extensive preliminary tests involving such varied materials as Duco Household Cement, Vellumoid, etc. Experience showed it [illegible] that the back of the gage after affixing [illegible] after about 12 [illegible] the surface of the adhesive was hard enough to permit [illegible], while the main body of the adhesive was pliable, enough to [illegible] compression. When dry the adhesive seemed to be [illegible]; when wet, it [illegible] and [illegible]. The adhesive did not harden under water, and readily permitted removal of the [illegible] or [illegible] of a [illegible].

Experience with the first models showed the vulnerability of the seams to leakage along the seam. Accordingly, the seams and seam straps were generously plied with solvent - resulting in the use of more solvent on the seams than might otherwise be required.

For Model No. 53, the dial gage arrangement was checked out in the inverse position before assembling the model, and before bolting the model to the steel flange. For this model the dial gages were mounted at mid-height of the lower panel, and clear of the seam. Dial gage readings were taken up to the point of failure.

In mounting Models Nos. 52 and 51, the upper "Lucite" diaphragm was left bolted to the steel flange, and the shell and then the lower diaphragm glued on. The test of Model No. 52 was interrupted by a serious leak at the lower end of the seam. The model was removed from the tank, this crack was sealed with solvent, and the test re-started and carried to conclusion without further incident. No dial gage readings were taken.

Similarly, no dial gage readings were taken on Model No. 51, but careful visual and touch observations were made. This test was carried through without incident. This test pressure exceeded calculated pre-

dictions, and threatened to go beyond the limits of the pressure gage; the critical pressure was reached just as the usable range of the gage was approached.

Model No. 50 suffered all the mechanical breakdowns and material failures avoided by Models Nos. 51-53. To provide for the logical increase in pressure above Model No. 51, prior to the test of Model No. 50 the authors procured and installed a high pressure hand hydraulic pump and a 200 pounds per square inch capacity pressure gage, as shown on Photograph No. 1 and Figure XVIII. Because of the difficulty in examining the entire inner surface of the shell and frames in the time allowed under the chosen load rate, dial gages were again mounted, as shown in Figure VIII. clear of frames and seam in the middle frame space. The function of these dial gages was to detect the yield point or point of buckling of the model by any non-linearity of deflection readings. Model No. 50 was first fitted with the same end diaphragms as used on Models Nos. 51-53 and fitted as shown for such models on Figure VI. The lower diaphragm flange sheared off in Test A, however, under a relatively low pressure. For later tests the lower diaphragm was modified, and both diaphragms were re-installed, as detailed for distinct, are considered to be beyond the limits of the pressure range the artificial pressure was reached just as the plastic range of the case was approached.

Model No. 49 suffered all the mechanical break-downs and material failures typical of models Nos. 51-56. To provide for the lateral increase in pressure above model No. 44, prior to the test of Model No. 49 the authors designed and installed high pressure test hydraulic pumps and 8,000 pounds per square inch hydraulic pressure range, as shown in Photograph No. 3 and Figure XVIII. Because of the difficulty in retaining the entire inner surface of the shell and frames in the time allowed under the design load tests, this shell was again repeated, as shown by Figure VIII. Water of frames and mostly the middle frame space. The function of these dial gages was to record the yield point or point of buckling of the model by any non-linearity of deflection readings. Model No. 49 was first filled with the same end thicknesses as used on models Nos. 51-56 and fitted as shown the loop models on Figure VI. The inner-diaphragm flange sheared off in Test 4, however, under a relatively low pressure. For later tests the inner diaphragm was modified, and with diaphragms were re-installed, as detailed for-

Model No. 50 on Figure VI. The lower head quilting bolts, and the load-spreading washers shown, were waterproofed with cotton grommets smeared with miracle adhesive. As will be noted from the results, Model No. 50 failed prematurely at a lower pressure than Model No. 51; accordingly, there was no need to use the hand pump that had been provided, and the maximum pressure was obtained directly from line pressure.

APPENDIX C

Data and Calculations

Tables VII-XVII contain a summary of the test data taken during tests of "Lucite" and "Plexiglas" columns.

"Plexiglas" data were taken in the form in which tabulated as the tests were being run.

The "Lucite", "Nylon" and Cellulose Acetate data were automatically recorded during the actual tests by an ink graph of force vs. time made by the testing machine. The authors recorded the readings for lateral and vertical deflection on these graphs at the appropriate values of force and time. The graphs are ten inches wide and have a total length of approximately 80 feet; the tables that follow are a summary of the data recorded on these graphs.

APPENDIX "B" describes the procedure followed by the authors in conducting the tests of plastic columns.

APPENDIX C

Data and Calculations

Tables VII-XVII contain a summary of the test data taken during tests of "[illegible]" and "[illegible]" columns.

"[illegible]" data were taken in the form in which tabulated as the tests were being run.

The "[illegible]", "[illegible]" and [illegible] data were automatically recorded during the actual tests by an X-Y [illegible] of [illegible], made by the [illegible] company. This [illegible] recorded the results for lateral and vertical deflection at these points at the appropriate values of force and time. The [illegible] are two inches wide and have a total length of approximately 30 feet; the tables that follow are a summary of the data recorded on these graphs.

APPENDIX "D" describes the procedure followed by the authors in computing the [illegible] of elastic columns.

APPENDIX "D"

Supplementary Discussion

Shapes of Stress-Strain Curves

Typical shapes of stress-strain curves for shipbuilding steels are indicated on Figure XXIV. Most of the steel curves are characterized by a distinct and definite yield point, which often occurs in the characteristic "drop of the beam" phenommnon as illustrated by the "Medium Steel" curve of Figure XXIV. Many High Tensile steels exhibit the other stress-strain curve shown on the same figure; these HTS curves show high values of E, $\sigma_{p.l.}$, $\sigma_{y.p.}$, and a distinct, rapid, and permanent drop in the value of E at the yield point. The third and last curve on Figure XXIV, in comparison, is typical of the methyl methacrylates (regardless of rate of load) including its lack of a distinct yield point. Thus, for "Lucite" we are forced to employ some arbitrary definition of "yield point" involving a percentage of elongation, or percentage of initial modulus, etc.

Comparison of the steel and plastic curves in Figure XXIV is informative. At low stresses the two

Table No. VII

Summary of Experimental Column Data

In Tables Below: L = Length of Equivalent Pin Ended Column, ρ = The Gyradius And σ_{yp} Equals The .002 Yield Stress

Plexiglas And Lucite Column Data

Model	Stress (σ_u)	L/ρ	σ_{ult}/σ_{yp}	$L/\rho \sqrt{\sigma_{yp}/E}$	$\frac{\sigma_{yp}}{E} \times 10^4$
0	13,320 psi	5	1.90	0.686	
1	10,400	10	1.48	1.372	
2	8,630	15	1.23	2.06	
3	7,200	20	1.03	2.75	
4	5,800	25	.829	3.44	
5	4,270	30	.610	4.12	
6	3,720	35	.531	4.81	
7	2,710	40	.387	5.50	
8	2,200	45	.314	6.19	59.2
9	1,745	50	.249	6.87	47.2
16	8,820	13.5	.983	2.34	
16 (Retest)	9,120	13.5	1.010	2.34	
17	8,220	18.2	.913	3.15	
18	5,030	23.0	.559	3.98	
19	3,960	27.6	.440	4.78	
20	2,280	32.3	.253	5.60	
21	1,845	52.0	.205	9.00	63.9
22	10,795	12.2	1.20	2.12	
23	11,300	12.7	1.26	2.20	
24	10,600	11.0	1.22	1.91	

Models 0-9, σ_{yp} = 7000, E = 370,000   Models 16-24, σ_{yp} = 9,000, E = 300,000

Steel Column Data

σ_{yp} = 44,000 psi   E = 31.3×10^6

Model	L/ρ	Stress (σ_u)	$L/\rho \sqrt{\sigma_{yp}/E}$	σ_{ult}/σ_{yp}	$\sigma_{yp}/E \times 10^4$
	145	14,000	5.44	.318	4.46
	116	23,000	4.35	.523	7.35
	104	29,000	3.90	.659	9.26
	90	36,000	3.37	.819	11.50
	87	39,000	3.26	.886	12.45
	73	43,000	2.74	.977	13.72
	59	44,000	2.21	1.000	14.05
	50	44,000	1.875	1.000	14.05
	48	42,000	1.80	.956	13.40
	52	45,000	1.912	1.020	14.38
	38	47,000	1.425	1.068	15.00
	30	50,000	1.125	1.135	16.00
	175	9,500	6.56	.216	

Table No. VIII

Test Data For Nylon And Cellulose Acetate Models

Tests By E. F. Durfee And V. D. Johnson

Model .328" x .310" x .1516" Cellulose-Acetate

Force	Stress	Vert. Defl.	Unit Strain
47#	1020#	4.0×10^{-3}	1220×10^{-5}
85#	1800	5.8	1768
114#	2380	6.7	2040
146	3100	8.0	2440
175	3720	9.2	2800
214	4560	11.0	3340
249	5310	13.7	4160
268	5700	15.9	4830
277	5900	18.0	5460
282	6000	19.8	6010
291	6200	21.6	6560
294	6250	23.6	7160
298	6340	25.7	7810
302	6420	27.4	8310
300	6380	29.0	8800
300	6380	29.5	8950

Rate of Loading — 800 psi/min

Model 14 .870" x .309" x .509 Nylon

Force	Stress	Vert. Defl.	Unit Strain
110#	696 psi	50×10^{-3}	575×10^{-5}
210	1335	76	874
360	2290	117	1342
520	3310	145	1667
680	4320	176	2020
770	4890	195	2240
860	5460	212	2435
1040	6590	248	2850
1190	7550	277	3180
1300	8240	301	3460
1350	8550	320	3680
1450	9190	344	3950
1525	9650	378	4350
1600	10130	406	4660
1625	10650	436	5020
1675	10800	474	5450
1700	10880	502	5760
1710	10880	532	6110
1710	10880	575	6610
1750	11120	615	7060

Table No IX

Test Data For Lucite Columns

Tests Run By E. F. Durfee Jr. and V. D. Johnson

Rate of Loading – 800 psi/min   Temp. 20.3°C

Model #16   4.02" x 0.617" x 0.743"

Force	Vert Defl.	Lateral Defl.	
2000#	70	3.8	
2230#	80	4.0	
2460	85	4.5	
2700	95	5.3	
2800	100	5.8	
2900	105	6.2	
2950	113	6.8	
3100	120	7.8	
3250	129	9.9	
3300	133	10.9	
3350	136	11.9	
3400	140	13.4	
3420	144	15.6	
3500		Visual	

From Plot, Critical Force = 3390# σ_{crit} = 8820 psi

Model #17   5.35" x 0.511" x 0.747"

Force	Vert. Defl	Defl. Left	Defl. Right
1570#	70	2.9	0.5
1850#	80	2.7	– 0.2
2100	90	2.1	– 1.0
2350	100	1.8	– 2.0
2600	110	1.0	– 3.0
2800	120	0.9	– 3.6
2900	127	0.9	– 3.9
3000	130	0.7	– 4.1
3100	135	1.1	– 4.1
3200	140	1.9	– 3.7
3250	145	2.9	– 2.9
3400	150	4.0	– 1.6
3450	155	6.9	+ 1.0
3530	160	Visual	Visual
3700			

From Plot, Critical Force = 3140# σ_{crit} = 8220 psi

Note: All Deflection Readings In 1/1000

Table No. X

Test Data For Lucite Columns

Test By E. F. Durfee Jr and V. D. Johnson

Rate of Loading - 800 psi/min   Temp. 20.3°C

Model #15   1.452" x .505" x .511"

Force	Vert. Defl.	Unit Defl.	Stress
57#	30 $\times 10^{-3}$"	210 $\times 10^{-5}$	220 psi
106	49	340	410
169	69	475	655
245	89	610	950
288	99	681	990
335	109	750	1300
374	118	812	1450
432	127	875	1670
513	147	1010	1990
573	160	1101	2220
660	176	1210	2560
770	198	1362	2984
812	207	1425	3150
915	225	1550	3540
1010	242	1665	3910
1261	286	1970	4890
1353	306	2105	5250
1497	332	2290	5800
1590	349	2401	6166
1639	358	2460	6350
1745	385	2650	6760
1880	420	2890	7286
2075	454	3121	8050
2150	471	3240	8330
2280	530	3462	8843
2405	542	3730	9320
2555	576	3970	9900
2655	606	4170	10290
2745	639	4400	10630
2815	665	4576	10910
3055	760	5230	11830
3170	825	5680	12280
3345	927	6380	12960
3445	996	6860	13350
3505	1060	7300	13580
3555	1116	7690	13780
3600	1198	8250	13950
3630	1255	8650	14070
3672	1488	10230	14220
3678	1529	10520	14245
3672	1669	11480	14220

Table No. XI

Test Data for Lucite Columns

Tests Ran By E.F. Durfee Jr and V.D Johnson

Rate of Loading - 800psi/min Temp. 20.3°C

Model #18 6.71" x 0.507" x 0.747" L/ρ = 46

Force	Vert. Defl.	Defl. Left	Defl. Right
740	40	4.1	-4.0
870	45	4.1	-4.0
970	50	4.1	-3.9
1080	55	5.0	-4.0
1190	60	5.0	-3.9
1410	70	5.1	-3.9
1640	80	5.2	-4.0
1775	85	5.2	-4.0
1830	90	6.2	-4.6
1950	95	6.2	-5.1
2030	100	8.0	-5.8
2150	105	9.5	-7.1
2500	110	11.1	-9.0
2600		Visual	Visual

From Plot, Critical Load = 2000# σ_{crit} = 5300 psi

Model #19 8.05" x 0.506" x 0.748" L/ρ = 55.1

Force	Vert. Defl.	Defl. Left	Defl. Right
845	45	3.1	-2.1
940	50	3.1	-2.9
1020	55	4.1	-2.9
1140	60	4.1	-3.0
1240	65	5.0	-3.6
1320	70	5.5	-4.3
1420	75	6.1	-4.5
1500	80	6.1	-4.6
1600	85	8.0	-6.2
1700	90	9.0	-7.1
1790	95	13.0	-11.5
1850	100	18.0	-17.0
1940		Visual	Visual

From Plot, Critical Load = 1500# σ_{crit} = 3960 psi

Note: All Deflections in 1/1000

Table No XII

Test Data For Lucite Columns

Tests By E.F. Durfee Jr. and V.D. Johnson

Rate of Loading - 800 psi/min Temp. 20.3°C

Model #20 9.386 x 0.504 x 0.741 L/ρ = 64.6

Force	Vert Defl.	Defl. Left	Defl. Right
80 #	5	- 4.2	5.3
220	15	- 6.1	7.0
410	27	- 7.0	7.8
490	32	- 7.2	8.0
605	40	- 7.8	8.8
782	50	- 8.4	9.8
918	60	- 10.0	11.7
1000	65	- 11.1	13.0
1160	75	- 14.2	16.7
1360	85	- 25.0	280
1490		Visual	Visual

From Plot, Critical Load = 850# σ_{crit} = 2280 psi

Model #21 14.98" x 0.498" x 0.751" L/ρ = 104

Force	Vert. Defl.	Defl. Left	Defl. Right
90 #		2	2
195		8	7
280		8	7
335		8	8
380		8	8
460		8	7
550		8	7
660		8	6
690		Visual	Visual

Critical Load = 690# $\sigma_{crit.}$ = 1845

Note: All Deflections in 1/1000

Table No. XIII

Test Data For Lucite Columns

Tests By E.F. Durfee Jr. and V. D. Johnson

Rate of Loading 300 #/min   Temp 22°C

Model #16 (Retest)   4.02" x 0.517" x 0.743"   L/ρ =

Force	Defl. Left	Defl. Right	Force	Defl. Left	Defl. Right
1450 #	0	1.0	3450 #	1.05	3.6
1950	0	1.9	3500	1.20	3.7
2300	0	2.5	3520	4.10	1.0
2550	0	3.0	3600	6.1	– 0.7
2750	0.15	3.1	3650	7.0	– 1.2
3000	0.15	3.7	3700	8.1	– 2.0
3240	0.40	3.5	3720	9.2	– 3.1
3260	1.04	3.2	3740	10.2	– 4.1

From Plot, Critical Force = 3500# σ_{ult} = 9120 p.s.i.

Model #23   3.65" x .496" x .740"   L/ρ = 25.4

Force	Defl Left	Defl. Right	Force	Defl. Left	Defl. Right
3230 #	0	4.2	4190	-1.1	10.7
3420	0	5.0	4200	-1.7	11.5
3630	0	5.6	4200	-2.1	11.9
3730	0	6.0	4210	-2.5	12.4
3780	0	6.3	4220	-3.3	13.3
3900	0	6.9	4220	-4.0	14.1
3970	0	7.3	4230	-5.0	15.6
4050	0	8.0	4240	-6.1	17.0
4110	0	8.5	4240	-7.1	18.1
4150	0	9.0	4250	-8.1	19.2
4170	-0.1	9.5	4250	-10.1	22.0
4180	-0.6	10.1			

From Plot, Critical Force = 4150# σ_{ult} = 11,300 p.s.i.

Note: All Deflection Reading in 1/1000

Table No XIV

Test Data For Lucite Columns

Tests By E.F. Durfee Jr. and V.D. Johnson

Rate of Loading 300#/min Temp. 22°C

Model #22 3.57" x .510" x .750" L/ρ = 24.3

Force	Defl. Left	Defl. Right	Force	Defl. Left	Defl. Right
3200#	0	4.5	4070#	3.0	5.1
3400	0	4.9	4100	3.0	5.1
3475	0	5.1	4150	3.0	5.5
3600	0	5.6	4175	4.9	3.9
3700	0	6.0	4200	4.9	4.0
3830	1.0	5.6	4220	7.9	1.2
3900	1.0	5.9	4227	8.0	1.3
3950	1.0	6.1	4300	13.0	-3.0
4000	1.0	6.5	4320	15.1	-5.0
4050	1.0	6.9	4330	19.0	-8.8

Critical Force From Plot = 4110# $\sigma_{ult.}$ = 10,790 p.s.i.

Model #24 3.19" x .500" x .746" L/ρ = 22.0

Force	Defl. Left	Defl. Right	Force	Defl. Left	Defl. Right
770#	0	0.7	3950#	.10	6.0
1200	0	1.0	4050	1.1	5.6
1850	0	2.0	4150	1.7	5.4
2500	0	3.0	4170	2.1	5.1
3070	0	4.0	4250	3.1	4.8
3430	.05	4.7	4320	4.0	4.1
3630	.09	5.0	4400	6.0	3.0
3800	.10	5.5			

Critical Force From Plot = 3950# σ_{ult} = 10,600 psi

Note: All Deflection Readings in 1/1000

Table No. XV

Test Data For Plexiglas Columns

Test By R.T. Miller

Rate of Loading - 400 #/min

Model O   1.44" x 1.00" x .51"   L/ρ = 10

Force	Vert. Defl.	Stress (σ)	σ correct.	Unit Elong.
200 #	16.00	392 psi	0 psi	0 $\times 10^{-5}$
400	18.05	784	392	142
600	19.65	1176	784	253
800	20.10	1568	1176	285
1000	22.30	1960	1568	438
1200	23.90	2352	1960	549
1600	27.00	3136	2744	763
2000	30.08	3920	3528	978
2400	33.45	4704	4312	1212
2800	36.82	5488	5096	1446
3200	40.72	6272	5880	1719
3600	45.10	7056	6664	2021
4000	50.65	7840	7448	2406
4400	57.30	8624	8232	2868
4800	65.65	9408	9016	3448
5200	77.95	10192	9800	4302
5600	96.20	10976	10584	5569
6000	Visual	11760		
6400	"	12544		
6800	"	13328		
6850	Extreme Deformation	13426		

Note: Deflections in 1/1000 inch

Table No. XVI

Test Data For Plexiglas Columns

Tests By R. T. Miller

Model 4 7.20" x 1.00" x .50" L/ρ = 50

Force	Vert. Defl.	Force	Vert. Defl.	Force	Vert. Defl.
200#	11.00	1000#	43.10	2400	102.80
400	18.50	1200	51.00	2800	127.50
600	26.20	1600	67.40	2900	Visual Buckling
800	34.10	2000	85.30		

Critical Load = 2900 σ_{unit} = 5800 psi Rate of Loading = 400#/min

Model #5 8.65" x 1.00" x .50" L/ρ = 60

Force	Vert. Defl.	Force	Vert. Defl.	Force	Vert. Defl.
100#	45.10	800	77.05	1500	109.00
200	49.78	900	81.65	1600	113.92
300	54.35	1000	86.12	1700	118.60
400	59.10	1100	90.45	1800	Visual Buckling
500	63.62	1200	95.05	1900	
600	68.10	1300	99.48	2135	
700	72.55	1400	104.28		

Critical Load = 2135 σ_{unit} = 4270 psi Rate of Loading = 200#/min

Model 6 10.08" x 1.00" x .51" L/ρ = 70

Buckling Load Recorded only — Load = 1900# σ_{unit} =

Rate of Loading = 400#/min

Model 7 11.52" x 1.00" x .51" L/ρ = 80

Buckling Load Recorded Only — Load = 1380# σ_{unit} =

Rate of Loading = 400#/min

Model 8 12.96" x .99" x .51" L/ρ = 90

Buckling Load Recorded Only — Load = 1110# σ_{unit} =

Rate of Loading = 400#/min

Model 9 14.4" x 1.00" x .51" L/ρ = 100

Buckling Load Recorded Only — Load = 890# σ_{unit} =

Rate of Loading = 400#/min

Table No. XVII

Test Data For Plexiglas Columns

Tests By R. T. Miller

Rate of Loading 400#/min

Model 1 — 2.88" x 1.00" x .50" — $L/\rho = 20$

Force	Vert. Defl.	Force	Vert. Defl.	Force	Vert. Defl.
200#	9.36	1600#	31.75	4000	83.50
400	13.00	2000	38.20	4400	98.80
600	16.20	2400	45.10	4800	122.00
800	19.30	2800	52.60	5200	} Visual Buckling
1000	22.10	3200	61.65	5600	
1200	25.40	3600	70.90		

Critical Load = 5200 σ_{crit} = 10,400 psi

Model #2 — 4.32" x 1.00" x .51" — $L/\rho = 30$

Force	Vert. Defl.	Force	Vert. Defl.	Force	Vert. Defl.
200#	1.00	1200#	23.65	3200	77.20
400#	5.90	1600	35.00	3600	92.40
600#	10.10	2000	42.90	4000	111.30
800#	14.90	2400	53.50	4400	} Visual Buckling
1000#	19.25	2800	64.80	4800	

Critical Load = 4400 σ_{crit} = 8630

Model #3 — 5.77" x 1.00" x .50" — $L/\rho = 40$

Force	Vert. Defl.	Force	Vert. Defl.	Force	Vert. Defl.
200#	8.35	1000#	33.70	2400#	80.75
400	15.12	1200	39.05	2800	96.20
600	20.42	1600	52.28	3200	114.20
800	26.90	2000	65.85	3600	Visual

Critical Load = 3600 σ_{crit} = 7200 psi

Note: All Deflections in 1/1000 in.

Table No XVIII

Tangant And Reduced Modulus Values For Plexiglas In Compression

Stress	E_T	E_R
3000 psi	3.7×10^5 psi	3.7×10^5 psi
5000	3.2 "	3.43 "
7000	2.35 "	2.90 "
8000	1.84 "	2.52 "
9000	1.32 "	2.06 "
10000	0.84 "	1.47 "
11000	0.81 "	1.50 "

Tangant And Reduced Modulus Values For Lucite In Compression

Stress	E_T	E_R
5000 psi	3.0×10^5 psi	3.0×10^5 psi
6000	2.9 "	2.95 "
7000	2.58 "	2.78 "
8000	2.42 "	2.67 "
9000	2.08 "	2.48 "
10000	1.83 "	2.31 "
11000	1.48 "	2.04 "
12000	1.04 "	1.65 "
13000	0.83 "	1.42 "
14000	0.20 "	0.50 "

materials both have a linear relationship between stress and strain, but the plastic stretches more for an equal increase in stress. At the yield stress of the steel, however, the instantaneous value of the modulus (E_T) for steel drops drastically. (A steel model experiencing this stress would fail through yield; or, more properly, through instability caused by the lowered value of E accompanying yield). At the arbitrarily set "yield stress" of the plastic, in contrast, the plastic behaves almost exactly as before; for the same increment in stress as viewed before, the increment of strain is a little larger, but only a little larger. The tendency towards instability failure - which is inversely proportional to E - is a little greater to the same extent that the instantaneous value of E_T has decreased. (A plastic model experiencing this stress would probably show no changes at all unless by sheer coincidence the gradual reduction in instantaneous E to this point was just sufficient to induce instability failure).

<u>Crazing</u>

Model No. 51, which reached the maximum absolute pressure of the four plastic submarine models tested, was the only one of the four models to exhibit the

phenomenon of crazing. Figure XVIII shows the location of the crazing in relation to the fracture and to the overall geometry of the model. Figure XIX details the crazing along the central portion of the line of fracture, and the smaller region of crazing on the edge of the adjacent frame. Both areas of crazing were observed immediately following the hydrostatic test. The crazing appeared in the form of tiny, hairlike cracks on or under the surface of the model, and could be detected only by careful lighting. Rough sketches were promptly made of the phenomenon with descriptive measurements. At the time of first examination, no definite determination was made as to which surface contained the tiny cracks. No detectable surface irregularities existed on either surface.

This model was next examined with a magnifying glass approximately three (3) days after the date of the hydrostatic test. At this examination, and at all subsequent re-examinations, no trace of the frame edge crazing could be found.

The crazing along the line of fracture remained unchanged and apparently stable. Figure XIX represents, therefore, the appearance of the phenomenon in the fractured area both immediately on conclusion of the test, and on 21 April 1951 when the drawing was made.

movement of cracking. Figure XVIII shows the location of the cracking in relation to the fracture and to the overall geometry of the model. Figure XIX details the cracking along the vertical portion of the initial fracture, and the small region of cracking on the edge of the adjacent frame. Both areas of cracking were observed immediately following the hydrostatic test. The cracking appeared in the form of tiny, hairline cracks on or under the surface of the model, and could be detected only by careful scanning. Rough sketches were promptly made of the appearance with appropriate measurements. At this time of close examination, no reliable determination was made as to which surface contained the tiny cracks. No noticeable surface irregularities existed on either surface.

This model was next examined with a magnifying glass approximately three (3) days after the date of the hydrostatic test. At this examination, and at all subsequent re-examinations, no trace of the frame edge cracking could be found.

The cracking along the line of fracture remained unchanged and apparently stable. Figure XIX represents, therefore, the appearance of the phenomenon in the fractured area both immediately on completion of the test, and on 12 April 1963 when the reading was made, This permanent crazing has been determined to be at, or immediately adjacent to, the inner surface of the shell. No finite surface breaks or irregularities exist.

The literature concerning the field of plastics contains much pertaining to the phenomenon of crazing - there is little agreement or unanimity regarding it; References (10) and (11). Among the possible causes of crazing are listed the following: the existence of a tensile stress at or near a yield stress, or, the existence of a relative tensile stress which may be superimposed on a general compressive stress field as durihg bending; instability of the plastic due to formula, conditions of molding and environment and atmosphere during manufacture; and reactions in the surface of the plastic due to the presence of solvents or oils, including human skin oils. The latter causes are essentially a form of material instability, or susceptibility to environmental effects, and are not considered pertinent to the crazing occurring in Model 51 for the following reasons: the material used was standard commercial "Lucite", and exhibited no other case of crazing during the manufacture, handling, and test of the models in spite of constant handling and exposure to water, oil, and ethylene dichloride solvent.

It is believed that the first mentioned cause of crazing is applicable to Model 51: the existence of a tensile stress at or near a yield stress, or, the existence of a relative tensile stress. Since the existence of crazing does not necessarily reduce the ultimate strength of a tensile specimen, the occurrence of crazing is not necessarily an indication that any portion of the material has reached the ultimate stress. All authorities consulted by the authors concurred that the observed crazing indicated an absolute or relative tensile stress field in the area affected. The permanent crazing at the center of the apparent fracture bulge is located at the inner surface of the model. It is believed that this crazing occurred when the formation of such a bulge produced bending in the shell, and caused a tensile stress at the inner surface relative to the general compression stress through the shell and at the outer surface.

No firm conjecture can be advanced in regard to the temporary crazing over the frame edge inasmuch as the exact surface location of this region is not known.

It is believed that the first mentioned phase of crazing is applicable to Model (1): the existence of a tensile stress at or near a yield stress, viz, the existence of a relative tensile stress. Since the existence of crazing does not necessarily reduce the ultimate strength of a tensile specimen, the occurrence of crazing is not necessarily an indication that any portion of the material has reached the ultimate stress. All authorities consulted by the author concurred that the observed crazing indicated an absolute or relative tensile stress field in the area affected. The permanent crazing at the bottom of the apparent fracture which is located at the inner surface of the model. It is believed that this crazing occurred when the formation of such a hole produced bending in the shell, and caused a tensile stress at the inner surface relative to the general compressive stress through the shell and at the outer surface.

A firm conclusion can be reached in regard to the necessary [illegible] prior to the [illegible] edge [illegible] in the outer surface portion of this region is not known.

APPENDIX E

Bibliography

(1) E. WENK, JR., "Model Tests and Analysis of a Cylindrical Foundation For a 5-Inch 38-Caliber Gun", DTMB Report R-255 (RESTRICTED), Feb. 1948.

(2) F.R. SHANLEY, "Applied Column Theory", Proceedings of American Society of Civil Engineers, vol. 75, June 1949, pp. 759-788.

(3) F.R. SHANLEY, "Inelastic Column Theory", Jnl. Aeron. Sci., vol. 14, no. 5, May 1947, pp. 261-268.

(4) D.F. WINDENBURG and C. TRILLING, "Collapse by Instability of Thin Cylindrical Shells Under External Pressure", DTMB Report 385, July 1934.

(5) C. TRILLING, "The Influence of Stiffening Rings on the Strength of Thin Cylindrical Shells", DTMB Report 396, Feb. 1935.

(6) Plastics Materials Manufacturers' Association - "Technical Data on Plastic Materials".

(7) W. RAMBERG and W.R. OSGOOD, "Description of Stress-Strain Curves by Three Parameters", Technical Notes, NACA, No. 902, July 1943.

(8) HOFF, BOLEY and COAN, "The Development of a Technique for Testing Stiff Panels in Edgewise Compression", Proceedings of Society of Experimental Stress Analysis, vol. V, no. II, pp. 14-34.

(9) R. VON MISES, "Critical External Pressure of Cylindrical Tubes Under Uniform Radial and Axial Pressure", DTMB Report No. 366.

(10) J. R. McLOUGHLIN, "Crazing of Polystrene Films", Princeton University Plastics Laboratory Technical Report 12B.

(11) "Notes and Comments of Section C", Princeton Project, Preliminary Report to ASTM concerning the Phenomenon of Crazing.

(12) SIMMONDS and ELLIS, "Handbook of Plastics".

(13) TIMOSHENKO, S., "Theory of Elastic Stability," pp. 64-170

(14) TIMOSHENKO, S., "Strength of Materials", vol. II, p. 141.